Title
Holocene Peatland Carbon Accumulation, Ecology, and Hydrology in the Canadian James Bay Lowlands

Author
Holmquist, James R.

Publication Date
2013

Peer reviewed|Thesis/dissertation

UNIVERSITY OF CALIFORNIA

Los Angeles

Holocene Peatland Carbon Accumulation, Ecology, and Hydrology in the Canadian James Bay Lowlands

A dissertation submitted in partial satisfaction of the requirements for the degree Doctor of Philosophy in Biology

by

James Robert Holmquist

2013

ABSTRACT OF THE DISSERTATION

Holocene Peatland Carbon Accumulation, Ecology, and Hydrology in the Canadian James Bay Lowlands

by

James Robert Holmquist

Doctor of Philosophy in Biology

University of California, Los Angeles, 2013

Professor Glen MacDonald, Chair

Northern peatlands contain some of the largest terrestrial stores of organic soil carbon (C) which may grow due to increases in productivity, or decline due to higher decay under projected warming and drought scenarios. However, models of peatland growth lack data on basic peatland history for the remote James Bay Lowlands (JBL) region of Canada, as well as the relationships between climate and productivity, and the history of Holocene precipitation. This dissertation presents C accumulation, vegetative macrofossil, and proxy-climate reconstruction data from eight previously unpublished sites in the JBL, as well as synthesizes currently available data. Peatlands in the JBL initiated lagging the retreat of the Laurentide ice sheet, and the drainage of glacial lakes by an average of 2,900 years. Most of the peatlands studied initiated as mineral rich fens, which transitioned to nutrient poor bogs an average of 3,800 years after they

initiated. Over the Holocene they have acted as a sink of CO_2, accumulating between 71.5 and 171.2 kgC m^{-2}, with median long-term apparent C accumulation rates (LARCA) ranging from 13.8 to 31.6 gC m^{-2} yr^{-1}. Peatland C accumulation was variable within and between sites, but was driven by productivity rather than decay during the late-Holocene. The depths of late-Holocene peat deposits correlate positively with growing season length, and photosynthetically active radiation, and were negatively affected by permafrost occurrence. A single site provides evidence for a relatively dry pre-Holocene Thermal Maximum period, and a relatively wet Holocene Thermal Maximum, with a small but positive influence of water table depth on LARCA. Although there was some variation due to site-specific conditions, multiple sites indicate that the warm Medieval Climate Anomaly was a wet period in the JBL, consistent with modern precipitation anomalies, whereas the Little Ice Age was dry. The Little Ice Age may have been locally complex due to precipitation variability, or the formation of permafrost. On the short term, peatland C-stores may grow faster if temperature and seasonality changes occur within their physiological and ecological limitations. However long-term peatland stability in the area will likely be dependent on precipitation, which may fluctuate due to the positions of the Arctic and Pacific fronts, and stochastic interactions between the atmosphere and sea surface temperatures.

The dissertation of James Robert Holmquist is approved

Thomas W. Gillespie

Philip W. Rundel

Lawren Sack

Glen M. MacDonald, Committee Chair

University of California, Los Angeles

2013

To Mom and Dad, for instilling the values of curiosity and perseverance in me, and for giving me everything that I need to succeed.

and to Jennifer Sargent for making the last five years the best of my life.

Table of Contents

Abstract……..…….(ii)

List of abbreviations……...……(x)

List of figures and tables.…….……..(xii)

Acknowledgements……..……..(xx)

Curriculum vitae…….……..(xxi)

1. Introduction…….……(1)

2. Peatland Initiation, Succession and Carbon Accumulation in the James Bay Lowlands…….(9)

2.1 ABSTRACT……..(9)

2.2 INTRODUCTION……...…(10)

2.3 MATERIALS AND METHODS……(13)

2.3.1. Field Sites and Previously Published Sites……..(13)

2.3.2. Age Depth Modeling……..(18)

2.3.3. GIS Data……..(22)

2.3.4. Macrofossil Analysis……..(23)

2.3.4. Soil C Estimates…….……..…(23)

2.4 RESULTS……...(24)

2.4.1. Peatland initiation and succession in the JBL……..…..……...(24)

2.4.2. Carbon Accumulation in the JBL……(35)

2.5. DISCUSSION……(38)

2.5.1. Geographic patterns of Peat Initiation and Succession……..(38)

2.5.2. Carbon Storage and LARCA……..(40)

2.6. CONCLUSION……...(43)

3. Climate Drivers for Late-Holocene Vertical Peat Accumulation in the Hudson and James Bay Lowlands……..(44)

3.1. ABSTRACT……..(44)

3.2. INTRODUCTION……..(44)

3.3. MATERIALS AND METHODS……...(48)

3.3.1. Average apparent rate of C accumulation……(49)

3.3.2. Statistical Analysis……(49)

3.4. RESULTS……..(50)

3.4.1. 2 ka Soil C in JBL……(50)

3.4.2. Climate and 2 ka Depth……...(54)

3.4.3 Permafrost Occurrence and Peat Depth……(61)

3.5. DISCUSSION……(62)

3.5.1. C Accumulation in the JBL……..(62)

3.5.2. MAAT, GDD_0 and PAR_0 as Drivers of Post-2 ka Vertical Peat Accumulation……(63)

3.5.3. The Effect of Permafrost on Peat Depth……....(66)

3.6. CONCLUSION……..(67)

4. Mid to Late-Holocene changes in Hydrology, Peatland Ecology, and Carbon Accumulation in the Canadian James Bay Lowland……..……(69)

4.1. ABSTRACT……...(69)

4.2. INTRODUCTION……..(70)

4.3. MATERIALS AND METHODS……..……..(74)

4.3.1. Study site and core information……..……..……..(74)

4.3.2. TA processing……..……(77)

4.3.3. Statistics……(79)

4.4. RESULTS……..(80)

4.4.1. TA and WTD……..(81)

4.4.2. WTD changes associated with Macrofossil and LARCA Record……...(83)

4.5. DISCUSSION……(85)

4.5.1. Mid-Holocene WTD Changes……(85)

4.5.2. Late-Holocene WTD changes……(87)

4.5.3. Vegetation Changes in the Mid-Holocene……(89)

4.5.4. Correlation between WTD and LARCA…..……..(90)

4.6. CONCLUSIONS……...(92)

5. Impact of the Medieval Climate Anomaly, Little Ice Age, and Recent Warming on Hydrology and Carbon Accumulation in the James Bay Lowlands…….(93)

5.1. ABSTRACT……...(93)

5.2. INTRODUCTION……..(94)

5.3. MATERIALS AND METHODS……...(96)

5.4. RESULTS……..(99)

5.4.1. TA Assemblages……(100)

5.4.2. WTD……..(106)

5.4.3. TA assemblages, WTD, and LARCA……..(107)

5.5. DISCUSSION…….(109)

5.5.1. Hydroclimatology and WTD During the MCA, LIA, and Recent Periods……....(109)

5.5.2. MCA Hydroclimatology in North America…….....(112)

5.5.3. Inconsistent relationships between WTD and LARCA…….(119)

5.6. CONCLUSION……(120)

6. Conclusion……..(121)

7. Works Cited……...(127)

List of abbreviations

1,000 calendar years before present (ka)

Bulk density (BD)

Calendar years before present (ybp)

Carbon (C)

Change in relative humidity with respect to present (ΔRH% wrt present)

Ecosystem respiration (ER)

El Niño Southern Oscillation (ENSO)

Growing degrees over 0°C (GDD_0)

Holocene Thermal Maximum (HTM)

Hudson Bay Lowlands (HBL)

James Bay Lowlands (JBL)

Little Ice Age (LIA)

Long-term apparent rate of C accumulation (LARCA)

Loss on ignition at 550°C (LOI_{550})

Mean annual air temperature (MAAT)

Mean annual precipitation (MAP)

Medieval Climate Anomaly (MCA)

Net ecosystem productivity (NEP)

Net primary productivity (NPP)

Nitrogen (N)

North Atlantic Oscillation (NAO)

Organic Matter (OM)

Photosynthetically active radiation integrated over the growing season (PAR_0)

Radiocarbon (^{14}C)

s. dev. (±)

Testate Amoebae (TA)

Water Table Depth (WTD)

West Siberian Lowlands (WSL)

List of Figures and Tables

Figure 1 (page 14): My study sites were located in the JBL, and were supplemented by a review of four additional reports of basal dates and timings of fen to bog transitions. Pictured are also maps of peatland extent (Tarnocai et al., 2011), and the borders of discontinuous and continuous permafrost zones (Brown et al., 1998).

Figure 2 (page 15): A. - D. Landscapes that are representative of the surface cover in the JBL including: *Picea mariana* dominated stands, uncovered *Sphagnum* bogs, minerotrophic thin fens, and open water. Photos are courtesy of David Beilmen, and are used with permission (Beilman, Personal Communication).

Figure 3 (page 19): Age-depth models from eight sites in the JBL area. Grey lines refer to minimum and maximum measurements, black lines refers to best estimates from Bacon age-depth modeling software.

Figure 4 (page 26): JBL1 BD, LOI_{550}, LARCA, and qualitative macrofossil zones plotted against time.

Figure 5 (page 27): JBL2 BD, LOI_{550}, LARCA, and qualitative macrofossil zones plotted against time.

Figure 6 (page 28): JBL3 BD, LOI_{550}, LARCA, and qualitative macrofossil zones plotted against time.

Figure 7 (page 29): JBL4 BD, LOI_{550}, LARCA, and qualitative macrofossil zones plotted against time.

Figure 8 (page 30): JBL5 BD, LOI_{550}, LARCA, and qualitative macrofossil zones plotted against time.

Figure 9 (page 31): JBL6 BD, LOI_{550}, LARCA, and qualitative macrofossil zones plotted against time.

Figure 10 (page 32): JBL7 BD, LOI_{550}, LARCA, and qualitative macrofossil zones plotted against time.

Figure 11 (page 33): JBL8 BD, LOI_{550}, LARCA, and qualitative macrofossil zones plotted against time.

Figure 12 (page 34): The upper plot represents LARCA values from all cores combined into 1,000-year bins. Central lines represent medians. Box edges represent the first upper and lower quantiles, and whisker lines represent third upper and lower quantiles. The central plot and bottom plot are the Z-scores for LARCA plotted for cores in the discontinuous permafrost and non-permafrost, and zones respectively.

Figure 13 (page 37): The upper plot represents LARCA values from all cores combined into 1,000-year bins. Central lines represent medians. Box edges represent the 25% upper and lower quartiles. Whisker lines represent least and greatest values. The central plot and bottom plot are the Z-scores for LARCA plotted for cores in the non-permafrost, and discontinuous permafrost zones respectively.

Figure 14 (page 47): My study sites were located in the JBL, and were supplemented by a review of seventeen additional age-depth models from the entire HBL-JBL. Pictured are also maps of peatland extent (Tarnocai et al., 2011), and the borders of discontinuous and continuous permafrost zones (Brown et al., 1998).

Figure 15 (page 51): Post-2 ka C accumulated in the eight JBL sites arranged by latitude. (-) Represent the upper and lower estimates of Post-2 ka C masses based on upper and lower estimates of 2 ka by 'Bacon' models. * Represents permafrost peat.

Figure 16 (page 55): Age-depth models from seventeen review sites in the HBL-JBL area. Grey lines refer to minimum and maximum measurements, black lines refer to best estimates from Bacon age-depth modeling software.

Figure 17 (page 56): Age-depth models from seventeen review sites in the HBL-JBL area. Grey lines refer to minimum and maximum measurements. Black lines refer to best estimates from Bacon age-depth modeling software.

Figure 18 (page 61): Four scatterplots correlating 2 ka depth as a function of environmental variables. Figures are arranged from left to right and top to bottom in order of the linear model's r^2 value. Solid lines represent the best fit for linear regressions. Dashed lines represent to the best fit for an exponential regression. Triangles represent new JBL site data. Circles represent review data.

Figure 19 (page 62): Bar and whisker plot of 2 ka depths in permafrost and non-permafrost peat. Central lines represent medians. Box edges represent the 25% upper and lower quantiles. Whisker lines represent least and greatest values.

Figure 20 (page 76): JBL7 is located in area that is crucial to understand because of its high levels of soil C, precipitation anomalies, and local hydrology. Top: JBL7 and notable review sites mentioned in the text, as well a peatland C mass, and permafrost distribution (Brown et al., 1998; Tarnocai, 2011). Bottom left:. A map showing compiled precipitation anomalies for the seven most extreme La Niña events since 1949 according to the Multivariate ENSO Index (1949-51, 1954-56,1964-66,1970-1972,1973-75, 1988-90, 2010-2011; NOAA/ESRL, 2013a,b), as well as the modern position of the arctic front (Ladd and Gajewski, 2009). Bottom right: Local surface hydrology, and both

fen and bog distribution near JBL7 (Provincial Land Cover Data Base, Second Edition; 2000).

Figure 21 (page 77): The age-Depth Model for JBL7 using multiple ^{14}C ages, and 'Bacon' statistical software (Blaauww et al., 2011).

Figure 22 (page 80): An xy plot with a list of common taxa identified in JBL7, as well as their mean WTD and minimum and maximum tolerances (Booth, 2008).

F**igure 23 (page 82):** Stratigraphy data for JBL7 including, age, TA species > at least 20% at some point in the core, WTD reconstructions, and TA zones based on a constrained cluster analysis. Grey bars represent periods of low TA data.

Figure 24 (page 84): JBL7 shows mid-Holocene synchronicities with a central Canadian compiled record of change in relative humidity with respect to present (∆RH% wrt present; Edwards et al., 1996), and late-Holocene synchronicities with a WTD reconstruction from another JBL record (Bunbury et al., 2012). JBL7 WTD reconstructions are also compared with macrofossil and LARCA data from the same core (Ch. 2). The solid line indicates the mean WTD value for the entire record. The dashed line represents the mid-Holocene, and late-Holocene averages.

Figure 25 (page 85): Scatter plot showing correlation between WTD and LARCA, as well as a plot of standard residuals relative to a linear model with WTD as the causal variable and LARCA as the dependent variable.

Figure 26 (page 97): A map of the James Bay Lowlands, showing the sites of testate amoeba based reconstructions, notable review sites mentioned in the text, peatland concentration (Tarnocai, 2011), and the southern boarders of continuous and discontinuous permafrost in the region (Brown et al., 1998).

Figure 27 (page 99): A xy plot with a list of common taxa identified in JBL8, JBL2, JBL4, as well as their mean WTD and minimum and maximum tolerances (Booth, 2008).

Figure 28 (page 101): Representations of common and notable tests found in JBL material: a. *Amphitrema wrightianum* type*,* b. *Arcella catinus* type*,* c*. Archerella flavum,* d. *Assulina muscorum,* e. *Bullinularia indicum,* f. *Difflugia pristis* type*,* g. *Difflugia pulex,* h. *Habrotrocha angusticollis*, i. *Heleopera* spp.*,* j. *Hyalosphenia elegans,* k. *Hyalosphenia papilio,* l. *Trigonopyxis* spp.

Figure 29 (page 103): Stratigraphy data for JBL8 including, age, notable TA species, WTD reconstructions, LARCA, and TA zones based on a cluster analysis.

Figure 30 (page 104): Stratigraphy data for JBL2 including, age, notable TA species, WTD reconstructions, LARCA, and TA zones based on a cluster analysis.

Figure 31 (page 106): Stratigraphy data for JBL4 including, age, notable TA species, WTD reconstructions, LARCA, and TA zones based on a cluster analysis.

Figure 32 (page 111): Z-scores of WTD for JBL8, JBL2, JBL7, and JBL4 over the late-Holocene.

Figure 33 (page 114): A map showing reported medieval surface moisture conditions from Ch. 4, Ch. 5, and a review of literature (Tab. 21, 22), as well as compiled precipitation anomalies for the seven most extreme La Niña events since 1949 according to the Multivariate ENSO Index (1949-51, 1954-56,1964-66,1970-1972,1973-75, 1988-90, 2010-2011; NOAA/ESRL, 2013a,b)

Table 1 (page 16): Site information for eight new JBL sites collected in the summer of 2008, and four review sites.

Table 2 (page 17): 2008 climate data from 3 stations in the JBL.

Table 3 (page 20): ^{14}C-AMS samples, depth, ^{14}C ages, and best fit 'Bacon' model calibration estimates for new eight southwest JBL cores. [a.]Refers to dates that contain ^{14}C from atomic weapons testing. [b.]Refers to outliers that were eliminated by 'Bacon'.

Table 4 (page 21): ^{14}C-AMS samples, depth, ^{14}C ages, and best fit 'Bacon' model calibration estimates for new eight southwest JBL cores. [a.]Refers to dates that contain ^{14}C from atomic weapons testing. [b.]Refers to outliers that were eliminated by 'Bacon'.

Table 5 (page 22): ^{14}C-AMS samples, depth, ^{14}C ages, and best fit 'Bacon' model calibration estimates for new eight southwest JBL cores. [a.]Refers to dates that contain ^{14}C from atomic weapons testing. [b.]Refers to outliers that were eliminated by 'Bacon'.

Table 6 (page 35): Lists the timings of deglaciation linearly interpolated from Dyke et al., (2003), peat initiation times, the timing of *Sphagnum*-dominance derived from ordinal macrofossil analysis, % time as fen, the timing of rootlette-lichen dominance in two permafrost sites. *JBL6 was omitted from the average basal date because it was recovered without a basal section.

Table 7 (page 36): Data for LOI_{550}, mean BD, and total C accumulation, as well as as well as min, max, mean, standard deviation, and median values for LARCA for each JBL core.

Table 8 (page 49): Site information from seventeen HBL-JBL ombrotrophic peat profiles with millennially resolved age-depth models, listed by author.

Table 9 (page 53): Peatland basal ages, basal depths, and 2 ka depths for seventeen review and eight new HBL-JBL cores. Data for apparent rate of C accumulation, and C mass data since inception, and post-2ka, are displayed as well.

Table 10 (page 54): r^2 values for JBL peatland 2 ka apparent rate of C accumulation, 2 ka depths, and HBL-JBL synthesis with MAP, MAAT, GDD_0 and PAR_0. *Refers to significance at the p<0.05. **Refers to significance at p<0.001. ***Refers to significance at p<0.0001. ^{e} Refers to an exponential regression rather than a linear regression.

Table 11 (page 57): ^{14}C-AMS samples, depth, ^{14}C ages, and best fit 'Bacon' model calibration estimates for seventeen from the HBL-JBL area. $^{a.}$Refers to dates that contain ^{14}C from atomic weapons testing. $^{b.}$Refers to outliers that were eliminated by 'Bacon'.

Table 12 (page 58): ^{14}C-AMS samples, depth, ^{14}C ages, and best fit 'Bacon' model calibration estimates for seventeen from the HBL-JBL area. $^{a.}$Refers to dates that contain ^{14}C from atomic weapons testing. $^{b.}$Refers to outliers that were eliminated by 'Bacon'.

Table 13 (page 59): ^{14}C-AMS samples, depth, ^{14}C ages, and best fit 'Bacon' model calibration estimates for seventeen from the HBL-JBL area. $^{a.}$Refers to dates that contain ^{14}C from atomic weapons testing. $^{b.}$Refers to outliers that were eliminated by 'Bacon'.

Table 14 (page 60): ^{14}C-AMS samples, depth, ^{14}C ages, and best fit 'Bacon' model calibration estimates for seventeen from the HBL-JBL area. $^{a.}$Refers to dates that contain ^{14}C from atomic weapons testing. $^{b.}$Refers to outliers that were eliminated by 'Bacon'.

Table 15 (page 79): A list of taxa (Booth, 2008) that were combined in this analysis because of ecological and morphological similarity.

Table 16 (page 80): Transfer function performance statistics for JBL7.

Table 17 (page 83): Zones, dominant taxa, and WTD descriptive statistics for JBL7, listed for each zone.

Table 18 (page 99): Transfer function performance statistics for JBL8, JBL2, and JBL4.

Table 19 (page 102): Zones, dominant taxa, and WTD descriptive statistics for four cores in the James Bay Lowlands, listed for the entire core, and for each zone.

Table 20 (page 109): The results of linear models with WTD as the independent variable and LARCA as the dependent variable for all four cores

Table 22 (page 115): The results of a literature review of reported moisture conditions across various proxies in North America.

Table 23 (page 116): The results of a literature review of reported moisture conditions across various proxies in North America.

ACKNOWLEDGEMENTS

I would like to acknowledge the National Science Foundation for funding this research (NSF-0843685; NSF-0628598). Part of my time at UCLA was also supported by a Ecology and Evolutionary Biology departmental fellowship. All chapters are based off of manuscripts in press or in preparation coauthored with Glen MacDonald. Chapter 2 and Chapter 3 are based on a manuscript coauthored with Angela Gallego-Sala, and a version of it is in press with the Journal of Arctic, Antarctic, and Alpine Research. Chapters 4 and 5 are based on manuscripts in preparation, coauthored with Robert Booth. Dave Beilman contributed to the 2008 fieldwork, and generously allowed me to use his photographs in Chapter 2. Matt Zebrowski generated the black and white maps presented in Chapter 3 and Chapter 5. I would like to acknowledge the efforts of my many hardworking undergraduate research assistants over the past five years: Siduo Zhang, Luis Rodriguez, Jennifer Kim, Karly Wagner, Nicolai Kondov, Scott Guzman, Michelle Lim, Alvin Li, Julianne Lee, Loren Quintanar, and Sam Geldin. I would like to thank Nigel T. Roulet and one anonymous reviewer for their constructive criticisms and suggestions for improving the Journal article which portions of Chapters 2 and 3 are based on. I would finally like to thank the people of the communities of Thunder Bay, Pickle Lake, and Big Trout Lake for their assistance and hospitality.

James R. Holmquist

Curriculum vitae

Education

B.S. Biology, Loyola Marymount University (2008)

Loyola High School, Los Angeles (2004)

Publications

Holmquist, J. H., MacDonald, G. M., Gallego-Sala, A. (In Press). Peatland Initiation, Carbon Accumulation, and 2 ka Depth in the James Bay Lowland and Adjacent Regions. *Journal of Arctic, Antarctic, and Alpine Research.*

Work Experience

- Graduate Researcher and Teaching Assistant: University of California, Los Angeles (2008-2013)
- Teaching Assistant: Loyola Marymount University and Roatán Institute for Marine Sciences (2008)
- Undergraduate Researcher and Teaching Assistant: Loyola Marymount University (2005-2008)
- SCUBA Equipment Specialist: Sport Chalet, Long Beach, CA (2005-2007)

Fellowships, Scholarships, and Awards

- Short Stay Research Fellowship: University of Utrecht (2011)

- Alfred R. Sedoux Prize for Field and Marine Biology: Loyola Marymount University (2008)
- Howard Towner Memorial Scholarship: Loyola Marymount University (2007-2008)
- Reverend Alfred Kilp Memorial Scholarship: Loyola Marymount University (2004-2005)

Presentations

- 4 December 2012: American Geophysical Union
- 23 February 2011: Living with Lakes: Sudbury Restoration Conference, Laurentian University
- 3 March 2011: GEOTOP: 61st Annual Arctic Research Conference, University of Quebec at Montreal
- 18 May 2010: EEB Graduate Research Seminar Series, University of California, Los Angeles
- 15 April 2010: Biology Department Seminar Series, Loyola Marymount University

1. Introduction

The Intergovernmental Panel on Climate Change's 2007 synthesis report contains models predicting global warming driven by anthropogenic greenhouse gasses, however these models contain no consensus on a range of possible carbon (C) cycle feedbacks (IPCC, 2007). Global warming is predicted to disproportionately affect northern latitudes by increasing average annual temperature, increasing the lengths of the growing season, and disrupting patterns of precipitation (IPCC, 2007). In addition to being particularly sensitive to climate change, northern latitudes contain 30% of the world's terrestrial soil C in peatlands, wetlands that form highly organic soil made up of partially decayed, compressed plant matter (Gorham, 1991; Turetsky et al., 2002). Peatlands have served as Holocene C sinks that need to be effectively modeled for general circulation models, and international climate agreements (Roulet, 2000; Waddington et al., 2009; Wania et al., 2009a, 2009b; Carlson et al., 2010; Dunn and Freeman, 2011; Freeman et al., 2012). Peatland systems have potential feedbacks with atmospheric changes in precipitation, temperature, and growing season length and understanding relations between climate and peatland C dynamics is of importance. At the same time, peatlands serve as archives of past climate change and C dynamics and can shed light on the future impacts of climate change (Gorham, 1991; Dise, 2009; Yu, et al., 2009; Chambers et al., 2011; Yu et al., 2011).

Peatlands store 270 to 450 Pg of C (Gorham, 1991), and have had an estimated net global cooling effect of -0.2 to -0.5 W m^{-2} since their initiation, after an early net warming effect of 0.1 W m^{-2} due to CO_2 and CH_4 emissions (Frolking and Roulet, 2007).

Peatlands are dynamic systems that change naturally over time due to site specific, or autogenic, events, but can also be driven by allogenic, or external forcing events such as watershed or climate change (Clymo, 1984; Belyea and Baird, 2006). Peatlands may be subdivided into fens and bogs. Fens, which typically occur in geologically young areas, are dominated by calciphilous vascular vegetation, and tend to have both higher net primary productivity and ecosystem respiration than bogs, which are dominated by mosses (van Breemen, 1995; Pastor, 2002). Fens typically undergo succession when their accumulated depth of organic matter limit access to nutrient-rich ground water, and acidity increases due to accumulated humic acid (van Breemen, 1995; Pastor, 2002). Bogs are commonly dominated by *Sphagnum* and have lower net primary productivity (NPP) and lower ecosystem respiration (ER) relative to fens (Blodau, 2002). They maintain their state by actively acidifying groundwater, and increasing the recalcitrance of peat with lignin-like biochemicals (van Breemen, 1995). *Sphagnum* dominated bogs have lower CH_4 emissions because of the lower activity of methane producing bacteria, as well as CH_4 recycling mediated by symbiotic methanotrophic bacteria (Raghoebarsing et al., 2005). Holocene peatland initiation likely increased atmospheric levels of methane, whereas subsequent succession from fen to bog may have decreased peatland emissions by 150 ppbv between 11 and 4 ka (ka = 1,000 calendar years before present [ybp]); Brook et al., 2000; MacDonald et al., 2006).

Peatlands exist in a climatic envelope constrained by temperature, and moisture (Yu et al., 2009). Relatively short growing season lengths and low rates of plant decay in northern latitudes support high NPP relative to ecosystem respiration ER, causing positive net ecosystem productivity (NEP) and C storage in peat soils (Clymo, 1984; van

Breeman, 1995; Blodau, 2002; Dise, 2009; Yu et al., 2009). High water tables, in poorly drained wetland networks negatively impact ecosystem respiration by causing anoxic conditions. Future changes in temperature, seasonality, and precipitation, could increase, decrease, or reverse this sink by changing the balance between NPP and ER (Gorham, 1991; Clymo et al., 1998; IPCC, 2007; Dise, 2009; Loisel et al., 2012; Yu, 2011; Charman et al., 2013). Increases in temperature and growing season length could increase NPP relative to ER causing an increase in peat formation and a negative feedback to future warming (Clymo et al., 1998; Beilman et al., 2009; Loisel et al., 2012; Charman et al., 2013). Studies on the influence of thermal drivers indicate that the rates of peat formation within the peatland climatic envelope are often constrained by productivity rather than decay. In the West Siberian Lowlands peatland vertical growth over the late-Holocene correlates significantly and positively with modern estimates of mean annual air temperature (Beilman et al., 2009). Other studies indicate that growing season length and photosynthetically active radiation are the dominant drivers of *Sphagnum* productivity (Loisel et al, 2012), and peat accumulation rates over the last 1,000 ybp (Charman et al., 2013). Many studies show that apparent C accumulation increases over the Holocene thermal maximum (HTM), which varies regionally (Kaufman et al., 2004; Yu et al., 2009; Bartlein et al., 2011; Yu et al., 2011). Increases in temperature can also cause the melting of permafrost, which has the contradictory effects of releasing CH_4 into the atmosphere, potentially increasing the release of stored C, and also reactivating CO_2 storage by increasing peat productivity (Beilman et al., 2009; Koven et al., 2011).

Precipitation changes may also have a drastic influence on the direction and magnitude of C cycle feedbacks in peatlands (Yu et al., 2009). C accumulation in bogs can be highly dependent on moisture thresholds of *Sphagnum* species (Strack et al., 2009). Some studies indicate that water table depth (WTD) drawdown can decrease *Sphagnum* productivity (Robroek et al., 2009), and increase peat decay (Fenner and Freeman, 2011). Wetter conditions can cause higher NEP in peatlands because of lower decay rates of submerged peat (Laiho, 2006). However, others studies claim that phenotypic plasticity of *Sphagnum* species increase the recalcitrance of peat under drought conditions (Breeuwer et al., 2008). Hydrological changes can also affect long-term apparent rate of C accumulation (LARCA) by shifting the dominant plant ecology. Ecosystem shifts to woodier vegetation can occur during droughts, raising C accumulation by increasing the density and recalcitrance of peat (Loisel and Garneau, 2010). Thus changes in precipitation and surface moisture can have potentially complex and contradictory effects on peatland soil C accumulation.

There has been progress in modeling Holocene peatland C accumulation, however there are still three major sources of uncertainty (Frolking et al., 2010; Quillet et al., 2013; Tuittila et al., 2013). 1. There is a lack of basic information on peat initiation, peatland succession, peatland C masses, and apparent rates of C accumulation for remote under-researched areas such as the James Bay Lowlands (JBL) of Canada. 2. The effect of climate, especially growing season length and photosynthetically active radiation, on peat productivity adds to the uncertainty of models. 3. Holocene surface moisture records are required to parameterize peatland development models, and are rare in northern latitudes. The JBL and Hudson Bay

Lowlands (HBL) are the second largest continuous peatland complex in the world, and are understudied relative to their importance as a global soil C store (Keddy, 2000; Glaser et al., 2004a; Riley, 2011; Bunbury et al., 2012; O'Reilly, 2012). Therefore the goal of this dissertation was to provide peat initiation, accumulation, and succession data, to test hypotheses regarding climate controls on C accumulation, and to reconstruct Holocene hydrology in the JBL.

In Chapter 2 I provide details on peatland initiation and the lag in peatland initiation following deglaciation and landscape change between 8 and 4 ka, as well as the timing of the transitions from *Carex*-dominated fens to *Sphagnum*-dominated bogs. Data on high-resolution reconstructions of LARCA are also presented. Peat initiation lagged deglaciation and coastal emergence by an average of 2,900 ± s. dev. (±) 1,200 years. Fen to bog succession lagged peat initiation by 3,800 ± 1,400. This average timing, deduced from radiocarbon dated peat cores, is also reflected in modern transition from geologically younger fen dominated coastal areas to geologically older bog dominated inland areas. Although LARCA was highly variable, the four oldest sites had local LARCA maximums at approximately 6.1 ka, possibly indicating the influence of synchronous autogenic processes, or the influence of a regional allogenic climatic event. Close in time, LARCA was not elevated during the warm Medieval Climate Anomaly (MCA = 1000 – 700 ybp) in comparison to the cooler Little Ice Age (LIA = 500 – 200 ybp). Either positive and negative temperature anomalies during the MCA were not sufficient to alter LARCA on a relatively short time scale, or autogenic processes were the dominant drivers of post-1 ka LARCA variability. The establishment of permafrost vegetation during the late-Holocene was coincident with extreme low

LARCA values in two sites, indicating a possible negative control of permafrost on LARCA.

In Chapter 3 I will report data on C accumulation, with a focus on the past 2 ka from eight new sites in the JBL. I will also review available data from previous publications, and modern gridded climate estimates, to test hypotheses regarding the control of four climate variables on vertical peat accumulation over the late-Holocene. Vertical peat accumulation was constrained by productivity rather than decay and the 2 ka year depth of peat correlated significantly and positively with mean annual precipitation, and mean annual air temperature, and had the highest correlation with growing degrees over 0°C (GDD_0) and photosynthetically active radiation integrated over the growing season (PAR_0). Permafrost occurrence produced decreased productivity throughout the mid and late-Holocene. In the study area peat accumulation was likely constrained by productivity rather than decay, and could be positively influenced by increasing temperature, and longer growing seasons due to anticipated future warming.

In Chapter 4, I will present a record of reconstructed WTD from 7.4 ka to present day obtained from a bog in the central JBL. Arctic air masses likely dominated central Ontario from 7.4 to 4.5 ka, causing relatively dry conditions, whereas the moister Pacific Front likely dominated central Ontario from 4.5 to 2.5 ka, causing relatively wet conditions. I also observed dry periods around 6.1 ka coincident with elevated LARCA, and 2.5 ka coincident with neoglacial cooling. I observed a relatively wet MCA, and a relatively dry LIA, which is consistent with other records in surrounding regions, as well and modern precipitation anomalies under La Niña and El Niño conditions respectively.

I also compared fluctuations in WTD to previously published macrofossil reconstructions to investigate an unusual succession event. At approximately 4.5 ka the site exhibited a shift in ecology from a *Sphagnum* dominated bog to an herbaceous dominated fen that was associated with an extreme wet period. The inundation of a *Sphagnum* peatland by calcium rich water could have given a competitive advantage to calciphilous fen vegetation. Although a 6.1 ka spike in LARCA was associated with a drought, there was a low but positive correlation between surface moisture and LARCA over the whole 7.4 ka record, indicating a possible complex relationship between peat productivity, decay rates, and hydrologically extreme conditions.

In Chapter 5 I will present a comparative study of high-resolution records of surface moisture, focusing on the MCA, LIA, and modern warming, for four sites in the JBL. The MCA and LIA were relatively wet and dry, respectively, for the three most southern sites. This conclusion is consistent with modeled and observed variation in La Niña and El Niño related precipitation patterns reflecting to changes in the planetary wave and westerly storm track. The northern-most site displayed the opposite trend with a dry MCA and wet LIA, possibly due to the spatial limit of positivity precipitation anomalies, or the effect permafrost on surface water pooling or draining. Despite the differing latitudinal pattern of medieval wetness/dryness accompanying warming, all four sites provide evidence modern drying. Despite the hydroclimatic sensitivity of the region, no distinct relationship was observed between variations in WTD over the MCA, LIA and recent warming with LARCA.

The JBL are an important and previously understudied region. This dissertation reinforces their importance as a Holocene C sink. Although future C cycle fluxes are

highly uncertain, the positive relationship between growing season and peat productivity, as well as the consistent positive precipitation anomalies under large-scale droughts, indicate that the JBL may act as a positive feedback to warming, if they remain within the climatic envelope for northern peatlands. However the climatic envelop of peatlands is poorly understood, and future precipitation anomalies are likely to be dependent on incompletely understood and yet un-modeled interactions between the atmosphere and sea surface temperatures. Additional work should be done to collect and analyze data from more cores in the JBL, to assess the robustness of the results presented here and refine the geographic boundaries of the greater moisture seen at southern regions during the MCA. More broadly, future studies are needed to replicate this work in other under-studied regions, to investigate the effects of peatland community composition, temperature, and hydrology on CH_4 emissions, and to integrate climate drivers of productivity, such as growing season length, into peatland development models.

2. Peatland Initiation, Succession, and Long Term Apparent Carbon Accumulation in the James Bay Lowlands

2.1 ABSTRACT

Basic knowledge of post-glacial peatland history, and carbon (C) accumulation are lacking for the Canadian James Bay Lowlands (JBL), despite their importance as a terrestrial C-store. This chapter utilizes radiocarbon (^{14}C) dates, plant macrofossil analysis, and soil C estimates from an eight core transect of the JBL to document the timings of peat initiation, fen to bog transitions, peatland C storage, and the ranges of long term apparent rate of C accumulation (LARCA). Peatland initiation lagged the retreat of the Laurentide ice sheet, the drainage of glacial lakes, and isostatic uplift by 2,900 ± s. dev. (±) 1,200 years. Transition from *Carex*-dominated fen to *Sphagnum*-dominated bog had an average timing of 3,800 ± 1,400 years following peatland establishment. JBL peatlands currently store between 71.5 and 171.2 kgC m^{-2}, and median LARCA ranged from 13.8 to 31.6 gC m^{-2} yr^{-1}. The four oldest sites had local LARCA maximums at approximately 6.1 ka, possibly indicating the control of synchronous autogenic processes, or the influence of a yet undocumented allogenic event. LARCA was not elevated during the warm Medieval Climate Anomaly (MCA) compared to the cooler Little Ice Age (LIA), despite a 2 - 4°C difference. However, there was indication that the establishment of modern permafrost during the late-Holocene negatively affected C accumulation.

2.2 INTRODUCTION

At present northern peatlands store 270 to 450 Pg of carbon (C; Gorham, 1991), making them a significant terrestrial C sink. Due to C storage, peatlands are estimated to have had a net global cooling effect of -0.2 to -0.5 W m^{-2} since their initiation, after an initial net warming effect of approximately 0.1 W m^{-2} due to CO_2 and CH_4 emissions (Frolking and Roulet, 2007). The timings of peatland initiation and succession have been used to build models of peat accumulation (Clymo, 1998; Frolking et al., 2001), and identify peatlands as a Holocene source of CH_4 (MacDonald et al., 2006). Reconstructions of past surface ecology, and long-term apparent rate of C accumulation (LARCA) can be used to investigate regional post-glacial history (Klinger and Short, 1996; Glaser et al., 2004a), to quantify patterns in C accumulation (Beilman et al., 2009; Loisel and Garneau, 2010), and to determine the possible effects of allogenic controls on LARCA (Bridgham et al., 2006; Beilman et al., 2009). Although information on peatland initiation, succession, and C storage is valuable, it is not yet available for many remote and understudied regions in the north.

The James Bay Lowlands (JBL) of Ontario are part of the second largest peatland complex in the world and contain some of the most remote and concentrated peatlands in the world (Riley, 2011). They occupy poorly drained land left in the depression produced by the Laurentide ice sheet (Dyke et al., 2003; Riley, 2011). The JBL remained largely covered by the ice sheet and glacial lakes Agassiz and Ojibway until the first land emergence around 9 ka (ka = 1,000 calendar years before present [ybp]; Dyke et al., 2003). Many peatlands in the southern lowlands formed after the

catastrophic drainage of the glacial lakes Agassiz and Ojibway due to the breaking of the Laurentide ice dam at 8.4 ka (Lajeunesse and St-Onge, 2008). The rest of the land became available for peatlands gradually due to the isostatic rebound of the crust underlying the Sea of Tyrell, which changed into the present day Hudson and James Bays. Although rates of land emergence were variable due to the interaction between isostatic sea level retreat, and normal cycles in eustatic sea level change, rates of land emergence were generally higher from 8.2 – 6 ka. This pattern of isostatic sea level retreat, periodic eustatic sea level changes, and cycles of storm strength were responsible for the north to south moraines mapped along the former coastline of the sea of Tyrell in the Hudson Bay Lowlands (HBL)-JBL (Hillaire-Marcel and Fairbridge, 1978). The HBL-JBL has some of the fastest rates of isostatic uplift globally with some areas raising an average of 1.2 m century^{-1} (Webber et al., 1970). A review of Laurentide deglaciation and peatland initiation in North America estimated that there is typically a 4,000-year lag between deglaciation and peatland initiation (Halsey et al., 2000; Gorham et al., 2007).

The timings of peatland community ecological changes, notably fen to bog transitions, are important to C cycle feedbacks, but have not been reported or synthesized for the JBL. Fen peat tends to initiate in down-slope areas of a watershed (Bauer et al., 2003). Overland and groundwater eventually become less accessible to surface plants as peat accumulates. Humic acids buildup and cations are leached as the peat conductivity decreases, and water input shifts to precipitation dominated. *Sphagnum* colonizes and builds bogs, engineering its own habitat by further acidifying water and insulating vascular plant roots (van Breemen, 1995; Pastor, 2002). These

transitions are apparent in the patterning of fen dominance around the Western coast of the James Bay on relatively recently emergent land, and bog dominance further inland on older surfaces (Klinger and Short, 1996; Glaser et al., 2004b; Tarnocai et al., 2011; Riley, 2011). Studies show that young fens tend to be higher emitters of CH_4, and CH_4 emission declines following succession to bogs (Roulet et al., 1994; Martikainen et al., 1995; Raghoebarsing et al., 2005; Frolking and Roulet, 2007).

On average, peatlands contain 130 kg C m^{-2} (Gorham, 1991), and as high as 180 kg C m^{-2} (Sheng et al., 2004). Previous studies indicate that LARCA is highly variable and dependent on local conditions, autogenic process, and climate, but high values are often associated with positive temperature and seasonality anomalies. High LARCA values have been linked to increased productivity during the Holocene thermal maximum (HTM) in Alaskan (11.0 – 9.0 ka; Yu et al., 2011), and eastern Canadian peatlands (5.0–3.0 ka; Yu et al., 2009). More recently, the shorter duration Medieval Climate Anomaly (MCA; 1000 – 700 ybp) and the Little Ice Age (LIA; 500 – 200 ybp) occurred during the late-Holocene (Lamb, 1965; Broecker, 2001; Viau et al., 2002; Moberg et al., 2005; Mann et al., 2009; Ljungqvist et al., 2010; Graham et al., 2011) and likely had a change of 2°C and -2°C (Christiansen and Ljungqvist, 2011). Studies in the JBL indicate that a brief increase in LARCA was associated with a wet and warm MCA (Bunbury et al., 2012). A global synthesis of peatland age-depth models show that modeled C accumulation increased during the MCA due to increases in growing season length and photosynthetically active radiation (Charman et al., 2013). Studies also cite permafrost occurrence as having a negative effect on LARCA (Beilman et al., 2009).

Based on the current lack of information of the specific history of peatland history in the JBL and current knowledge regarding climate-LARCA relations over the Holocene, I examine five research questions in this chapter. 1. What were the timings of, and spatial patterns of peat initiations, and fen to bog transitions? 2. How much C has accumulated over the Holocene? 3. What were the magnitudes and variability of LARCA in the JBL? 4. Do LARCA increases coincide with positive temperature and seasonality anomalies during mid-Holocene, or during the MCA? 5. Was there any influence of permafrost on LARCA?

2.3 MATERIALS AND METHODS

2.3.1. Field Sites and Previously Published Sites

The Ontario JBL, in which the study sites are located (Fig. 1), covers 221,000 km^2. Of the total wetlands present there some 35% are bogs mainly dominated by *Sphagnum* (Riley, 2005, 2011). The HBL-JBL contain *Picea mariana* dominated forests in the south (Fig. 2) and mixed *P. mariana* and *Larix larcina* forests in the north (Riley, 2005, 2011). These are interspersed with unforested bog and fen complexes dominated by *Sphagnum* mosses and *Carex* spp. respectively (Fig. 2). Northern permafrost bogs have drier surfaces and are often typified by a surface cover of *Cladonia*. The HBL-JBL formed following the retreat of the Laurentide ice sheet commencing at approximately 10 ka.

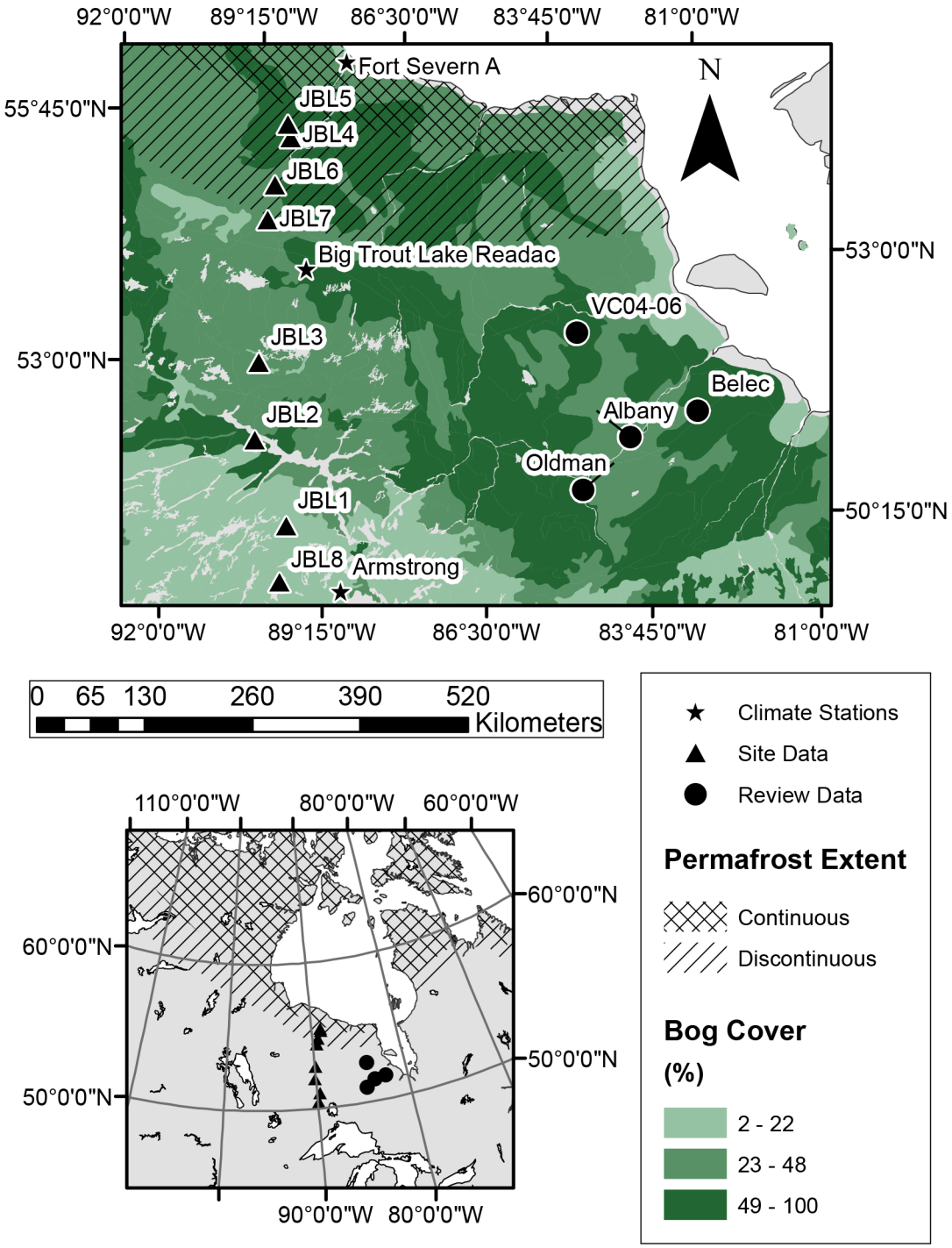

Figure 1: My study sites were located in the JBL, and were supplemented by a review of four additional reports of basal dates and timings of fen to bog transitions. Pictured are also maps of peatland extent (Tarnocai et al., 2011), and the borders of discontinuous and continuous permafrost zones (Brown et al., 1998).

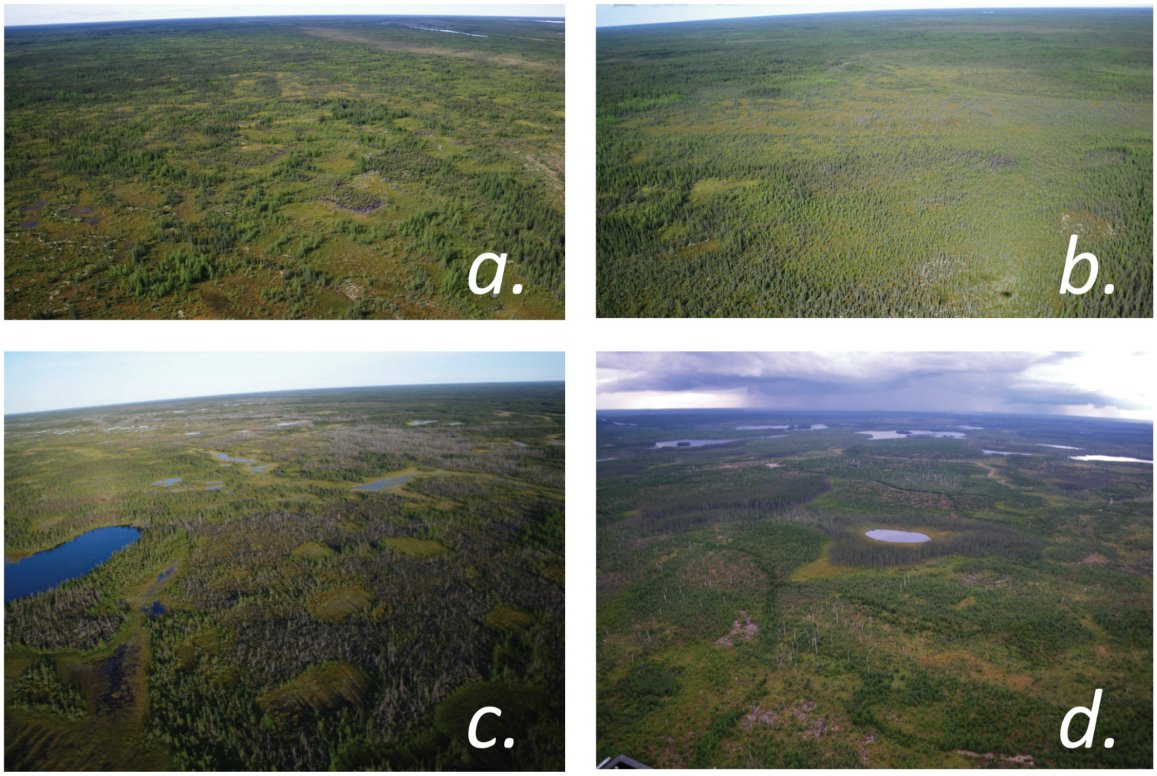

Figure 2: A. - D. Landscapes that are representative of the surface cover in the JBL including: *Picea mariana* dominated stands, uncovered *Sphagnum* bogs, minerotrophic thin fens, and open water. Photos are courtesy of David Beilmen, and are used with permission (Beilman, Personal Communication).

Permafrost occurs in the northern and costal HBL-JBL, dominates the landscape in the north within ~80 km of the coast, and occurs along the coast in the south within a slimming margin of approximately 20 to 40 km wide (Fig. 1; Zoltai and Tarnocai, 1975; Riley, 2005). Along the coast, continuous permafrost, and subarctic vegetation can be found anywhere where soil temperatures remain below 0°C annually, and permafrost discontinuously south of this isotherm due to the efficient insulating qualities of peat soils (Riley, 2005).

The JBL of central and northern Ontario are accessible almost exclusively by helicopter, boat, and winter ice road, and remain both sparsely populated and understudied. Some peatland basal dates and paleoecological information are

available from studies focused near the Albany River (Glaser et al., 2004a), Churchill Rail Line (Dredge and Mott, 2003), and Victor Mine (O'Reilly, 2011; Bunbury et al., 2012). Eight bog cores were collected from eight sites by helicopter during the summer of 2008 (Fig. 1; Tab. 1). The sites form a latitudinal transect from 50˚27' N to 55˚24' N. All cores were collected from raised, ombrotrophic peat landforms. MAP and MAAT data from three climate stations within the approximate range of the sites are included in Table 2 (Fig. 1; Environment Canada, 2013). In 2008 these climate stations were within the peatlands' temperature-precipitation space described in Yu et al. (2009), ranging from -4.88 to 3.03°C, and 607.8 to 683.5 mm (Tab. 2).

Table 1: Site information for eight new JBL sites collected in the summer of 2008, and four review sites.

Core	Source	Coordinates (d m s)	Elevation (m)	Peatland Type
JBL1	-	51°03'53" N, 89°47'34" W	371	*Sphagnum* bog
JBL2	-	52°01'07" N, 90°07'53" W	362	*Sphagnum* bog
JBL3	-	52°51'37" N, 89°55'46" W	270	*Sphagnum* bog
JBL4	-	55°16'09" N, 88°55'50" W	108	*Sphagnum* bog
JBL5	-	55°24'55" N, 88°57'06" W	143	Permafrost plateau
JBL6	-	54°46'21" N, 89°19'10" W	140	Permafrost bog
JBL7	-	54°23'43" N, 89°31'20" W	150	*Sphagnum* bog
JBL8	-	50°27'33" N, 89°55'42" W	407	*Sphagnum* bog
Albany	Glaser et al., 2004a	51°26' N, 83°37' W	82	*Sphagnum* bog
Belec	Glaser et al., 2004a	51°37' N, 82°17' W	64	*Sphagnum* bog
Oldman	Glaser et al., 2004a	51°01' N, 84°34' W	101	*Sphagnum* bog
VC04-06	Bunbury et al., 2012	52°42'36" N, 84°10'48" W	105	*Sphagnum* bog

Table 2: 2008 climate data from 3 stations in the JBL.

Climate Station (DMS)	Total Precipiation (mm)	MAAT (°C)
Fort Severn A (56°01'12"N, 87°40'48"W)	NA	-4.88
Big Trout Lake Readac (53°49'12"N, 89°54'00"W)	683.5	-3.13
Armstrong (50°17'24"N, 88°54'36"W)	608.7	3.03

Six cores - JBL1, JBL2, JBL3, JBL4, JBL7, JBL8 - were from *Sphagnum fuscum* dominated hummock surfaces and were permafrost free (Tab. 1). These hummocks existed in complexes with *S. angustifolium* hollows and intermediate *S. magellanicum* sections. Notable vascular species include tree species: *Picea mariana*, *Larix larcina*, shrubs species: *Chamaedaphne* spp., *Vaccinium* spp., *Salix* spp., *Betula* spp., *Eriophorum* spp., as well as *Carex* spp. and *Equisetum* spp. in hollows. JBL2 and JBL3 existed as bog islands in larger poor-fen complexes. JBL4 was from the discontinuous permafrost zone and contained examples of boreal vegetation as well as subarctic *Cladonia* spp. on higher microsites. Two cores, JBL5 and JBL6, were from permafrost sites with *Cladonia* dominated surfaces underlain by *Sphagnum*-dominated peat. JBL5 was a degraded permafrost plateau with large cracks filled with melt-water. JBL5's surface cover was predominantly *Cladonia* spp., *Ledum* spp., and unvegetated surfaces of decayed peat. In addition to these original sites, I also included for comparative analysis four other sites selected after a review of well-dated peat bog macrofossil records in the JBL region (Glaser et al., 2004a; Bunbury et al., 2012).

I sampled the first 0.8 to 1m of each core with a box corer, and subsequent depths with a Russian auger for non-permafrost peatlands or a motorized SIPRE drill for

permafrost. Seven of the cores contained complete profiles from the surface to the mineral/peat interface. I recovered JBL6 without the basal section, and therefore omitted it from basal date, and total C accumulation datasets. I wrapped cores in plastic-wrap and aluminum foil while in the field, and placed them in a freezer on their arrival at the University of California, Los Angeles. I subsampled all core, while they were frozen, into 1 cm increments on a bandsaw.

2.3.2. Age Depth Modeling

I established chronologies for the JBL cores were established using multiple radiocarbon (^{14}C) dates (Fig. 3; Tab. 3 - 5). My goal was to select dates in order to have approximately millennially resolved chronologies pre-1 ka, and bicentennially resolved chronologies post-1 ka. I separated plant based macrofossils from peat with distilled H_2O and removed fungal hyphae and plant rootlettes using forceps, under a dissecting microscope. I used bulk-peat when no single macrofossils were identified. I pretreated samples using acid-base-acid treatments at 65°C to remove carbonates, humic acids, and dissolved organic C (Olsson, 1986). I vacuum-sealed samples in quartz tubes with CuO powder and Ag wire and combusted them for 4 hours at 900°C. Samples were graphitized, and atomized in an accelerator mass spectrometer at the University of California, Irvine's Keck Laboratory. The ratio of ^{14}C to ^{12}C was calculated

relative to blank and standards from dendrochronologically dated wood.

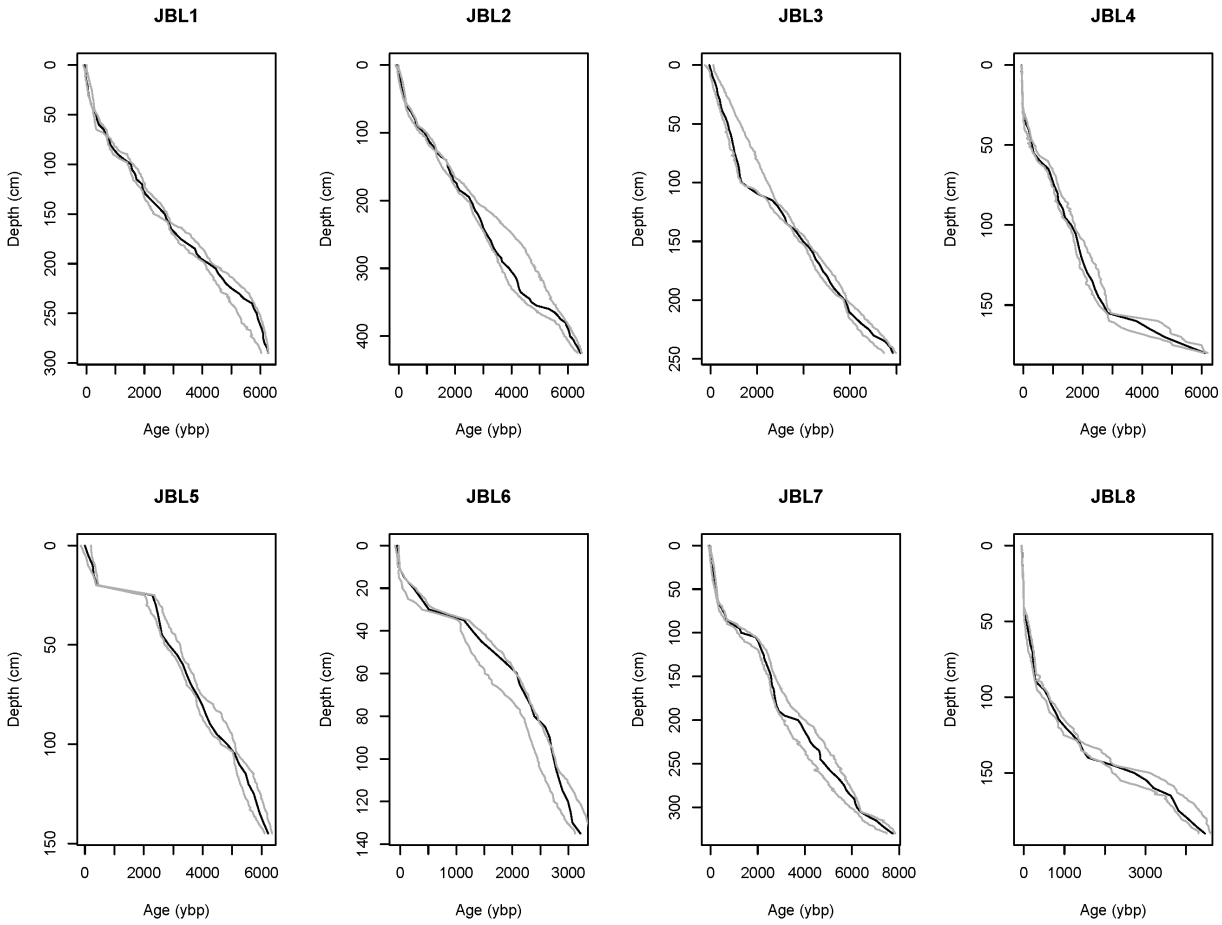

Figure 3: Age-depth models from eight sites in the JBL area. Grey lines refer to minimum and maximum measurements, black lines refers to best estimates from Bacon age-depth modeling software.

I used calibrated multiple ^{14}C dates (Fig. 3; Tab. 3 – 5) and created age-depth model for each core using 'Bacon', a flexible Bayesian age-depth modeling software (Blaauw and Christen, 2011) written in R (R core development team, 2012). For calibration purposes, I used INTCAL09 (Reimer et al., 2009), and NH1 for post-bomb dates (Hua and Barbetti, 2004). I assumed a date of -58 BP for the surface of each new JBL core except for JBL5, which had surface peat that dated pre-modern (15 ^{14}C age; Fig. 3; Tab. 4).

Table 3: ^{14}C-AMS samples, depth, ^{14}C ages, and best fit 'Bacon' model calibration estimates for new eight southwest JBL cores. [a.] Refers to dates that contain ^{14}C from atomic weapons testing. [b.] Refers to outliers that were eliminated by 'Bacon'.

Core	Depth (cm)	Lab I.D. #	Material	^{14}C age	±	Age Range (ybp)	Best Fit (ybp)	
JBL1	44-45	UCI AMS 107067	*Sphagnum* stems	110	20	219-274	228	
JBL1	57-58	UCI AMS 90508	Cyperaceae leaf	225	30	288-248	402	
JBL1	70-71	UCI AMS 107068	Moss stem	795	20	664-739	694	
JBL1	83-84	UCI AMS 93975	Cyperaceae stems and rhizome	970	30	805-1055	918	
JBL1	96-97	UCI AMS 115836	Cyperaceae leaves	1565	20	1320-1515	1394	
JBL1	123-124	UCI AMS 91703	Cyperaceae fragment	1985	20	1869-2029	1938	
JBL1	155-156	UCI AMS 90509	Wood	2680	15	2690-2875	2782	
JBL1	195-196	UCI AMS 91704	Cyperaceae fragments	3745	20	3916-4251	4006	
JBL1	239-240	UCI AMS 91705	Amblystegiaceae stems	4960	25	4978-5793	5713	
JBL1	285-286	UCI AMS 67693	Bulk peat	5265	15	5982-6262	6242	
JBL1	285-286	UCI AMS 96178	Amblystegiaceae stems	5195	35	5982-6262	6242	
JBL2	55-56	UCI AMS 90510	*Sphagnum* stems	75	15	229-264	239	
JBL2	71-72	UCI AMS 91706	*Sphagnum* stems	375	20	355-555	512	
JBL2	87-88	UCI AMS 90511	Cyperaceae leaf	625	15	564-664	641	
JBL2	103-104	UCI AMS 91707	*Sphagnum* stems	1065	30	863-1043	950	
JBL2	125-126	UCI AMS 76592	Bulk peat	1390	15	1266-1346	1341	
JBL2	162-163	UCI AMS 97814	Cyperaceae leaves	1915	25	1779-1959	1879	
JBL2	200-201	UCI AMS 67694	Bulk peat	2530	20	2473-2753	2562	
JBL2	267-268	UCI AMS 96179	Cyperaceae leaves	3915	20	3263-4408	4408	
JBL2	324-325	UCI AMS 76591	Bulk peat	3285	20	3933-5173	4237	b.
JBL2	335-336	UCI AMS 93976	Amblystegiaceae stems	3845	30	4156-5311	4349	
JBL2	375-376	UCI AMS 91708	Amblystegiaceae stems	5030	50	5437-5897	5771	
JBL2	420-421	UCI AMS 93977	Amblystegiaceae	5900	180	6247-6462	6395	
JBL2	421-422	UCI AMS 67695	Bulk peat	5560	20	6265-6460	6407	
JBL3	83-84	UCI AMS 90512	*Sphagnum* fronds	-625	15	1076-2096	1175	a.,b.
JBL3	95-96	UCI AMS 93978	Cyperaceae leaf, Ericaceous leaf	1290	20	1212-2347	1275	
JBL3	111-112	UCI AMS 93979	Cyperaceae leaves	2415	20	2272-2722	2294	
JBL3	135-136	UCI AMS 97815	Cyperaceae leaves	3240	20	3319-3579	3334	
JBL3	151-152	UCI AMS 76593	Bulk peat	3760	15	3963-4213	4079	
JBL3	173-174	UCI AMS 97816	Equisetum fragments	2020	80	4514-5104	4795	b.
JBL3	195-196	UCI AMS 91709	Wood fragments	4920	25	5426-5806	5583	
JBL3	211-212	UCI AMS 90513	Needle fragments	4380	70	5915-6475	6066	b.
JBL3	244-245	UCI AMS 93980	*Sphagnum* fronds	6930	60	7457-7977	7835	
JBL3	244-245	UCI AMS 67696	Bulk peat	7145	45	7457-7977	7835	

I preferred 'Bacon' to linear interpolation between dates because the latter can be too restrictive if cores are longer than 1 m, and do not have high resolution dating (Blaauw and Heegaard, 2012). 'Bacon' deals with outliers in a standardized way using

a robust Student's T method (Christen and Pérez, 2009). Bayesian algorithms require priors. I used the program's default settings for the priors: shape (2), memory strength (4), and memory mean (0.7). For the accumulation rate prior I used a default value of 20 yr cm^{-1}, and used 50 yr cm^{-1} if the default did not produce a parsimonious age-depth model. Only JBL7 required a different accumulation prior of 40 yr cm^{-1}.

Table 4: ^{14}C-AMS samples, depth, ^{14}C ages, and best fit 'Bacon' model calibration estimates for new eight southwest JBL cores. [a.]Refers to dates that contain ^{14}C from atomic weapons testing. [b.]Refers to outliers that were eliminated by 'Bacon'.

Core	Depth (cm)	Lab I.D. #	Material	^{14}C age	±	Age Range (ybp)	Best Fit (ybp)	
JBL4	25-26	UCI AMS 76594	Bulk peat	-2175	15	-31--11	-12	a.
JBL4	36-37	UCI AMS 107070	*Sphagnum* stems	130	20	29-144	95	
JBL4	45-46	UCI AMS 107071	*Sphagnum* stems	85	20	122-267	253	
JBL4	54-55	UCI AMS 107072	*Sphagnum* stems	340	20	326-481	346	
JBL4	64-65	UCI AMS 107073	*Sphagnum* stems	1030	20	740-985	848	
JBL4	75-76	UCI AMS 76595	Bulk peat	1150	15	975-1180	1054	
JBL4	100-101	UCI AMS 76596	Bulk peat	1750	15	1533-1733	1641	
JBL4	150-151	UCI AMS 76597	Bulk peat	2610	15	2589-2824	2731	
JBL4	167-168	UCI AMS 96180	*Picea* Needle	4325	45	3965-4985	4563	
JBL4	175-176	UCI AMS 67697	Bulk peat	5245	20	5251-6021	5569	
JBL4	175-176	UCI AMS 94022	Moss fronds	5450	110	5251-6021	5569	
JBL5	0-1	UCI AMS 90522	*Betula* leaf	15	15	-146-204	-5	
JBL5	7-8	UCI AMS 107074	Lichen frags	115	20	75-280	204	
JBL5	11-12	UCI AMS 107075	Bulk peat	-140	20	179-364	277	a.,b.
JBL5	15-16	UCI AMS 76598	Bulk peat	300	15	308-423	321	
JBL5	19-20	UCI AMS 107076	*Sphagnum* stems	360	20	374-459	414	
JBL5	25-26	UCI AMS 107077	*Sphagnum* stems	2200	20	2064-2379	2315	
JBL5	26-37	UCI AMS 96181	*Sphagnum* stems	2400	25	2398-2738	2513	
JBL5	55-56	UCI AMS 93981	Herbaceous fragment	2965	20	3055-3315	3170	
JBL5	72-73	UCI AMS 67698	Bulk peat	3420	15	3636-3886	3722	
JBL5	100-101	UCI AMS 76599	Bulk peat	4350	15	4733-5108	4885	
JBL5	140-141	UCI AMS 67699	Bulk peat	5320	20	5949-6294	6108	
JBL5	140-141	UCI AMS 93982	Cyperaceae leaves, Spruce needle fragments, Moss stems	5170	25	5949-6294	6108	

Table 5: ^{14}C-AMS samples, depth, ^{14}C ages, and best fit 'Bacon' model calibration estimates for new eight southwest JBL cores. [a.]Refers to dates that contain ^{14}C from atomic weapons testing. [b.]Refers to outliers that were eliminated by 'Bacon'.

Core	Depth (cm)	Lab I.D. #	Material	^{14}C age	±	Age Range (ybp)	Best Fit (ybp)	
JBL6	10-11	UCI AMS 90514	Coniferous needles	-1020	15	-46--11	-23	a.
JBL6	15-16	UCI AMS 107078	Lichen fragments	125	20	-2-103	73	
JBL6	19-20	UCI AMS 107079	Bulk peat	-90	20	36-226	206	a.,b.
JBL6	27-28	UCI AMS 107080	Bulk peat	360	20	281-481	430	
JBL6	33-34	UCI AMS 90515	*Sphagnum* stems	1165	15	806-966	886	
JBL6	75-76	UCI AMS 67700	Bulk peat	2195	20	2055-2355	2331	
JBL6	100-101	UCI AMS 76600	Bulk peat	2440	15	2448-2773	2520	
JBL6	134-135	UCI AMS 67701	Bulk peat	3025	20	3110-3405	3187	
JBL7	51-52	UCI AMS 76601	Bulk peat	125	15	196-266	225	
JBL7	61-62	UCI AMS 93983	*Sphagnum* stems	190	15	268-303	283	
JBL7	71-72	UCI AMS 93984	*Sphagnum* stems	375	20	340-505	468	
JBL7	82-83	UCI AMS 93985	*Sphagnum* stems	645	20	559-669	656	
JBL7	92-93	UCI AMS 93986	*Sphagnum* stems	1205	30	955-1195	1103	
JBL7	121-122	UCI AMS 97817	*Sphagnum* stems	2310	15	2027-2387	2198	
JBL7	150-151	UCI AMS 67702	Bulk peat	2505	15	2471-2741	2569	b.
JBL7	177-178	UCI AMS 96182	Cyperaceae leaves and rhizome	2540	25	2692-3267	2755	
JBL7	205-206	UCI AMS 93987	*Sphagnum* stems	5190	25	3181-4251	3859	
JBL7	300-301	UCI AMS 67703	Bulk peat	5365	15	5994-6339	6241	
JBL7	327-328	UCI AMS 91710	*Sphagnum* stems	6840	25	7340-7790	7627	
JBL7	327-328	UCI AMS 93988	Bulk peat	6910	30	7340-7790	7627	
JBL7	329-330	UCI AMS 90516	Wood	3860	15	7487-7847	7731	
JBL8	25-26	UCI AMS 76602	Bulk peat	-1215	15	-11--6	-8	a.
JBL8	37-38	UCI AMS 90517	Salix leaf	-535	15	-7--7	-6	a.
JBL8	77-76	UCI AMS 91711	*Sphagnum* fronds	115	20	171-266	228	
JBL8	87-88	UCI AMS 90518	*Sphagnum* stems	210	15	259-374	280	
JBL8	99-100	UCI AMS 90519	*Sphagnum* stems	565	15	451-631	603	
JBL8	111-112	UCI AMS 91712	Coniferous needle fragments	950	40	713-913	814	
JBL8	125-126	UCI AMS 76603	Bulk peat	1385	15	1074-1334	1241	
JBL8	140-141	UCI AMS 91713	*Sphagnum* fronds	2075	20	1748-2143	1710	
JBL8	159-160	UCI AMS 94023	Cyperaceae leaves	3380	60	2983-3723	3205	
JBL8	186-187	UCI AMS 96183	Cyperaceae leaves	1840	70	4208-4568	4337	b.
JBL8	188-189	UCI AMS 67704	Bulk peat	4025	15	4319-4594	4428	

2.3.3. GIS Data

I mapped deglaciation patterns using shapefiles developed by Dyke et al., (2003). However I had to convert the ages of the layers from ^{14}C ages to calendar years before present using INTCAL09 (Reimer et al., 2009). I used linear interpolation between shapefiles to estimate the timing of land emergence.

2.3.4. Macrofossil Analysis

I used semi-quantitative analysis to describe the macrofossil abundances in the cores at 4 cm increments. I assigned ordinal values to major macrofossil categories, *Sphagnum*, herbaceous peat including, non-*Sphagnum* mosses, and *Carex*, and wood, based on their relative dominance in each sample (Barber, 1981; Lévesque, 1988). I also recorded lichen and rootlette dominated peat as a separate category since it was abundant in the active layers of two permafrost cores, but is ecologically distinct from fen-based herbaceous peat (Kuhry and Turunen, 2006; Kuhry, 2008). Although quantitative macrofossil analyses are preferable for performing high resolution and sensitive paleoecological reconstructions, or applying transfer functions for paleoclimatological applications, an ordinal approach is adequate for identifying major changes in past community ecology (Mauquoy et al., 2010).

2.3.5. Soil C Estimates

I estimated percentage C for every 1 cm increment as the product of dry bulk density (BD), loss on ignition at 550°C (LOI_{550}), and a %C assumption of 0.5 gC 1 g Organic

Matter (OM)$^{-1}$ (Turunen et al., 2002). I took samples for BD and LOI_{550} from subsampled cores with a stainless steel tube with a 1 cm diameter and measured subsamples lengthwise with digital calipers to calculate volume. I measured dry BD by dividing the dry weight by the sample volume after drying to a constant mass at 105°C. LOI_{550} was calculated as the mass lost after one hour ignition in a muffle furnace at 550°C (Sheng et al., 2004). LARCA was calculated as the mass of organic C divided by the rate of change in the age depth model at a 1 cm resolution (Eq. 1).

Equation 1: $$LARCA = \frac{BD \times LOI_{550} \times 0.5gC}{yr}$$

2.4 RESULTS

2.4.1. Peatland initiation and succession in the JBL

In the JBL cores, peat initiation had an average timing of 5,900 ± 1,200 years, and lagging the retreat of the Laurentide ice sheet, and the drainage of glacial lakes Agassiz and Ojibway at 8.2 ka (Fig. 3 - 10; Fig. 11). Paleo-land surface maps indicated that deglaciation and peak land emergence in the study area took place from 11.3 ka in the south to 6.6 ka in the north following isostatic rebound of land emerging from the sea of Tyrell (Tab. 6). Four sites (JBL4, JBL5, JBL6, JBL7) formed following the catastrophic drainage of Lake Agassiz. In the three most southern sites, there were longer periods between deglaciation and peat initiation, 4,000 – 6,000 years.

In all eight sites, I observed fen to bog transitions in the core stratigraphies (Fig. 4 - 11; Fig. 12; Tab. 6). Only in one case, JBL7, did I observe a potentially complex and rare mode of succession with *Sphagnum* dominated conditions initiating, followed by a transition herbaceous conditions, and a return to *Sphagnum* dominance near the surface. JBL1, JBL2, JBL3, JBL4, and JBL8 initiated as herbaceous dominated systems, and transitioned to *Sphagnum* dominated systems. All eight cores had brief to extensive sections where wood was dominant, or co-dominant with herbaceous or *Sphagnum* peat. JBL1, JBL2, JBL3, and JBL5 indicated a relatively quick transition from shrub cover and herbaceous fen to *Sphagnum* peatland, while JBL4, JBL6, JBL7, JBL8 had longer transitional periods during which *Sphagnum* and herbaceous peat were co-dominant. Of the two permafrost cores, JBL5 followed the fen to bog succession, and both cores had rootlette, lichen, and wood, dominated active layers overlaying *Sphagnum* dominated permafrost peat.

The results from these original sites were combined with the previously published results from the four additional sites (Tab. 1). Average land emergence time was 8.9 ± 1.4 ka, average peat initiation date was 6.0 ± 1.2 ka, lagging land emergence by 2,900 years. Average succession times for the entire data set was 3,800 ± 2,800 years following peatland initiation (Fig. 12; Tab. 6). Of the four most southern sites in the JBL transect, three had extended fen periods (91 – 97%).

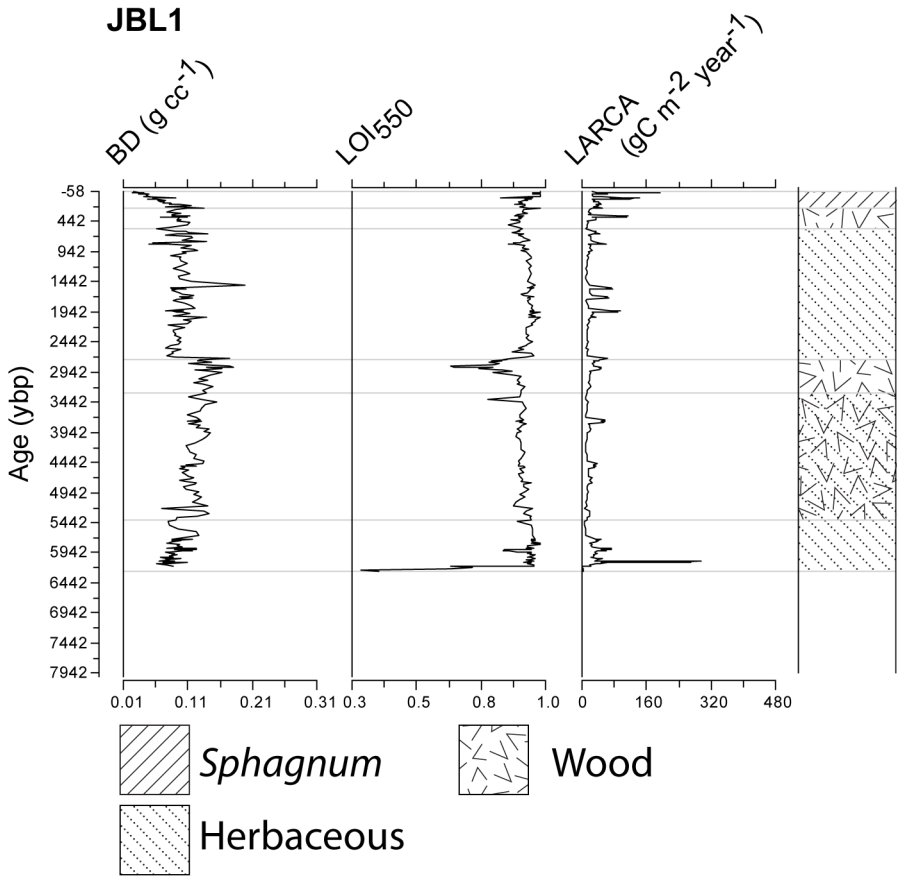

Figure 4: JBL1 BD, LOI_{550}, LARCA, and qualitative macrofossil zones plotted against time.

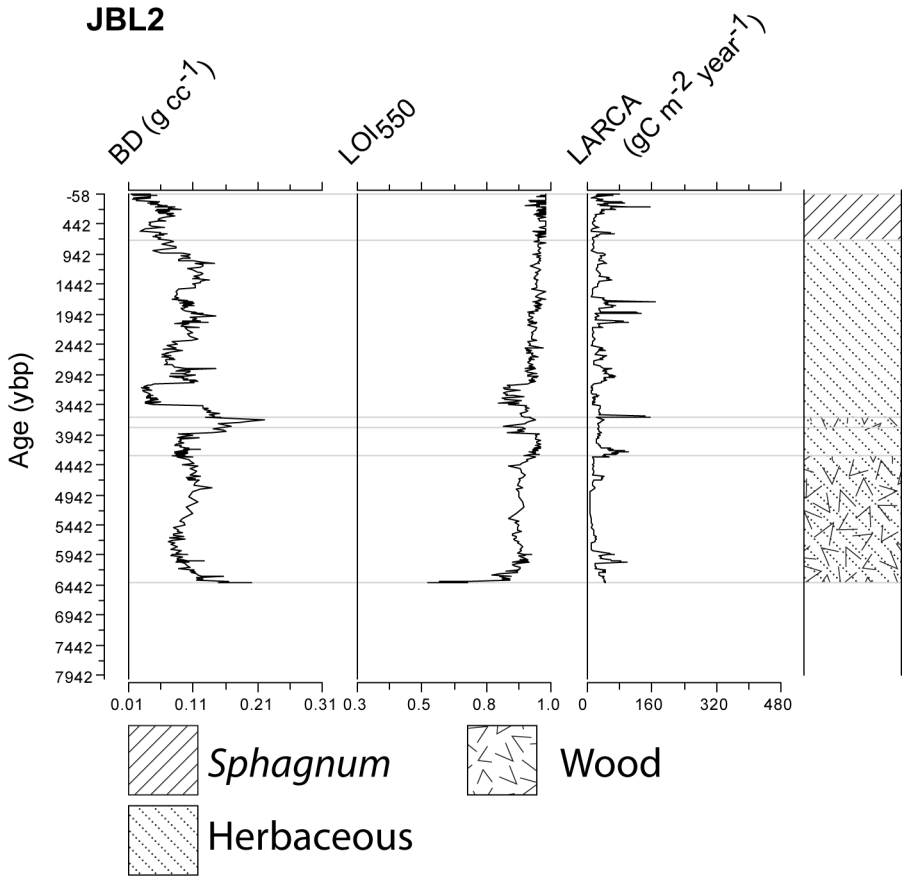

Figure 5: JBL2 BD, LOI_{550}, LARCA, and qualitative macrofossil zones plotted against time.

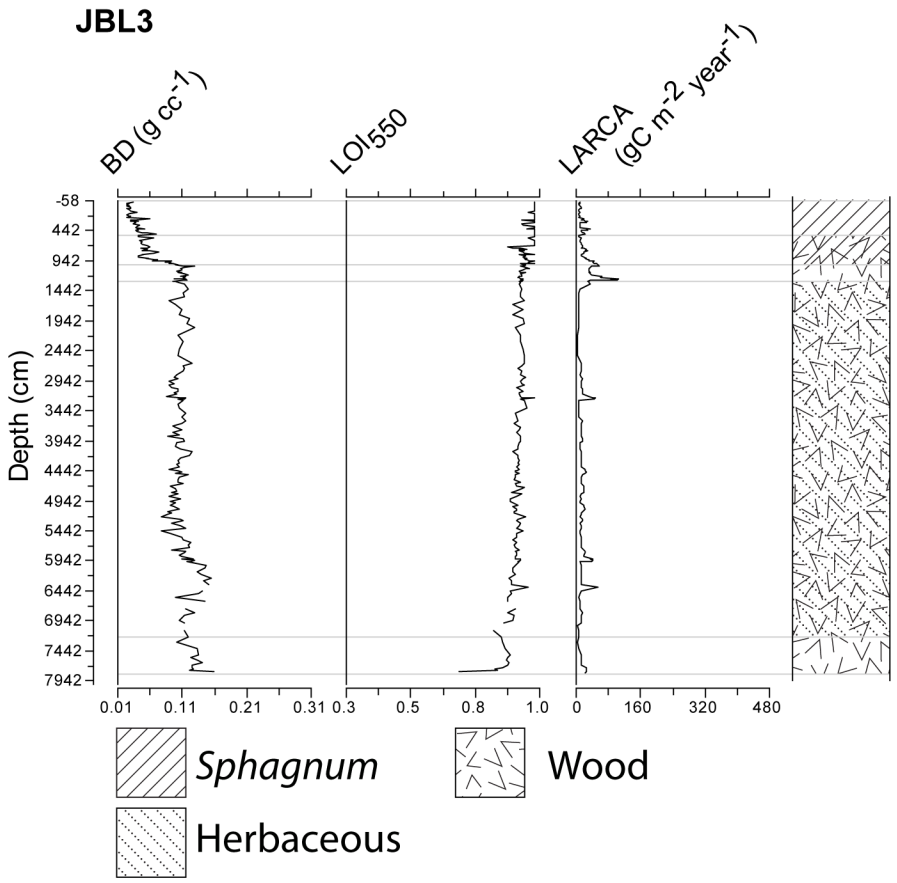

Figure 6. JBL3 BD, LOI_{550}, LARCA, and qualitative macrofossil zones plotted against time.

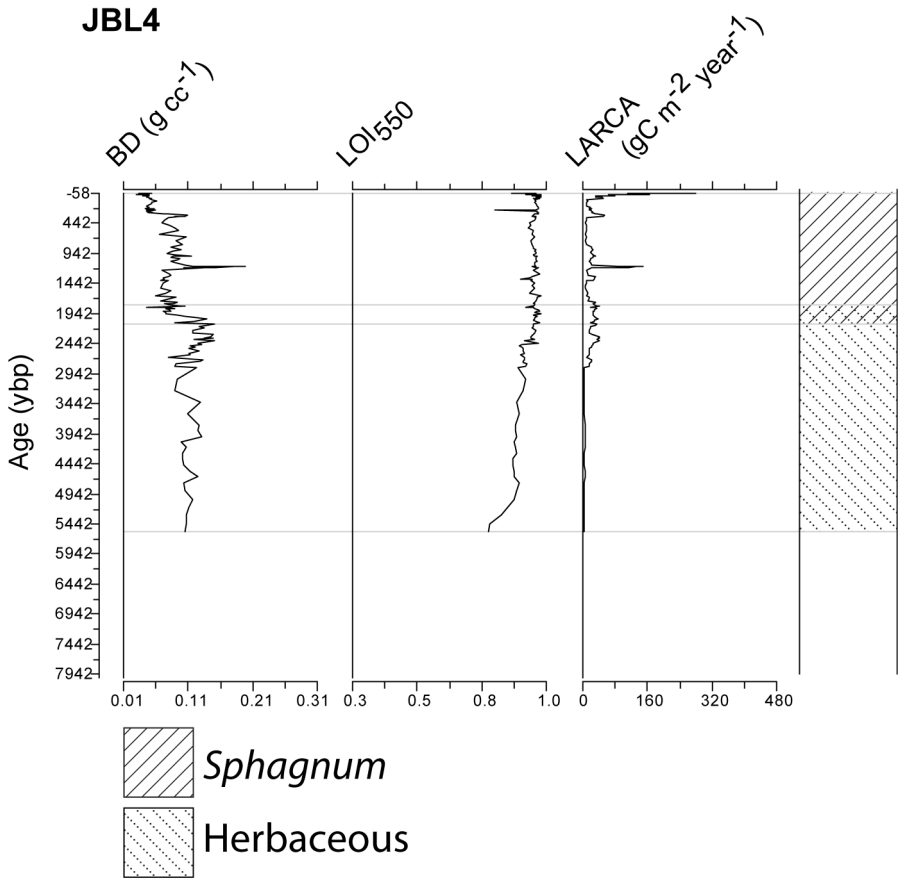

Figure 7: JBL4 BD, LOI_{550}, LARCA, and qualitative macrofossil zones plotted against time.

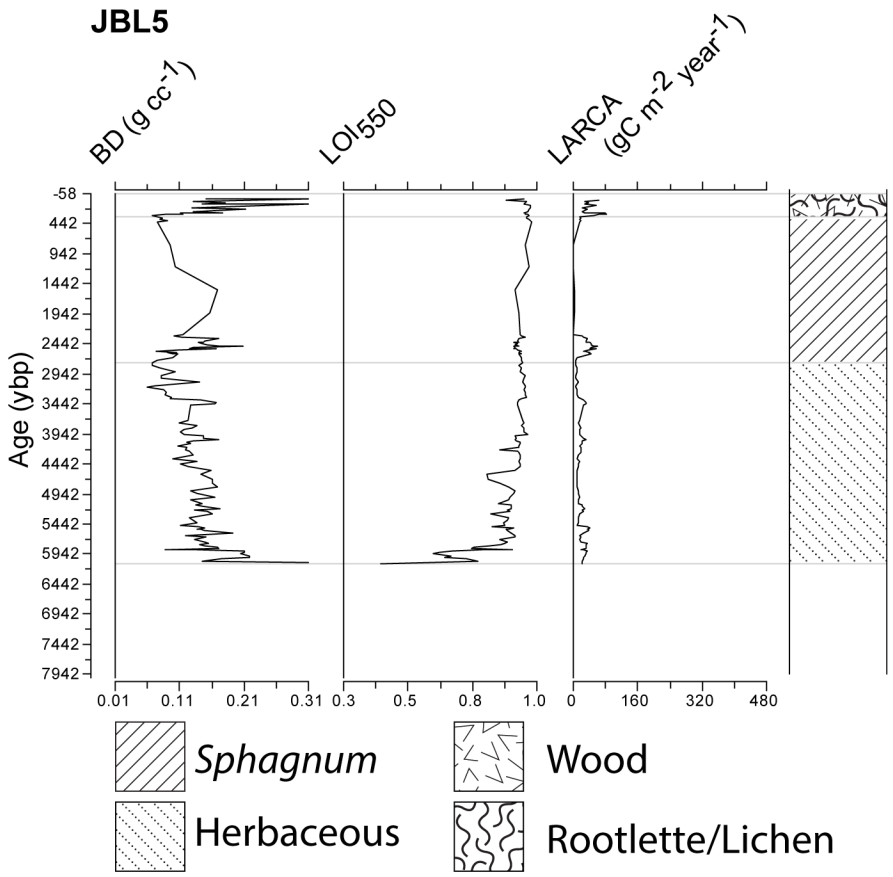

Figure 8: JBL5 BD, LOI_{550}, LARCA, and qualitative macrofossil zones plotted against time.

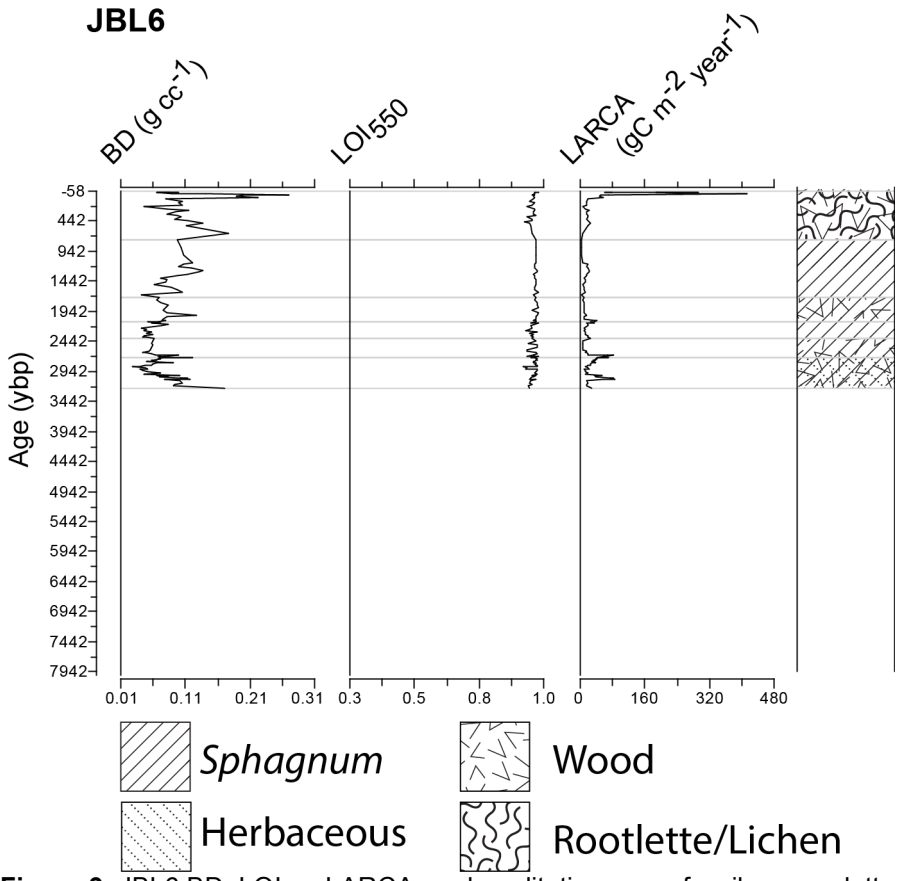

Figure 9: JBL6 BD, LOI_{550}, LARCA, and qualitative macrofossil zones plotted against time.

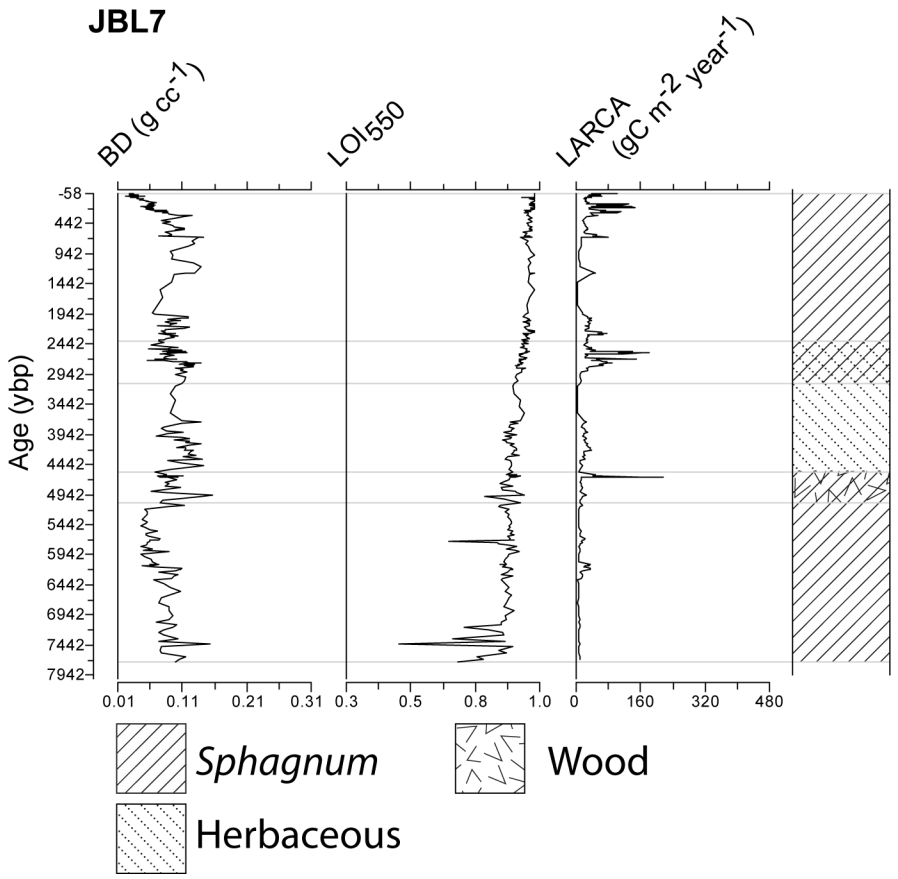

Figure 10: JBL7 BD, LOI_{550}, LARCA, and qualitative macrofossil zones plotted against time.

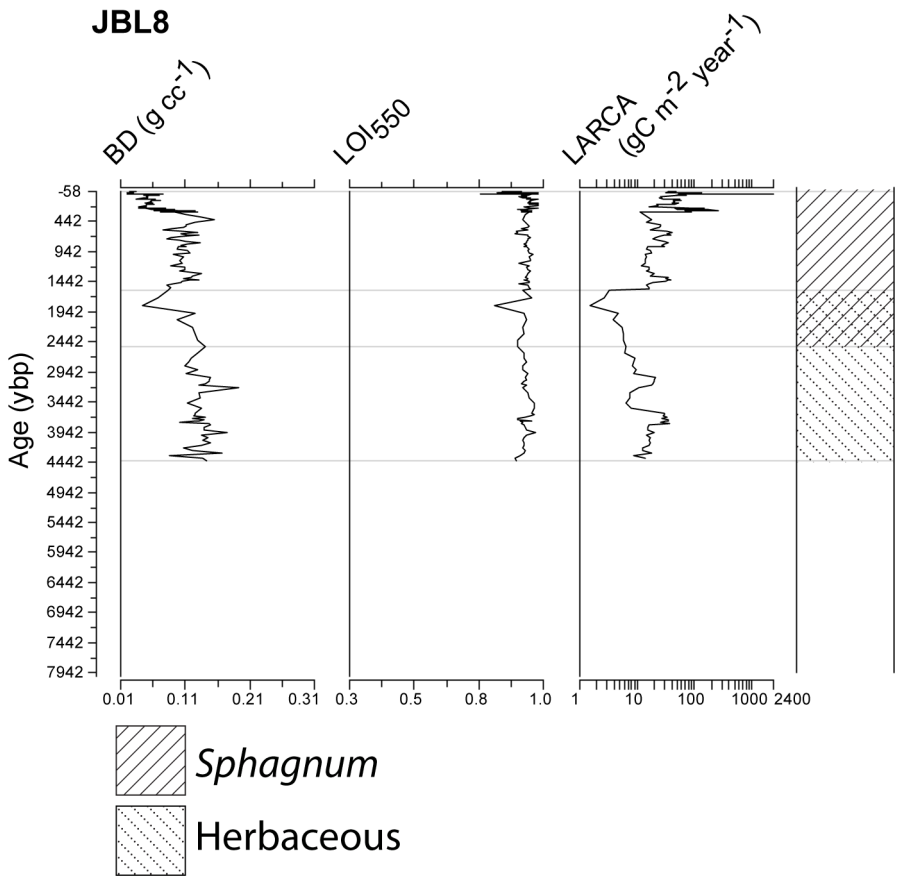

Figure 11: JBL8 BD, LOI_{550}, LARCA, and qualitative macrofossil zones plotted against time.

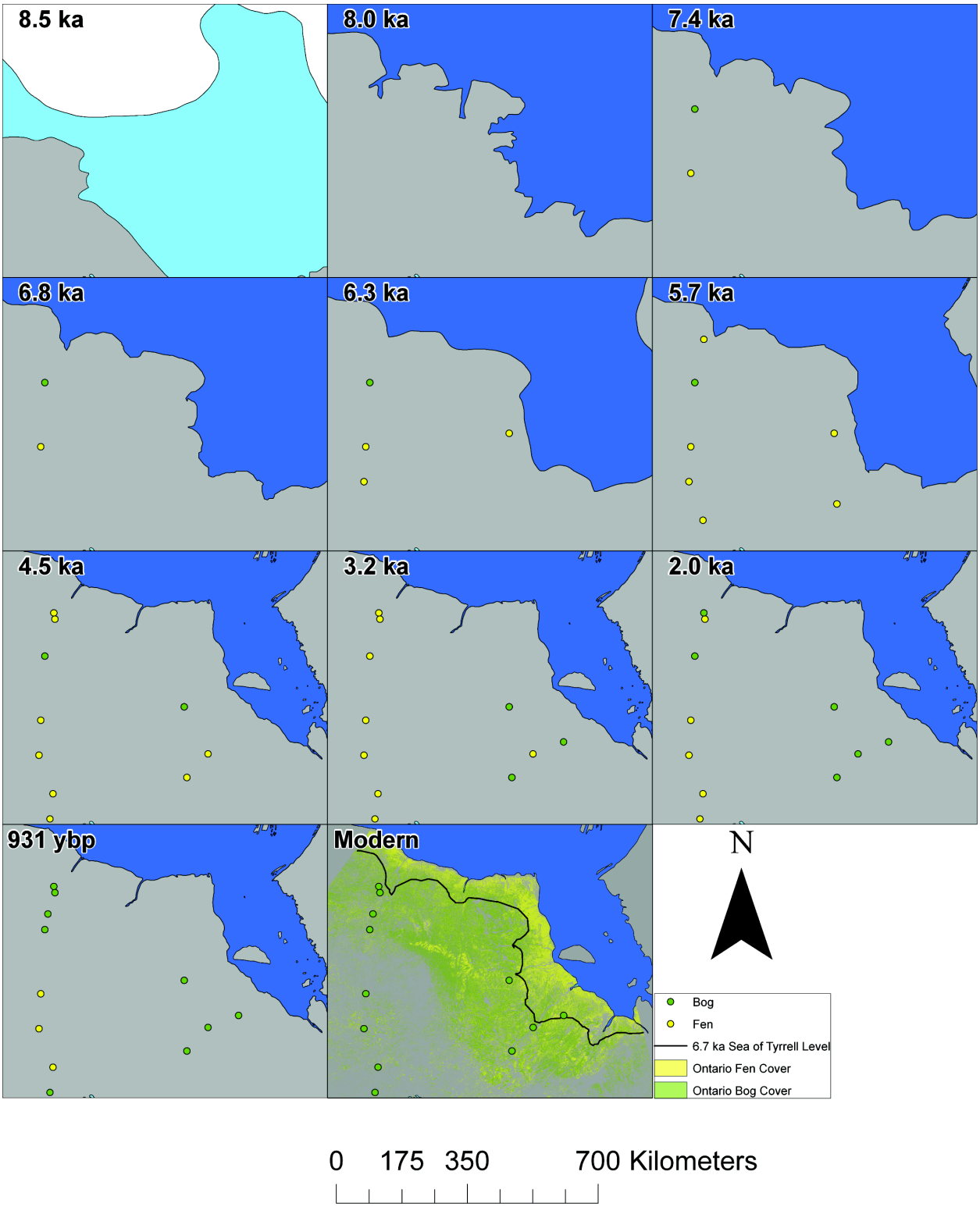

Figure 12: Deglaciation, glacial lake drainage, and isostatic uplift took place in the JBL during the Holocene (Dyke et al., 2003). Fen initiation lagged land availability in most cases and bog transition followed that. Modern land cover classifications indicate a gradient of fen to bogs dominance that coincides with land that is 5 - 7 ka years old.

Table 6: Lists the timings of deglaciation linearly interpolated from Dyke et al., (2003), peat initiation times, the timing of *Sphagnum*-dominance derived from ordinal macrofossil analysis, % time as fen, the timing of rootlette-lichen dominance in two permafrost sites. *JBL6 was omitted from the average basal date because it was recovered without a basal section.

Core	Deglaciation (ybp)	Initiation (ybp)	*Sphagnum* dominance (ybp)	Rootlette/lichen dominance (ybp)	Time as Fen (%)
JBL1	10292	6242	164	-	97
JBL2	10461	6407	584	-	91
JBL3	8983	7835	453	-	94
JBL4	8292	5569	1795	-	68
JBL5	8410	6108	2754	298	55
JBL6	8448	3187*	2678	636	-
JBL7	8470	7731	2276	-	-
JBL8	10442	4428	1405	-	68
Albany	7408	4810	2680	-	44
Belec	6566	3960	3430	-	13
Oldman	11272	5920	3690	-	38
VC04-06	8196	6700	4900	-	27

2.4.2. C Accumulation in the JBL

The mass of C accumulated at the sampling sites ranges from 71.5 to 171.2 kgC m^{-2} and averages 109.7 ± 36.2 kgC m^{-2} (Tab. 4). The highest LOI_{550} generally corresponds with the low-density acrotelm and active layer sections (Fig. 4 - 11). The exception to this is JBL5, which has a densely packed rootlette-lichen active layer. The lowest LOI_{550} values generally correspond to highest BD values at the mineral dominated basal sections. The reported mean BD, 0.087 ± 0.03 is slightly lower than values for fens and bogs in Western Canada, 0.094 g cm^{-3} (Vitt et al., 2000a), and the range of measurements from the Mackenzie River Basin, Finland, and the WSL (0.092 to 0.094 g cm^{-3}; Makila, 1994; Sheng et al., 2004; Beilman et al., 2009). Peat generally has lower BD and higher LOI_{550} in the top meter of peat, and higher BD and lower LOI_{550} in deeper peat due to decay and compaction over time in deeper peat. The young age and shallow depths of the JBL peat may account for the lower BD recorded here.

LARCA varies over four orders of magnitude ranging from 1.3 to 2369.3 gC m^{-2} yr^{-1} (Fig. 4 - 11; Tab. 7). The highest values in JBL8 skew its' mean artificially high, and may be artifacts of ^{14}C uncertainty, so I present median values in addition to means and ranges. Drastic changes in LARCA, in some cases could be attributed to changes in the slope of the age-depth model, or to changes in density or C content coinciding with changes in dominant macrofossil assemblage. A summary of the LARCA Z-scores across the eight cores at 1 cm resolution, and LARCA values compiled by 1 ka year increments is available in Figure 13. There is evidence for synchronous increases in LARCA across four different cores at approximately 6.1 ka, causing the 7 to 6 ka interval to have the highest median LARCA.

Table 7: Data for LOI_{550},, mean BD, and total C accumulation, as well as as well as min, max, mean, standard deviation, and median values for LARCA for each JBL core.

Core	LOI_{550} mean	BD mean ± s. dev ($g\ cm^{-3}$)	C mass ($kg\ C\ m^{-2}$)	LARCA mean ($gC\ m^{-2}\ yr^{-1}$)	LARCA min - max ($gC\ m^{-2}\ yr^{-1}$)	LARCA median ($gC\ m^{-2}\ yr^{-1}$)
JBL1	0.94 ± 0.04	0.098 ± 0.031	129.8	37.3 ± 40.9	1.4 - 294.4	24.9
JBL2	0.97 ± 0.02	0.079 ± 0.029	171.2	38.9 ± 29.5	3.4 - 169.3	31.6
JBL3	0.95 ± 0.03	0.093 ± 0.045	104.4	20.4 ± 17.4	4.2 - 103.5	13.8
JBL4	0.96 ± 0.04	0.086 ± 0.033	71.5	41.4 ± 54.1	2.2 - 279.2	23.6
JBL5	0.93 ± 0.08	0.135 ± 0.046	82.0	24.6 ± 15.9	1.3 - 83.5	21.2
JBL6	0.98 ± 0.09	0.084 ± 0.037	NA	35.1 ± 54.0	3.8 - 411.8	18.2
JBL7	0.94 ± 0.05	0.08 ± 0.026	129.2	38.0 ± 39.4	2.8 - 215.3	24.7
JBL8	0.95 ± 0.03	0.087 ± 0.041	77.1	119.2 ± 362.9	1.5 - 2369.3	30.2

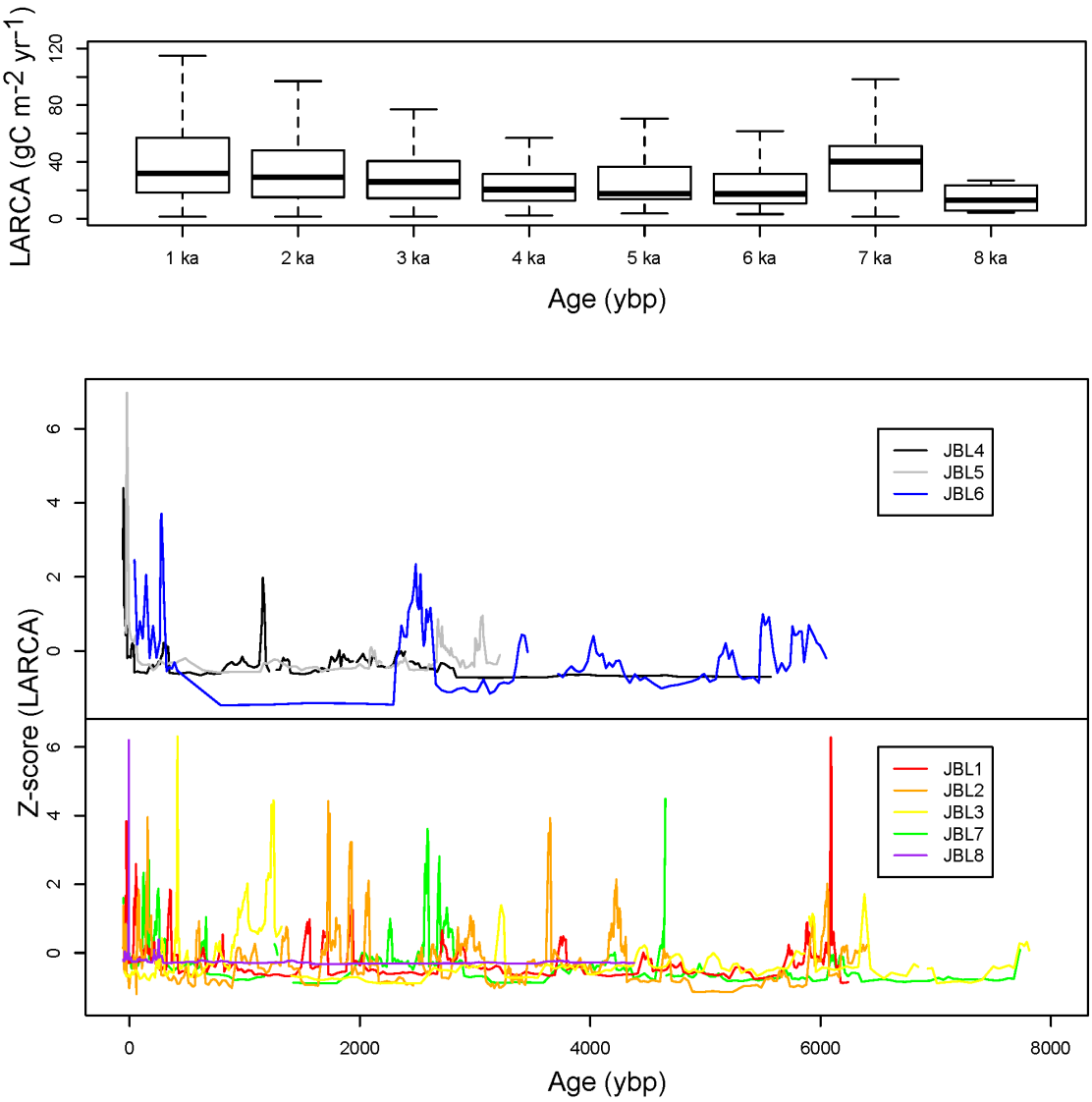

Figure 13: The upper plot represents LARCA values from all cores combined into 1,000-year bins. Central lines represent medians. Box edges represent the first upper and lower quantiles, and whisker lines represent third upper and lower quantiles. The central plot and bottom plot are the Z-scores for LARCA plotted for cores in the discontinuous permafrost and non-permafrost, and zones respectively.

Extreme low LARCA values are either associated with peat initiation, or ecological transition to modern permafrost conditions (Fig. 4 - 11). Basal layers typically have some of the lowest C accumulation rates due to either initial low slopes in the age-depth models (overall slow rates of sediment deposition/accretion), or low LOI_{550}

because of high mineral content. In JBL1 the lowest LARCA values occur in the basal section due to low BD and low LOI_{550}, due to inorganic sediment content. In JBL2 the basal section displays initially moderate C accumulation rates caused by a simultaneously high accumulation rate, and low LOI_{550} due to mineral content. However, JBL5 and JBL6 have extremely low LARCA values that were coincident with shifts from *Sphagnum* to lichen and rootlette dominated peat, vegetation indicative of dry permafrost surfaces. LARCA in JBL5 ranged from 1.3 - 83.5 g C m^{-2} yr^{-1}, containing both the lowest minimum and maximum LARCA out of all eight cores analyzed (Tab. 7). In JBL6 there was also a decrease in LARCA during the transition from *Sphagnum* to rootlette, lichen, and wood dominated peat.

2.5. DISCUSSION

2.5.1. Geographic patterns of Peat Initiation and Succession

Average site initiation lagged deglaciation or glacial lake drainage by 2,900 ± 1,200 years with spatial variability (Fig. 4 - 11; Tab. 6). A review of North American peat initiation describes a 4,000-year lag between deglaciation and peat initiation (Halsey et al., 2000; Gorham et al., 2007). The drainage of glacial lakes was a major lag factor, as well as the cold 8.2 ka event. The 8.2 ka event was caused by the catastrophic dranaige of glacial lakes Agassiz and Ojibway interrupting thermohaline circulation in the North Atlantic causing widespread cool-dry conditions, and likely discouraged major peat formation (Barber et al., 1999). Halsey et al., (2000) postulated that this lag was

partially due the time it took for land to become amenable to peat formation, and the random chance of dispersal of, and colonization by peat forming species. The dispersal of peat forming species has been estimated at about 2,700-years following major deglaciation (Gorham et al., 2007). One of the weaknesses of this study is the single site, single core approach, and peat initiation can be heterogeneous within a single site. The expansion of peatlands could be important the observed timing of peatland initiation, but is not readily analyzed in this study (Bauer et al., 2003).

The four northern sites had a shorter lag between deglaciation and peatland initiation (Fig. 4 - 11; Tab. 6). A hypothesis for this difference could be that the igneous shield bedrock of the southern portion of the field area, and the lacustrine and marine sediments underlying the JBL (Josenhans and Zevenhuizen, 1990) have different reliefs, pHs, nutrient statuses and permeabilities causing differences in peatland initiation (Korhola, 1995). The four southern sites also showed longer times between initiation and fen to bog transition. The three sites in the Albany River region and JBL site VC04-06 are more analogous to the four northern JBL transect sites (Glaser et al., 2004a; Bunbury et al., 2012), with shorter lags between land availability and peat initiation.

Fen to bog transition lagged peat initiation by 3,800 years and land availability by 6,700 years. The average lag between the timing of land availability and fen to bog transition scales with modern landscape patterns in the isostatically rising JBL (Fig. 4 - 11; Tab. 6). Previous studies have documented a transition from geologically younger costal fens to geologically older inland bogs in the JBL (Klinger and Short, 1996; Glaser et al., 2004a). *Sphagnum* is the dominant cover past ~40 km distance from the bay

(Klinger and Short, 1996; Provincial Land Cover Data Base, 2000; Tarnocai et al., 2011). The estimated level of the Sea of Tyrrell at 6.7 ka roughly corresponds with the transition from costal fen dominance to inland bog dominance (Fig. 13).

Presently wetlands in the Hudson Bay Lowlands (HBL)-JBL are a negligible producer of CH_4 (Roulet et al., 1994), but may have been higher emitters in the past due to higher ER, anaerobic conditions, and CH_4 transport to the surface through *Carex* arenchyma (Whalen, 2005). Peatland contributions to atmospheric CH_4, measured by the oldest peatland initiation within a 2° x 2° grid show initiation, and CH_4 from ice cores, increase lagging the HTM (12.0 – 11.5 ka; MacDonald et al., 2006). Following this increase, atmospheric methane levels decreased from 700 to 550 ppbv between 11 and 4 ka (Brook et al., 2000; MacDonald et al., 2006). Although the JBL is the second largest complex in the world, there is no apparent peak in CH_4 emissions at this time in ice cores during peak peat initiation (5.9 ka; Brook et al., 2000; MacDonald et al., 2006). CH_4 emissions from the JBL may have been mitigated by fen to bog transitions occurring in European, Asian, and Alaskan peatlands (MacDonald et al., 2006). Fen to bog succession occurring around 2.4 ka, could have contributed to the low observed in CH_4 during that time. However, further studies need to be done to evaluate the contributions of large peatland fen to bog transitions to atmospheric CH_4 over the mid to late-Holocene.

2.5.2. C Storage and LARCA

The mass of C pools in the JBL range from 71.5 to 171.2 kgC m^{-2} and have an average value 109.7 ± 36.2 kgC m^{-2} (Tab. 7). This approximately matches the range and variability from another large Canadian survey of peat mass from the Mackenzie River Basin, as well as global surveys, which provide values ranging between 53 to 165 kg m^{-2} and averaging 130 kgC m^{-2} (Gorham et al., 1991). Mean estimates from the JBL are likely lower than global mean estimates because the deglacial history of the JBL makes them younger on average than other major peatlands which had earlier deglaciation times, or remained ice free during the last glacial maximum (Kuhry and Turunen, 2006; MacDonald et al., 2006).

Although highly variable, the four oldest sites have anomalously high LARCA values at approximately 6.1 ka (Fig. 4 - 11; Fig. 13). There are two possible explanations for this pattern. 1. The 6.1 LARCA increase could have been caused by autogenic peat accumulation that occurred coincidentally at all four sites because of their similar initiation timing and surface conditions (Clymo, 1984; Belyea and Baird, 2006). 2. The 6.1 LARCA increase could have been caused by a punctuated extreme autogenic event such as climate or watershed changes that have not yet been previously identified because of the paucity of data in the JBL. It could have been caused by, or intercorrelated with, drought events between 6.2 – 6.0 ka recorded in low mid-Atlantic lake levels (Li et al., 2007). It also could have been caused by, or intercorrelated with, the final deglaciation of Laurentide ice northeast of the JBL in the Ungava Bay region 6.4 - 6.1 ka (Dredge, 2001), or the Foxe ice dome 8.5 – 6.5 ka (Dredge, 1990), or a brief cold period, caused by one of several meltwater discharges into Ungava Bay ~6.4 ka (Jansson and Kleman, 2004).

The HTM, and medieval warming did not have a significant influence on LARCA. LARCA was highly variable and had many brief increases during the Holocene (Fig. 13). JBL2, and JBL7 displayed LARCA peaks between 5 - 3 ka, however LARCA was not elevated across the 5 – 3 ka cohorts during the centuries connected with the HTM in eastern Canada. Similarly, JBL3 and JBL4 have LARCA peaks that coincide with the MCA, but there is not consistent pattern across all cores. Globally peatlands show a slight increase in LARCA during the MCA in response to changes in seasonal photosynthetically active radiation (Charman et al., 2013). However in our smaller, more localized, dataset, if there is a relationship, it may not be observable due to the high variability of LARCA, and the complication of succession events, and acrotelm – catotelm boundaries.

The minimum values of LARCA usually occurred in basal layer, which had the longest time to decay, under minerotrophic conditions with higher organic C turnover rates (Fig. 4 - 11). However, the two permafrost cores had their minimum values between *Sphagnum* sections and rootlette, lichen, and wood dominated sections that are indicative of modern permafrost conditions (Tab. 1). This supports recent evidence from the Western Siberian Lowlands, that permafrost has had a negative effect on C accumulation during the late-Holocene (Beilman et al., 2009). Permafrost can decrease peat formation by decreasing plant productivity, decreasing the amount of physical peat accumulation, and drying the surface by drainage through cracks in permafrost (Gorham, 1991). Although permafrost decreased apparent accumulation in JBL5 and JBL6, there is evidence for ongoing LARCA in the upper sections that can be relatively

high and variable due to the low decay rate of the woody matter under dry local topography, and short growing seasons.

2.6. CONCLUSION

Peatland initiation lagged glacial retreat in central and northern Ontario by 2,900 years, with shorter lags occurring in sites closer to the James Bay (Tab. 3). The timings of fen to bog transitions were variable, and included relatively quick transitions, protracted poor-fen stages, and one case that reversed the dominant trend. A 6,700-year lag in succession from fen to bog following land availability is reflected in both the available macrofossil records, and modern land surfaces of varying ages in the JBL. If the JBL was ever a significant source of CH_4, it was likely transitioning to a lower level source by 2.4 ka. The range of C mass accumulated throughout the Holocene is typical of boreal and subarctic peatlands. Spatial patterns in LARCA illuminated possible allogenic controls of LARCA between 7 to 6 ka, and a near shutdown in LARCA with the establishment of dry permafrost surface vegetation in two sites. Although the history of the JBL as a CH_4 source, and the origin of the 6.1 ka LARCA increase are uncertain, the JBL have acted as a constant, although dynamic, sink of CO_2 throughout the mid and late-Holocene. The next three chapters will present investigations of the climate drivers for peatland accumulation rates using naturally occurring gradients in precipitation, temperature, seasonality, and permafrost, and reconstructions of past hydrology using testate amoebae.

3. Climate Drivers for Late-Holocene Vertical Peat Accumulation in the Hudson and James Bay Lowlands

3.1. ABSTRACT

Climate drivers for the rates of peatland growth and C accumulation are important to understand because of their possible roles in future C cycle feedbacks to global warming. This chapter utilizes a transect of eight ombrotrophic peat cores from the under-studied James Bay Lowlands (JBL) of central and northern Ontario to quantify the magnitude and rate of C accumulation since peatland initiation and for the last 2 ka (ka = 1,000 calendar years before present [ybp]). Seventeen radiocarbon (^{14}C)-based age-depth models with well-resolved chronologies from a literature review covering the entire Hudson Bay Lowlands (HBL)-JBL region supplement this new data. Approximately 40% of total soil C has accumulated since 2 ka. The depth of peat that has accumulated over the past 2 ka correlates significantly and positively with modern gridded climate estimates for mean annual precipitation, mean annual air temperature, growing degree-days > 0°C, and photosynthetically active radiation integrated over the growing season. There are significantly shallower depths of peat accumulation in permafrost regions. Vertical peat accumulation was likely constrained by productivity rather than decay indicating the possibility of a positive feedback to future warming within peatlands' ecological and physiological tolerances.

3.2. INTRODUCTION

Peatland carbon (C) cycle feedbacks have the potential exhibit dynamic and complex shifts in magnitude and direction due to the influence of precipitation, growing season length, and photosynthetically active radiation on plant and peat production, and greenhouse gas emissions (Gorham, 1991; Clymo, 1998; MacDonald et al, 2006; IPCC, 2007; Dise, 2009; Loisel et al., 2012; Yu et al., 2012; Charman et al., 2013). In peatlands, oxygen poor and acidic inundated conditions, low mean annual temperatures, and short growing seasons lead to higher net primary productivity (NPP) relative to ecosystem respiration (ER) because the amount of C accumulated in catotelm section of the soil outpaces C losses through acrotelm and catotelm decay (Clymo, 1984; van Breeman, 1995; Blodau, 2002; Dise, 2009; Yu et al., 2009). This positive net ecosystem productivity may increase, decrease, or reverse due to projected anthropogenic climate change (Moore and Knowles, 1989; Davidson and Janssens, 2006; Tarnocai, 2006; Beilman et al., 2009; Loisel et al., 2012).

Precipitation and surface moisture may be important drivers of peat accumulation in *Sphagnum* bogs. *Sphagnum* mosses do not have stomata and cannot regulate water loss during CO_2 exchange making them vulnerable to large shifts in surface moisture (Loisel et al., 2012). Effective moisture has been found to be a significant driver of *Sphagnum* growth in some continental sites (Loisel et al., 2012). However, in a review of North American peat accumulation, precipitation was found to be significantly, but inversely, correlated with peat depth, and the rate of accumulation (Gorham et al., 2003). There is also some evidence that *Sphagnum* bogs can regulate their own water table depth because of their complex structure and ecohydrology; therefore they may

not be sensitive to precipitation related water stress within their ecological limit (Lahio, 2006; Dise, 2009). This internal feedback relationship has been included into many different peatland development models (Clymo, 1984; Belyea and Baird, 2006; Eppinga et al., 2009; Frolking et al., 2010).

Thermal characteristics such as air temperature, and growing season length are possible important drivers of *Sphagnum* growth and C accumulation. *Sphagnum* growth rate increases with temperature (Gunnerson, 2005; Breeuwer et al., 2008). *Sphagnum* productivity has also been globally linked to photosynthetically active radiation, and growing season length (Loisel et al., 2012). Studies have also observed significant, positive correlations worldwide between mean growing degree-days above 0°C (GDD_0) and rates of peat accumulation (Clymo et al., 1998). GDD_0, photosynthetically active radiation integrated over the growing season (PAR_0) was also shown to be a driver of post-1 ka (ka = 1,000 calendar years before present [ybp]) apparent C accumulation rate in a global peatland database (Charman et al., 2013). In an analysis of a widespread network of *Sphagnum* cores in the WSL, the depths of 2 ka peat correlate significantly and positively with mean annual air temperature (MAAT; Beilman et al., 2009). In the WSL 2 ka depths are also significantly shallower if permafrost is present, suggesting productivity, rather than low decomposition rates, may exercise greater control on peat accumulation at these sites (Beilman et al., 2009).

The James Bay Lowlands (JBL) and adjacent Hudson Bay Lowlands (HBL) of Quebec, Ontario, and Manitoba in Canada (Fig. 14), are second to the WSL as the largest continuous peatland complex in the world (Riley, 2005, 2011). Despite the importance of the HBL-JBL to global C cycling, only a few studies have estimated

average apparent rate of C accumulation over the broad regions of northern Ontario (O'Reilly, 2011; Bunburry et al., 2012). It is due largely to inaccessibility by surface transport that large portions of the JBL in central and northern Ontario remain understudied. In addition to this, no studies have synthesized current patterns, or analyzed connections between peat accumulation and climate in the HBL-JBL.

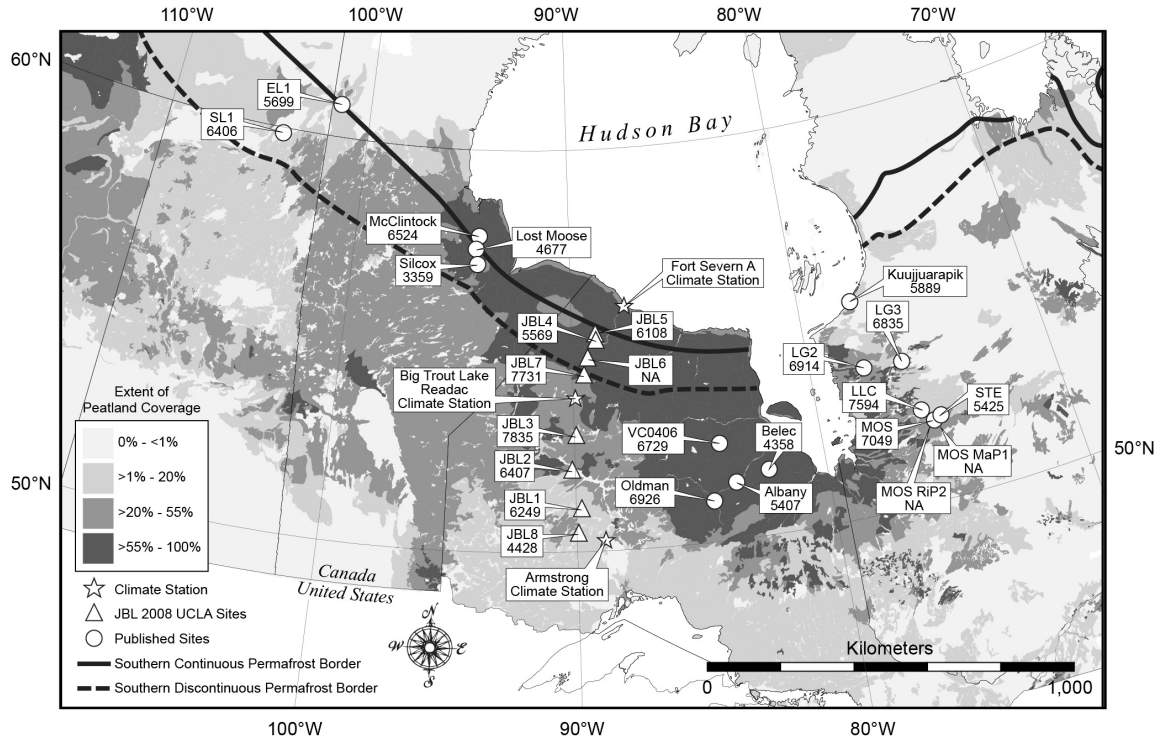

Figure 14: My study sites were located in the JBL, and were supplemented by a review of seventeen additional age-depth models from the entire HBL-JBL. Pictured are also maps of peatland extent (Tarnocai et al., 2011), and the borders of discontinuous and continuous permafrost zones (Brown et al., 1998).

This chapter focuses geographically on patterns in C storage in ombrotrophic peatlands relative to 2 ka in the HBL and JBL. Although the arctic and subarctic have experienced variation in climatic conditions over the past 2 ka, this time period represents the period of the Holocene during which natural radiative forcing, boundary

conditions and Arctic climate are the most similar to today (Kaufman et al., 2009). Data on peatland depth can be useful to make baseline estimates of peat production relative to decay and the potential impacts of climate change (Beilman et al., 2009).

The goal of this chapter is to determine the effect that climate has had on vertical peat accumulation in the wider HBL-JBL. I had four different research questions. 1. Do apparent C accumulation, and 2 ka depth correlate significantly and inversely with modern mean annual precipitation (MAP), and positively with modern MAAT, GDD_0, and PAR_0 in the eight cores from the JBL? 2. Did 2 ka depth correlate significantly inversely with MAP, and negatively with MAAT, GDD_0, and PAR_0 over the entire HBL-JBL? 3. Were relationships between climate and peat accumulation consistent between the eight-core JBL transect, and the larger HBL-JBL? 4. Did modern permafrost occurrence have a significant, and negative relationship with peat depth, and 2 ka depth with permafrost peatlands being significantly shallower than non-permafrost locations?

3.3. MATERIALS AND METHODS

Core collection and processing is detailed in Chapter 2. I supplemented my eight JBL cores with a review of seventeen other HBL-JBL cores. The entire data set ranges in latitude from 50°27' N to 60°50' N (Fig. 14; Tab. 1; Tab. 8). Out of the combined dataset, nineteen of the sites are from ombrotrophic bogs, whereas six are from permafrost plateaus, or polygonal peat formations. I avoided analyzing cores from fens, or with chronologies that were less than approximately millennially resolved.

Table 8: Site information from seventeen HBL-JBL ombrotrophic peat profiles with millennially resolved age-depth models, listed by author.

Author	Core Name	Coordinates (d m s)	Elevation (m)	Peatland Type
Arlen-Pouliot and Bhiry, 2005	Kuujjuarapik	55°20' N, 77°40' W	85	Palsa
Beulieu-Audrey, 2009	LG2	53°39' N, 77°44' W	173	*Sphagnum* bog
	LG3	53°34' N, 76°08' W	215	*Sphagnum* bog
Bunbury et al., 2012	VC0406	52 42'36" N, 84°10'48" W	105	*Sphagnum* bog
Dredge and Mott, 2003	Lost Moose	57°33.9' N, 94°19.0' W	109	*Sphagnum* bog
	Silcox	57°10.0' N, 94°14.2' W	141	*Sphagnum* bog
Glaser et al., 2004a	Albany	51°26' N, 83°37' W	82	*Sphagnum* bog
	Belec	51°37' N, 82°17' W	64	*Sphagnum* bog
	Oldman	51°01' N, 84°34' W	101	*Sphagnum* bog
Kuhry, 2008	McClintock	57°50' N, 94°12' W	80	Permafrost plateau
Sannel and Kuhry, 2009	EL1	60°50' N, 101°33' W	329	Permafrost plateau
	SL1	59°53' N, 104°12' W	390	Permafrost plateau
Loisel and Garneau, 2010	MOS MaP1	51°58' N, 75°24' W	304	*Sphagnum* bog
	MOS RiP2	51°58' N, 75°24' W	304	*Sphagnum* bog
van Bellen et al., 2011	LLC	52°17'15" N , 75°50'21" W	256	*Sphagnum* bog
	MOS	51°58'55" N, 75°24'06" W	299	*Sphagnum* bog
	STE	52°02'37" N, 75°10'23" W	303	*Sphagnum* bog

3.3.1. Average apparent rate of C accumulation

For the eight core JBL transect, I calculated the mass of C accumulated from initiation to the surface, and 2 ka depth to the surface (Beilman et al., 2009). For average Holocene apparent rate of C accumulation I summarized the mass of C and divided the mass by the amount of time since initiation. For post-2 ka apparent rate of C accumulation I summarized the amount of C accumulated since the closest approximation to 2 ka and divided the mass by that closest approximation.

3.3.2. Statistical Analysis

I statistically tested hypotheses regarding the relationships between climate and 2 ka depths, as well as permafrost occurrence on both total depths, and 2 ka depths. To test

the hypotheses that MAP, MAAT, GDD_0, and PAR_0 correlate significantly with 2 ka depth, I used linear regressions, and climate data from 0.5° x 0.5° integrated gridded databases for MAP and MAAT (1975 - 2005; Matsuura and Willmott, 2009). Initial analysis and previous research (Beilman et al., 2009) indicated the possibility of an exponential relationship between MAAT and 2 ka depth, so I included an exponential regression in my analysis of these two variables. For measurements involving seasonality I used 0°C as a base temperature since *Sphagnum* species are adapted to growth at low temperatures (Asada et al., 2003). I used a 0.5° x 0.5° gridded database for GDD_0 calculated from daily temperature values, and PAR_0 from latitude, orbital parameters and the fraction of sunshine hours (Prentice et al., 1993), using the CLIMATE 2.2 database (Kaplan et al., 2003). I also tested the hypothesis that permafrost peatlands are significantly shallower than non-permafrost peatlands, using a one-way ANOVA with permafrost occurrence as the independent variable, and total depth, or 2 ka depth as the dependent variable. All statistics were calculated with the computer language and statistical program R (R-core development team, 2012).

3.4. RESULTS

3.4.1. 2 ka Soil C in JBL

More C is present that was older than 2 ka than was younger in the eight new JBL cores (Tab. 7). This is not surprising as the pre-2 ka portion of the cores typically represents >5 ka to 2.4 ka of deposition. Post-2 ka C stocks range from 16.3 to 62.5 kg C m^{-2} and

averaged 40.5 ± 14.3 kg C m^{-2} (Fig. 15). In the JBL about 40% of the total C present in the cores is younger than 2 ka. Notable exceptions to this trend are JBL4 and JBL8 where pre-2 ka apparent rate of C accumulation is drastically lower than post-2 ka.

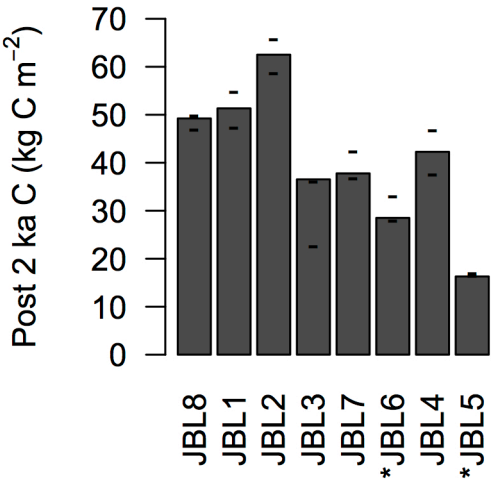

Figure 15: Post-2 ka C accumulated in the eight JBL sites arranged by latitude. (-) Represent the upper and lower estimates of Post-2 ka C masses based on upper and lower estimates of 2 ka by 'Bacon' models. * Represents permafrost peat.

Apparent rate of C accumulation was generally higher post-2 ka than total in the eight new JBL cores. Average apparent rate of C accumulation since initiation ranged from 12.8 to 26.7 g C m^{-2} yr^{-1}, with a mean of 17.4 ± 5.0 g C m^{-2} yr^{-1} (Tab. 9). These correspond to estimations of 13 to 30 g C m^{-2} yr^{-1} for North American peat bogs (Gorham, 1991; Turunen et al., 2002; Kuhry and Turunen, 2006), and fall in the range of observed global peatland C accumulation (8.4 to 38.0 g C m^{-2} yr^{-1}; Yu et al. 2009). Post-2 ka apparent rate of C accumulation ranged from 8.5 to 30.8 g C m^{-2} yr^{-1} and had an average of 20.2 ± 6.9 g C m^{-2} yr^{-1}. The lowest post-2 ka estimate in JBL5 (8.5 g C m^{-}

^{2} yr^{-1}) roughly corresponds with projected rates for subarctic Canada (9 g C m^{-2} yr^{-1}; Gorham, 1991), and the lowest observed arctic estimates from a global synthesis (8.4 g C m^{-2} yr^{-1}; Yu et al. 2009). Pre-2 ka apparent rate of C accumulation was generally lower than post-2 ka apparent rate of C accumulation, and ranged from 8.2 to 24.8 g C m^{-2} yr^{-1} and averaged 15.0 ± 5.6 g C m^{-2} yr^{-1}.

Table 9: Peatland basal ages, basal depths, and 2 ka depths for seventeen review and eight new HBL-JBL cores. Data for apparent rate of C accumulation, and C mass data since inception, and post-2 ka, are displayed as well.

				Total		Post-2 ka	
Core	Basal Age (ybp)	Depth (cm)	2 ka depth (cm)	C mass (kg C m^{-2})	C accumulation rate (g C m^{-2} yr^{-1})	C mass (kg C m^{-2})	C accumulation rate (g C m^{-2} yr^{-1})
JBL1	6249	286	128	129.8	20.8	51.3	25.6
JBL2	6407	422	173	171.2	26.7	62.5	31.2
JBL3	7835	245	109	104.4	13.3	35.5	17.9
JBL4	5569	176	122	71.5	12.8	42.3	21.2
JBL5	6108	141	24	82.0	13.4	16.3	8.5
JBL6	NA	NA	58	NA	NA	28.5	14.3
JBL7	7731	330	109	129.2	16.7	37.8	18.9
JBL8	4428	189	143	77.1	17.4	49.2	23.7
Albany	5407	264	106	-	-	-	-
Belec	4358	236	63	-	-	-	-
EL1	5699	186	8	-	-	-	-
Kuujjuarapik	5889	225	31	-	-	-	-
LG2	6914	397	72	-	-	-	-
LG3	6835	375	54	-	-	-	-
LLC	7594	483	123	-	-	-	-
Lost Moose	4677	135	73	-	-	-	-
McClintock	6524	166	64	-	-	-	-
MOS	7049	297	101	-	-	-	-
MOS MaP1	NA	NA	92	-	-	-	-
MOS RiP2	NA	NA	74	-	-	-	-
Oldman	6926	446	156	-	-	-	-
Silcox	3359	70	53	-	-	-	-
SL1	6406	196	63	-	-	-	-
STE	5425	286	108	-	-	-	-
VC0406	6729	304	105	-	-	-	-

In the eight new JBL sites, both apparent rate of C accumulation and 2 ka depth correlate significantly and positively with MAP with r^2 values of 0.56 and 0.58 respectively ($p<0.05$; Tab. 10). 2 ka depths also correlate significantly and positively with MAAT ($p<0.05$; $r^2=0.52$; Tab. 10).

Table 10: r^2 values for JBL peatland 2 ka apparent rate of C accumulation, 2 ka depths, and HBL-JBL synthesis with MAP, MAAT, GDD_0 and PAR_0. *Refers to significance at the $p<0.05$. **Refers to significance at $p<0.001$. ***Refers to significance at $p<0.0001$. ^{e}Refers to an exponential regression rather than a linear regression.

	New sites Post-2 ka apparent C accumulation rate (n=8)	New Sites 2 ka Depth (n=8)	HBL-JBL Synthesis 2 ka Depth (n=25)
MAP	0.56^{*}	0.58^{*}	0.20^{*}
MAAT	0.38	0.52^{*}	0.46^{**} / 0.49^{***e}
GDD_0	0.50	0.50	0.60^{***}
PAR_0	0.46	0.46	0.62^{***}

3.4.2. Climate and 2 ka Depth

Based on a combined dataset of my eight new cores and the seventeen previously published cores (Fig. 4 - 11; Fig. 16; Fig. 17; Tab. 3; Tab 4; Tab. 9; Tab. 11 - 14), peat depth at 2 ka correlates significantly and positively with MAP, MAAT, GDD_0, and PAR_0 (Fig. 17; Tab. 10). 2 ka depths range from 8 to 173 cm with a mean of 88.5 ± 41.1 cm. Overall peat depth ranges from 70 to 483 cm, meaning that the average proportion of peat vertical accumulation since 2 ka was 36.9 ± 19.1%, roughly similar to the 40% of C present younger than 2 ka in 8 new JBL sites. 2 ka depth correlates significantly and positively with MAP ($p<0.05$; $r^2=0.20$), MAAT ($p<0.001$; $r^2=0.46$), GDD_0 ($p<0.0001$; $r^2=0.60$), and PAR_0 ($p<0.0001$; $r^2=0.62$). An exponential regression between MAAT and 2 ka depth increases the r^2 value to 0.49 ($p<0.0001$). A linear regression defining PAR_0 as a predictor of 2 ka depth describes the most variance out of all of the variables I tested.

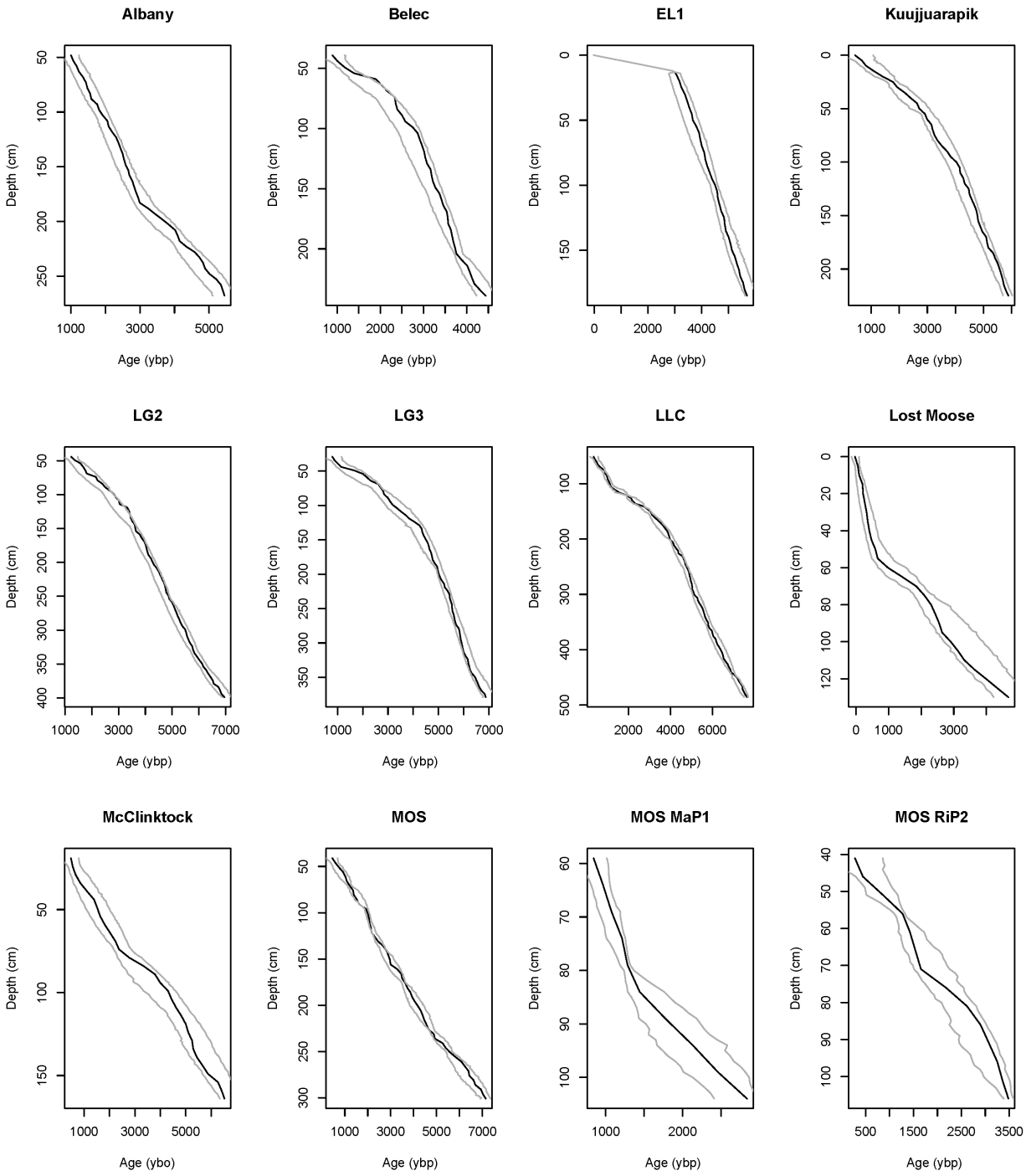

Figure 16: Age-depth models from seventeen review sites in the HBL-JBL area. Grey lines refer to minimum and maximum measurements, black lines refers to best estimates from Bacon age-depth modeling software.

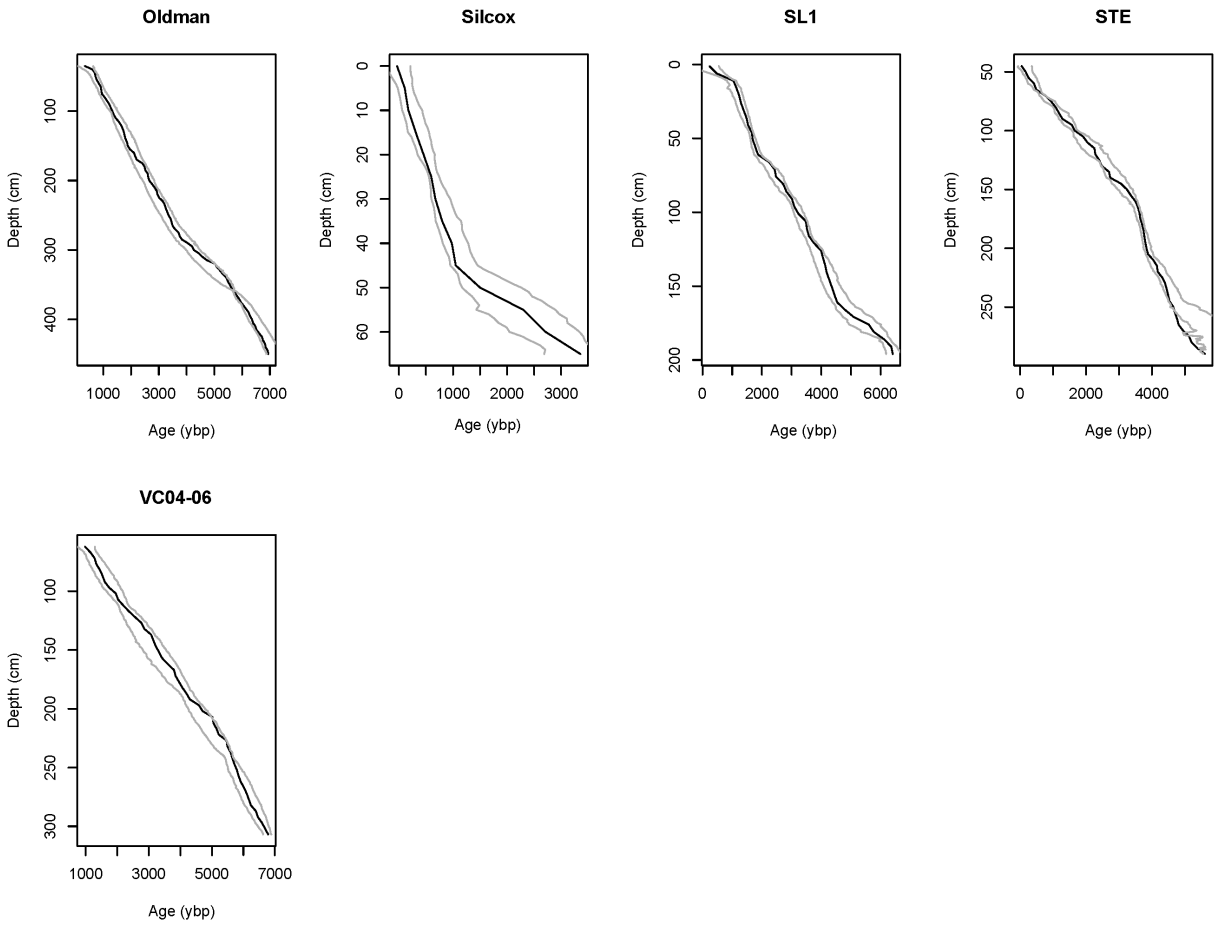

Figure 17: Age-depth models from seventeen review sites in the HBL-JBL area. Grey lines refer to minimum and maximum measurements. Black lines refer to best estimates from Bacon age-depth modeling software.

Table 11: ^{14}C-AMS samples, depth, ^{14}C ages, and best fit 'Bacon' model calibration estimates for seventeen from the HBL-JBL area. [a.] Refers to dates that contain ^{14}C from atomic weapons testing. [b.] Refers to outliers that were eliminated by 'Bacon'.

Core	Depth (cm)	Lab I.D. #	Material	^{14}C age	±	Age Range (ybp)	Best Fit (ybp)
Albany	47-49	Beta-44532	Peat	1110	70	785-1245	1031
Albany	101-104	Beta-44534	Peat	2020	70	1720-2105	1922
Albany	155-160	Beta-44535	Peat	2450	90	2441-2876	2697
Albany	178-183	Beta-44533	Peat	2680	80	2744-3284	2946
Albany	210-215	Beta-44536	Peat	3750	70	3696-4266	4091
Albany	259-264	Beta-44537	Peat	4810	70	4983-5648	5386
Belec	37-40	Beta-53065	Peat	900	70	504-1174	888
Belec	50-52	Beta-53066	Peat	1350	60	1092-1427	1301
Belec	73-76	Beta-53068	Peat	2280	50	1898-2353	2339
Belec	95-100	Beta-54595	Peat	2770	70	2326-2851	2716
Belec	145-150	Beta-54596	Peat	3070	70	2992-3387	3262
Belec	195-200	Beta-54597	Peat	3430	11	3619-3869	3721
Belec	231-236	Beta-54598	Peat	3960	60	4132-4587	4302
EL1	12-13	Hela-1051	NA	2850	70	2781-3206	3033
EL1	98-99	Poz-19644	NA	4010	30	4314-4584	4483
EL1	136-138	Hela-1052	NA	4260	45	4792-5217	4948
EL1	180-186	Hela-1053	NA	5065	70	5590-5995	5659
Kuujjuarapik	0-1	UL-2367	NA	360	60	-151-1069	418
Kuujjuarapik	24-25	UL-2593	NA	1810	60	1549-1954	1773
Kuujjuarapik	54-55	UL-2592	NA	2900	70	2771-3216	2915
Kuujjuarapik	99-100	UL-2591	NA	3770	70	3673-4218	4036
Kuujjuarapik	154-155	UL-2590	NA	4080	100	4524-4949	4811
Kuujjuarapik	179-180	UL-2589	NA	4490	70	4976-5361	5171
Kuujjuarapik	209-210	UL-2587	NA	4850	70	5449-5804	5688
Kuujjuarapik	224-225	UL-2358	NA	5020	80	5694-6029	5889
LG2	44-45	Beta-199811	*Sphagnum* remains	1250	40	952-1482	1244
LG2	95-96	Beta-199812	*Sphagnum* remains	2500	40	2373-2713	2721
LG2	146-147	Beta-199813	*Sphagnum* remains	3350	40	3420-3670	3610
LG2	199-200	Beta-199814	*Sphagnum* remains	3830	40	4089-4379	4275
LG2	250-251	Beta-199815	*Sphagnum* remains	4210	50	4635-4915	4876
LG2	326-327	Beta-199816	*Sphagnum* remains	4960	50	5596-5911	5767
LG2	350-351	Beta-199817	*Sphagnum* remains	5300	50	5977-6282	6139
LG2	395-397	Beta-199819	Terrestrial plants macroremains	6100	40	6798-6891	6891

Table 12: ^{14}C-AMS samples, depth, ^{14}C ages, and best fit 'Bacon' model calibration estimates for seventeen from the HBL-JBL area. [a.] Refers to dates that contain ^{14}C from atomic weapons testing. [b.] Refers to outliers that were eliminated by 'Bacon'.

Core	Depth (cm)	Lab I.D. #	Material	^{14}C age	±	Age Range (ybp)	Best Fit (ybp)
LG3	35-36	Beta-199818	*Sphagnum* remains	980	40	791-1271	932
LG3	75-76	Beta-199819	Terrestrial plants macroremains	2560	40	2374-2784	2749
LG3	130-131	Beta-199820	*Sphagnum* remains	3910	40	3802-4412	4281
LG3	190-191	Beta-199821	*Sphagnum* remains	4460	40	4881-5126	4959
LG3	249-250	Beta-199822	*Sphagnum* remains	4800	40	5411-5676	5542
LG3	329-330	Beta-199823	*Sphagnum* remains	5310	50	6111-6451	6187
LG3	374-375	Beta-180474	Terrestrial plants macroremains	5980	60	6715-7185	6835
LLC	51-52	UCI AMS 43480	*Sphagnum* stems	340	20	172-562	347
LLC	77-78	UCI AMS 58634	*Sphagnum* stems	915	15	773-913	885
LLC	102-103	UCI AMS 50203	*Sphagnum* stems	1205	15	1096-1276	1149
LLC	120-121	UCI AMS 57419	*Sphagnum* stems	1980	15	1882-1997	1919
LLC	140-141	UCI AMS 57421	*Sphagnum* stems	2550	15	2506-2771	2731
LLC	153-154	UCI AMS 50204	*Sphagnum* stems	2915	15	2969-3154	3101
LLC	201-202	UCI AMS 43479	*Sphagnum* stems	3745	20	3988-4188	4010
LLC	250-251	UCI AMS 58636	*Sphagnum* stems	4165	20	4594-4844	4783
LLC	293-294	UCI AMS 50205	*Sphagnum* stems	4450	15	5008-5298	5076
LLC	350-351	UCI AMS 43478	*Sphagnum* stems	4985	20	5636-5921	5792
LLC	439-440	UCI AMS 50206	*Sphagnum* stems	6055	15	6817-7032	6879
LLC	480-483	Beta-223743	Ericaceous Leaf Fragments	6640	40	7431-7676	7576
Lost Moose	40-45	GSC-5321	Peat	290	80	308-678	448
Lost Moose	50-55	GSC-5226	Peat	420	90	450-1050	636
Lost Moose	68-73	GSC-5284	Peat	1990	70	1543-2118	1897
Lost Moose	125-135	GSC-5221	Peat	4270	70	4225-5250	4677
McClintock	18-20	Hela-670	Bulk Peat	395	35	50-785	482
McClintock	70-72	AECV 1719C	Bulk Peat	2230	80	2047-2732	2287
McClintock	108-110	Hela-3850	Bulk Peat	4280	110	3992-5077	4616
McClintock	160-166	AECV 1718C	Wood	5810	90	6303-7098	6501
MOS	40-41	UCI AMS 57424	*Sphagnum* stems	355	15	168-678	452
MOS	70-71	UCI AMS 54958	*Sphagnum* stems	1270	25	1115-1305	1218
MOS	95-96	UCI AMS 64586	*Sphagnum* stems	1990	20	1863-2018	1927
MOS	108-109	UCI AMS 67515	*Sphagnum* stems	2065	25	2013-2148	2068
MOS	120-121	UCI AMS 54959	*Sphagnum* stems	2225	25	2177-2357	2164
MOS	136-137	UCI AMS 64588	*Sphagnum* stems	2490	20	2496-2746	2703
MOS	172-173	UCI AMS 54960	*Sphagnum* stems	3275	25	3396-3611	3553
MOS	224-225	UCI AMS 54961	*Sphagnum* stems	4185	25	4612-4882	4629
MOS	246-247	UCI AMS 57426	*Sphagnum* stems	4740	15	5289-5649	5437
MOS	296-297	Beta-223744	*Sphagnum* stems	6200	40	6709-7269	7049

Table 13: ^{14}C-AMS samples, depth, ^{14}C ages, and best fit 'Bacon' model calibration estimates for seventeen from the HBL-JBL area. [a.] Refers to dates that contain ^{14}C from atomic weapons testing. [b.] Refers to outliers that were eliminated by 'Bacon'.

Core	Depth (cm)	Lab I.D. #	Material	^{14}C age	±	Age Range (ybp)	Best Fit (ybp)	
MOS MaP1	60	UCI AMS 45796	*Sphagnum* stems, ericaceous leaves and coniferous needles	925	20	676-1031	867	
MOS MaP1	78	UCI AMS 45797	*Sphagnum* stems, ericaceous leaves and coniferous needles	1280	20	1160-1300	1269	
MOS MaP1	100-102	Beta-227710	*Sphagnum* stems, ericaceous leaves and coniferous needles	2610	50	2214-2874	2610	
MOS RiP2	42	UCI AMS 43471	*Sphagnum* stems	230	20	-182-868	309	
MOS RiP2	56	UCI AMS 43470	*Sphagnum* stems, ericaceous leaves and *Picea mariana* needles	1240	20	1099-1324	1272	
MOS RiP2	69-71	UCI AMS 43472	Ericaceous leaves and coniferous needles	545	20	1489-2199	1633	
MOS RiP2	75	UCI AMS 43473	Picea mariana needles	2350	100	1745-2460	2074	
MOS RiP2	101-102	UCI AMS 50320	Larix laricina and *Picea mariana* needles	3040	15	3124-3524	3383	
Oldman	33-36	Beta-44538	Peat	280	90	81-636	334	
Oldman	45-48	Beta-44539	Peat	870	90	497-777	703	
Oldman	63-66	Beta-44540	Peat	990	70	743-993	907	
Oldman	69-74	Beta-43025	Peat	1010	70	819-1064	932	
Oldman	97-102	Beta-43026	Peat	1520	70	1242-1517	1326	
Oldman	134-144	Beta-42375	Peat	2010	70	1657-2092	1793	
Oldman	158-163	Beta-43027	Peat	2940	70	1906-2321	2113	a.
Oldman	200-205	Beta-42376	Peat	2610	70	2465-2850	2715	
Oldman	255-260	Beta-42377	Peat	3060	70	3165-3620	3446	
Oldman	296	Beta-42378	Peat	3690	70	3894-4409	4212	
Oldman	350-355	Beta-43028	Peat	4910	11	5426-5681	5594	
Oldman	369-374	Beta-42379	Peat	5310	80	6124-6524	6255	
Oldman	413-417	Beta-42380	Peat	5980	100	6453-6913	6517	
Oldman	441-446	Beta-42381	Peat	5920	90	6811-7381	6908	

Table 14: ^{14}C-AMS samples, depth, ^{14}C ages, and best fit 'Bacon' model calibration estimates for seventeen from the HBL-JBL area. [a.]Refers to dates that contain ^{14}C from atomic weapons testing. [b.]Refers to outliers that were eliminated by 'Bacon'.

Core	Depth (cm)	Lab I.D. #	Material	^{14}C age	±	Age Range (ybp)	Best Fit (ybp)
Silcox	20-25	GSC-5265	Peat	550	50	495-685	542
Silcox	38-43	GSC-5266	Peat	1010	60	847-1302	993
Silcox	65-70	GSC-5245	Peat	3120	60	2688-3643	3359
SL1	1-2	Poz-19656	NA	115	0.36	-530-545	229
SL1	10-11	Poz-18597	NA	1120	30	833-1133	1042
SL1	41-42	Poz-16805	NA	1614	36	1445-1645	1559
SL1	45-46	Poz-10675	NA	1750	30	1563-1708	1658
SL1	58-59	Poz-19658	NA	1770	30	1716-1936	1834
SL1	66-67	Poz-19659	NA	2160	30	2002-2317	2278
SL1	83-84	Poz-16806	NA	2605	35	2566-2876	2784
SL1	91-92	Poz-19660	NA	2915	30	2907-3162	3027
SL1	114-115	Poz-19661	NA	3250	35	3397-3657	3567
SL1	124-126	AECV 1966c	NA	3690	90	3627-4027	3947
SL1	155-156	Poz-19662	NA	3890	35	4238-4848	4444
SL1	181.5-182.5	Poz-20142	NA	5250	40	5532-6217	5838
SL1	195-196	AECV 1905c	NA	5780	90	6181-6731	6406
STE	45-46	UCI AMS 54962	*Sphagnum* stems	105	30	-72-368	69
STE	67-68	UCI AMS 58645	Picea leaf fragments	600	20	559-669	650
STE	79-80	UCI AMS 64589	*Sphagnum* stems	1175	20	1001-1191	1078
STE	98-99	UCI AMS 54963	*Sphagnum* stems	1715	25	1552-1717	1641
STE	124-125	UCI AMS 65381	*Sphagnum* stems	2445	20	2345-2735	2399
STE	160-161	UCI AMS 54964	*Sphagnum* stems	3255	30	3356-3571	3512
STE	179-180	UCI AMS 67514	*Sphagnum* stems	3415	25	3608-3768	3703
STE	201-202	UCI AMS 65382	*Sphagnum* stems	3485	20	3777-3992	3853
STE	223-224	UCI AMS 54965	*Sphagnum* stems	3960	30	4183-4528	4287
STE	239-240	UCI AMS 58643	*Sphagnum* stems/Picea leaf fragments	3975	15	4423-4863	4493
STE	285-286	UCI AMS 40360	*Sphagnum* stems	6225	20	5632-7302	5425
VC0406	62-63	Beta-281000	*Sphagnum* stems	1130	40	786-1286	1004
VC0406	110-111	Beta-281001	Twigs	2140	40	2010-2330	2153
VC0406	185-186	Beta-281002	*Sphagnum* stems	3770	40	3967-4392	4168
VC0406	237-238.5	Beta-280032	Wood	4760	40	5274-5649	5605
VC0406	303-304	Beta-281003	Wood fragments	5820	40	6580-6855	6729
VC0406	303-304	Beta-281004	Conifer needles	5890	40	6580-6855	6729

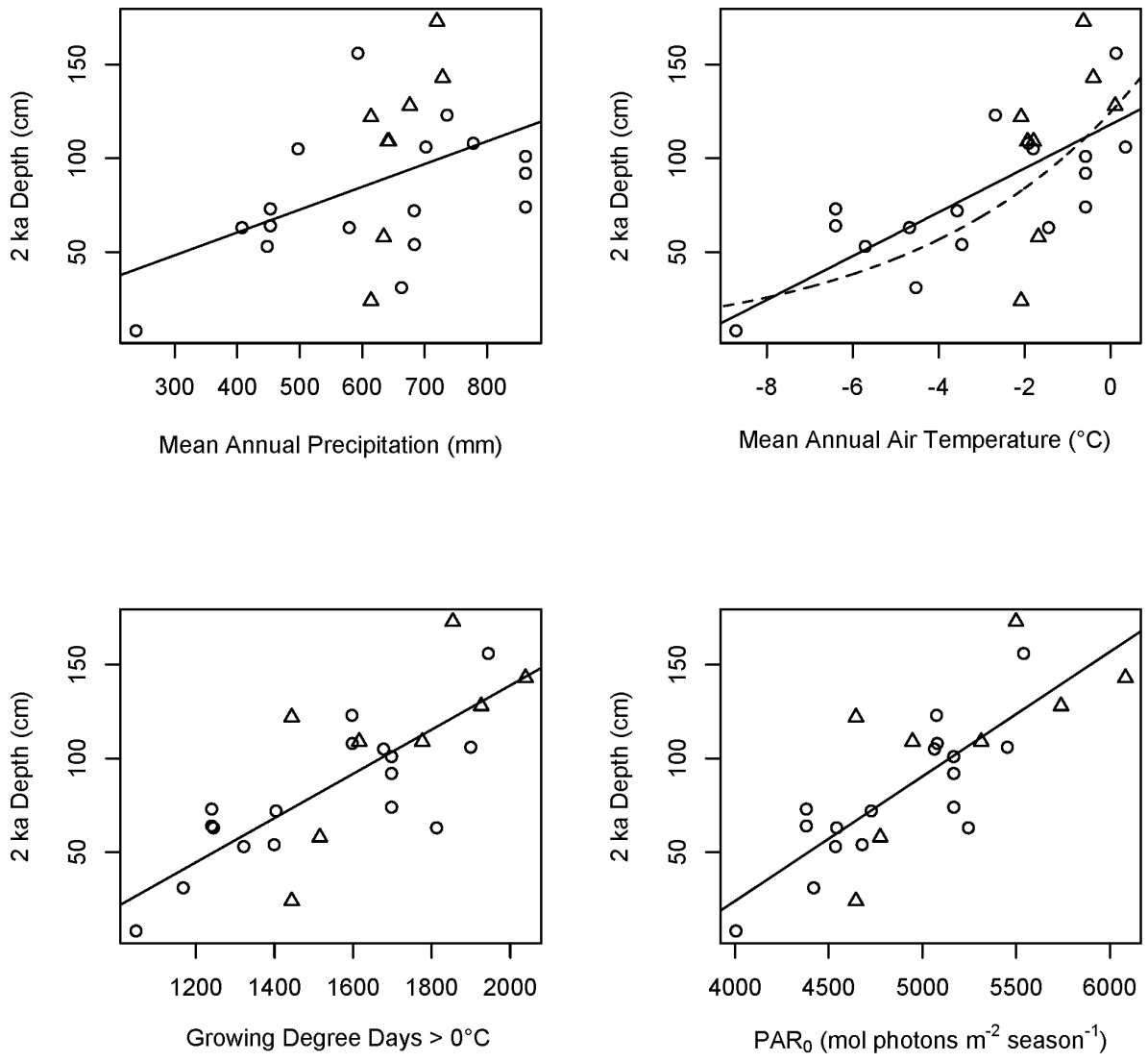

Figure 18: Four scatterplots correlating 2 ka depth as a function of environmental variables. Figures are arranged from left to right and top to bottom in order of the linear model's r^2 value. Solid lines represent the best fit for linear regressions. Dashed lines represent to the best fit for an exponential regression. Triangles represent new JBL site data. Circles represent review data.

3.4.3. Permafrost Occurrence and Peat Depth

Permafrost occurrence was found to have a significant effect on 2 ka depths, and total depths in the twenty-five HBL-JBL cores (Fig. 19). A one-way ANOVA determined that there is a statistically significant difference between the depths of permafrost peatlands, and non-permafrost peatlands ($p<0.05$). A one-way ANOVA showed that permafrost peatlands have a significantly shallower 2 ka depth than non-permafrost peatlands ($p<0.0001$). Permafrost total depths average 182.8 ± 31.6 cm, whereas non-permafrost total depth average 290.6 ± 112.0 cm. Permafrost 2 ka depths average 41.3 ± 23.6 cm for permafrost peatlands, while non-permafrost bogs average 103.4 ± 33.4 cm.

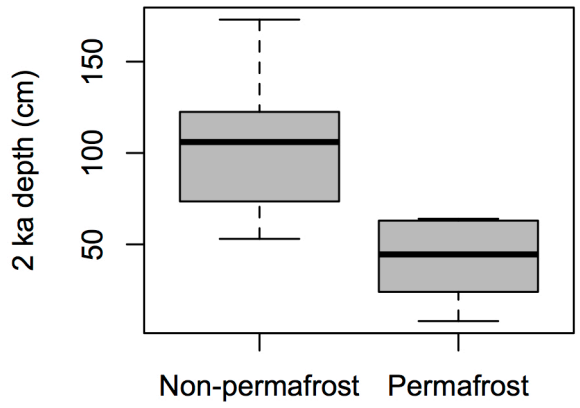

Figure 19: Bar and whisker plot of 2 ka depths in permafrost and non-permafrost peat. Central lines represent medians. Box edges represent the 25% upper and lower quantiles. Whisker lines represent least and greatest values.

3.5. DISCUSSION

3.5.1. C Accumulation in the JBL

C accumulation measurements in the eight new JBL sites showed that 40% of C is younger than 2 ka in the southwest JBL *Sphagnum* bogs. This is roughly comparable to estimates for WSL, where 41% of C is younger than 2 ka (Sheng et al., 2004; Beilman et al., 2009). Only two of my sites, JBL4 and JBL8, have more post-2 ka C than pre-2 ka C, which may have been caused by low relative pre-2 ka accumulation, relatively high belowground C mineralization, or a combination of both. Apparent rate of C accumulation is driven by autogenic drivers, allogenic drivers, and complex internal ecohydrological feedbacks, and has the potential to vary substantially among peatlands (Belyea and Baird, 2006).

3.5.2. MAAT, GDD_0 and PAR_0 as Drivers of Post-2 ka Vertical Peat Accumulation

In my analysis, differing scales show different correlations between post-2 ka apparent rate of C accumulation, 2 ka depth, and four climate variables. In the eight new JBL sites MAP significantly correlated with both post-2 ka apparent rate of C accumulation, and 2 ka depth. This correlation is also significant and positive in my review dataset, but was low relative to MAAT, GDD_0 and PAR_0. MAP may exercise some local control over peat accumulation in the JBL, but temperature, seasonality, and photosynthetically active radiation are likely the major drivers of vertical peat accumulation in the entire HBL-JBL. This supports the conclusions of a recent global synthesis of peatland C accumulation rates. Water table depths need to be persistently high for peat to form. However, once they are present, they do not explain any of the variance of C

accumulation rates (Charman et al., 2013). It is also possible that small sample size in the new JBL sites (n = 8) may lower the dataset's descriptive power.

In the entire HBL-JBL synthesis, there was a significant and positive correlation between 2 ka and MAP ($p < 0.05$; Tab. 10), however, we did not observe the inverse relationship with precipitation similar to that reported by a broad survey North American peatlands (Gorham et al., 2003). This may be due to the topographic controls in southern sites (Gorham et al., 2003) that are not present in the more topographically homogenous HBL-JBL, which I heavily sampled. This was also not a robust relationship because the correlation was heavily influenced by EL1 site data (MAP = 208 mm, 2 ka depth = 8 cm). If the point is deleted the r^2 value lowers to 0.087, and the statistical significance is eliminated.

My study showed that MAAT had a significant effect on vertical peat accumulation since 2 ka in the HBL-JBL (Fig. 18; Tab. 11). This is analogous to the relationship found between MAAT and 2 ka depth in WSL; however, there are key differences between the two areas. In WSL, data fits an exponential regression that explains more variation ($r^2 = 0.82$; Beilman et al., 2009) than the HBL-JBL data's exponential regression ($r^2 = 0.49$). In WSL there is less variability in 2 ka depth for permafrost sites, as well as deeper 2 ka depths in southern non-permafrost bogs (Beilman et al., 2009).

My hypotheses, that GDD_0, and PAR_0 are major drivers of peat accumulation in the HBL-JBL, are supported by significant and positive correlations between these variables and 2 ka depths. PAR_0 has the highest correlation ($p<0.0001$, $r^2=0.62$; Tab. 10). In a previous study that analyzed global *Sphagnum* productivity a linear regression

between PAR_0 and *Sphagnum* productivity explained a significant but comparatively small amount of variance (r^2=0.23; Loisel et al., 2012). PAR_0 integrates photosynthetically active radiation over the growing season length and can potentially influence two different aspects of peat formation. Photosynthetically active radiation and growing season length may both drive plant growth, and thus litter input (Clymo, 1998). Growing season length also affects the length of time each year that the ground is unfrozen and biomass can pass from the acrotelm to the catotelm (Clymo, 1998; Gorham et al., 2003). My results also support a global study of peatland apparent rate of C accumulation over the last 1000 years, in which GDD_0 and PAR_0 were found to correlate significantly with post-1 ka apparent rate of C accumulation (Charman et al., 2013). However, the significance of radiation as a driver of *Sphagnum* growth has been debated because of the high degree of shading in boreal peat bogs, and due to photoinhibition occurring in *Sphagnum* photosynthetic tissues (Harley et al., 1989; Murray et al., 1993).

The relationship of growing season length and photosynthetically active radiation to vertical peat accumulation is important because northern latitudes will be disproportionately affected by global warming. Models of future anthropogenic climate forcing predict disproportionate seasonality changes in northern latitudes, and increases in the length of the growing season (IPCC, 2007). Between 1982 and 1999 the effective start of the growing season advanced 5.4 days in the northern hemisphere (Jeong et al., 2011). Remote sensing images indicate that the plant growth in the Canadian low arctic has increased 0.46–0.67% yr^{-1} from 1982 to 2006 (Jia et al., 2009). However, there will

likely be complications modeling PAR_0 as a predictive bioclimatic variable because of the uncertainty in model prediction of future cloud cover (Charman et al., 2013).

3.5.3. The Effect of Permafrost on Peat Depth

Significantly shallower basal depths and 2 ka depths in permafrost peatlands compared to peatlands that were permafrost-free supported my hypothesis, that permafrost occurrence inhibits peat accumulation. My hypothesis, that permafrost occurrence significantly decreased post-2 ka vertical accumulation, was supported by significantly shallower 2 ka depths in permafrost peat, compared to non-permafrost peat ($p<0.0001$). Previous studies indicate that permafrost likely formed during the Little Ice Age (Vitt et al., 2000b) during the late-Holocene in Western Canada. However, the timing of permafrost formation in Eastern Canada is not as well understood. Either, permafrost establishment earlier than 2 ka, or general lower productivity due to constantly lower MAAT, GDD_0, and PAR_0 without the direct influence of permafrost, may explain overall shallower permafrost peat.

There was consistent vertical growth in peatlands post-2 ka. Only two cores, JBL5 and EL1, contained near surface macrofossils that dated pre-modern. JBL5 had dates of 204 and 207 ybp at 8 and 12 cm respectively (Tab. 4), and EL1 had a 13 cm depth dating near 3.0 ka (Tab. 11). Besides these two sites, there is little evidence for the recent shutdown of permafrost 2 ka C accumulation described in the WSL (Beilman et al., 2009). Post-2 ka depth measurements indicated diminished, but ongoing, vertical

accumulation, similar to the described activity in a survey of subarctic palsas (Olefeldt et al., 2012).

Controls of permafrost on late-Holocene peat growth show that productivity, rather than decay currently drives the significant climatically related differences in peat growth observed here. However, the resulting changes in hydrology and CH_4 emissions from melting permafrost will likely result in a greater uncertainty in peatland C cycle feedbacks (IPCC, 2007). Past studies of northern and southern regions in the HBL-JBL show that CH_4 emissions were lower than previously estimated (Roulet et al., 1994). If non-permafrost peatlands store C faster than permafrost peatlands, then peatlands could act as a negative feedback to future warming (Turetsky et al., 2007; Beilman et al., 2009) at least as transient reactions to warming. The effect of permafrost melt on hydrology is also controversial. Some studies project that permafrost melts will increase drainage (Jorgenson and Osterkamp, 2005; Riordan et al., 2006) while others claim that it will increase peatland extent (Payette et al., 2004).

3.6. CONCLUSION

In the eight peatlands that I studied in the JBL, approximately 40% of their total soil C, 16.3 to 62.5 kg C m^{-2}, is younger than 2 ka. In the entire HBL-JBL, vertical peat growth since 2 ka correlates significantly and positively with modern mean annual precipitation. 2 ka depth in the entire HBL-JBL also correlates significantly and positively with atmospheric thermal properties, and most closely with photosynthetically active radiation integrated over the growing season. There is also evidence for significantly

reduced, although continuing, post-2 ka peat accumulation in permafrost bogs. These two pieces of evidence suggest the possibility that initial increased productivity of northern peatlands due to projected climate change in the 21st century and the arctic amplification of warming could produce increased C storage and a potential negative feedback to potential climate warming at least in a transient fashion until the climatic envelope for peatland maintenance is exceeded in northern regions.

4. Mid to Late-Holocene changes in Hydrology, Peatland Ecology, and Carbon Accumulation in the Canadian James Bay Lowlands

4.1. ABSTRACT

Holocene hydrological and ecological variations are important for understanding high-latitude peatland dynamics because they affect the rates of soil carbon (C) accumulation. I reconstructed a 7.4 ka (ka = 1,000 calendar years before present [ybp]) record of water table depth (WTD) for a peatland in the James Bay Lowlands using testate amoebae. WTD varied from 6 to 35 cm over the last 7.4 ka with relatively dry conditions from 7.4 to 4.5 ka, and moister conditions from 4.5 to 2.4 ka likely reflecting large-scale changes in atmospheric circulation. The Medieval Climate Anomaly (1000 – 700 ybp) was a relatively wet event, and the Little Ice Age (500 – 200 ybp), was a relatively dry event. This pattern is consistent with other reported records in the region, as well as modern responses of precipitation patterns to periods of North American warming and cooling and La Nina/El Nino variations. I also compared fluctuations in WTD to macrofossil-based records of peatland ecological conditions. At approximately 4.5 ka the peatland exhibited a shift in ecology from a *Sphagnum* dominated bog to an herbaceous dominated fen that was associated with an extreme wet period. The inundation of a *Sphagnum* peatland by calcium rich water could have caused this unconventional ecological change. Generally high C accumulation rates at the site were associated with wet conditions. However, LARA also rose during brief droughts

indicating that extreme hydrological events have a complex relationship with peat productivity, and decay rates

4.2. INTRODUCTION

Peatlands serve a dual climatic role as important carbon (C) sinks and as archives of past events for which data from their stratigraphy can elucidate climate – C relations (Clymo, 1998; Bridgeham et al., 2006; Dise, 2009; Chambers et al., 2011). Peatland climate proxies can be used to generate data, and validate models of hydrology and precipitation patterns (Booth et al., 2006; Booth et al., 2012). Testate amoebae (TA) have proved useful for performing WTD and pH reconstructions in peatlands and lakes (Charman et al., 2000; Booth, 2008; Mitchell et al., 2008). Studies in Scandinavia (Andersson and Schoning, 2010), the Quebec James Bay Lowlands (JBL; Loisel and Garneau, 2010; Lamarre et al., 2012) and Ontario (Bunbury et al., 2012; Elliot et al., 2012) have reconstructed WTD with TA, and then compared WTD to peatland vegetation reconstructions using macrofossils, and/or long-term apparent rate of C accumulation (LARCA). Such work allows a direct linking of hydrology to vegetation change and variations in LARCA.

Globally TA based WTD records have been used to reconstruct both site-specific, and climate driven hydrological patterns. They have provided data on differential drainage between sites (Warner et al., 1992; Klein et al., 2013), and have been linked to autogenic changes such as shifts in surface plant community ecology (Lamentowicz et al., 2010, McMullen et al., 2004) and hummock-hollow development

(Andersson and Schoning, 2010). They have also been useful for reconstructing climate patterns related to solar intensity cycles (Hughes et al., 2006; Mauquoy et al., 2008), broad changes in precipitation related to the Holocene Thermal Maximum (HTM; Nichols et al., 2009), El Niño Southern Oscillation (ENSO; Mcglone and Wilmhurst, 1999; Booth et al., 2005), and North Atlantic Oscillation (NAO; Charman and Hendon, 2000). TA have been instrumental in documenting the effect of the Medieval Climate Anomaly (MCA; 1000 – 700 calendar years before present [ybp]; Bunbury et al., 2012; Booth et al., 2012), the Little Ice Age (LIA; 500 – 200 ybp; Bunbury et al., 2012; Lammare et al., 2012), modern climate change, and many droughts of regional to global scale (Booth et al., 2005; Booth et al., 2012).

Long-term apparent rate of C accumulation (LARCA; Gorham et al., 1991; Clymo, 1998) at individual sites is sensitive to water table fluctuations, peat vegetation composition, and rates of decay in addition to atmospheric thermal properties and photosynthetically active radiation (Laiho, 2006; Beilman et al., 2009; Loisel and Garneau, 2010; Loisel et al., 2012; Charman et al., 2013; Ch. 3). Future climate change may cause shifts in the magnitudes and directions of C fluxes; therefore, it is important be able to predict moisture changes, as well as the relationship between moisture and peatland C storage. In this chapter I present water table depth (WTD) reconstructions for a peatland in Ontario based on (TA) in order to test hypotheses regarding variations in Holocene circulation and precipitation patterns in boreal Canada. I also compare this hydrological reconstruction to previously published macrofossil, and LARCA data to elucidate the complex relationship between WTD, peat vegetation/macrofossil content, and LARCA.

The Hudson and James Bay Lowlands (HBL-JBL) of Canada are part of the second largest peatland complex in the world (Riley, 2011; Tarnocai, 2011), and are underrepresented by paleohydrology studies; currently having one TA based WTD reconstruction (Bunbury et al., 2012). Precipitation in Canada has been dependent, both historically and at present, on the position of the Arctic and Pacific Fronts, and the phases of ENSO and NAO. Before the HTM the arctic front had a relatively southern position as documented by stable isotope records ~7 ka (ka = 1,000 ybp; Edwards et al., 1996). The arctic front moved north during the HTM to its' most northern extent between 6 and 4 ka, along with the northernmost position of the tree line (Edwards et al., 1996; MacDonald et al., 1998; Beringer et al., 2001). During the MCA (Lamb, 1965; Broecker, 2001; Moberg et al., 2005; Mann et al., 2009; Ljungqvist et al., 2010; Graham et al., 2011), relatively cool, La Niña-like Pacific Sea surface temperatures (SST), possibly coupled with an anomalously warm North Atlantic, caused drought across most of North America (Booth et al., 2005). However, modern observations show that regions of Central Ontario are prone to positive precipitation anomalies under La Niña conditions (Seager et al., 2008; Fig. 20). TA analysis in the area indicates that the MCA and the LIA (Mauquoy et al., 2002; Viau et al., 2002; Moberg et al., 2005; Mann et al., 2009; Ljungqvist et al., 2010) were likely wet events (Bunbury et al., 2012). However, the LIA has been reported as more spatially variable in WTD reconstructions in Canada because of the southern movement of the Arctic front (Kaislahti Tillman et al., 2010), and hydrological changes caused by the formation of permafrost (van Bellen et al., 2011; Lammare et al., 2012). The modern extent of the Arctic front is variable, and dependent on temperature (Mamet and Kershaw, 2011).

It is important to understand the drivers of local hydroecological change because fen to bog transitions likely have a large effect on greenhouse gas emissions (MacDonald et al., 2006; Dise, 2009). Models of peatland development often treat fens and bogs as alternative stable states, which maintain competitive advantages by positive feedback with abiotic conditions (Meinders and van Breemen, 2005; Eppinga et al., 2009). Bogs outcompete fens by maintaining a positive feedback with groundwater chemistry (low pH, and low nutrient concentrations), whereas fen vegetation out-competes bog vegetation for light (van Breemen, 1996; Meinders and van Breemen, 2005; Eppinga et al., 2009). In Chapter 3, I presented the results of macrofossil analyses for eight cores in the JBL. In classic models of peat succession minerotrophic fens, dominated by herbaceous vegetation, transition to *Sphagnum* dominated, ombrotrophic bogs due to paludification by *Sphagnum* (van Breemen, 1995). However, several sources list possible modes of peatlands reversing this trend by transitioning from *Sphagnum* dominated systems to *Carex* dominated systems due to flooding (Mitchell and Niering, 1993; Lamers et al. 2002; Bauer et al., 2003).

Future precipitation change may induce C cycle feedbacks by directly or indirectly affecting the productivity and decay of peat. Although growing season length and photosynthetically active radiation are the dominant drivers of peat accumulation over the late-Holocene (Beilman et al., 2009; Loisel et al., 2012; Charman et al., 2013), peat needs to form within a climatic envelope dominated by surface moisture (Laiho, 2006; Yu et al., 2009). Multi-year observations of fens and poor fens in Alberta showed that productivity during drought years is constrained by available moisture (Adkinson et al., 2011). LARCA in bogs can be highly dependent on moisture thresholds of

Sphagnum species (Strack et al., 2009). However, drought can also change the density of peat because of bog collapse (Winston, 1994), and the phenotypic plasticity of *Sphagnum* mosses (Turetsky et al., 2008). Some studies indicate that WTD drawdown can decrease *Sphagnum* productivity (Robroek et al., 2009), as well as increase peat decay (Fenner and Freeman, 2011). While other studies show that *Sphagnum* is more competitive during fluctuating WTD conditions (Breeuwer et al., 2008).

In this chapter I address several research questions regarding Holocene hydrology, ecology, and C accumulation at a peatland in the JBL: 1. What was the range and variability of WTD throughout the pre-HTM and HTM of the mid-Holocene (7.4 – 2.5 ka; Kaufman et al., 2004) and cooler late-Holocene Neoglacial period (2.5 ka – present day)? 2. What was the range and variability of WTD during the warm MCA (1000 – 700 ybp) and cooler LIA (500 – 200 ybp)? 3. What hydrological change, if any, was associated with succession events that were previously reported for JBL7 (Ch. 2)? 4. How has LARCA responded to long and short-term changes in hydrology during the mid and late-Holocene, and were such responses to hydrological changes consistent for all wet and dry periods?

4.3. MATERIALS AND METHODS

4.3.1. Study site and core information

JBL7 (54°23’43.1” N, 89°31’19.7” W; Fig. 20) is a raised peat bog in the JBL. A stratigraphic core was collected in the summer of 2008 as part of an eight core transect

of central and northern Ontario. The site is part of a large wetland complex, with *Picea mariana* stands of varying ages, open *Ledum* spp., *Chamaedaphne* spp., and *Sphagnum fuscum* dominated hummocks, and occasional lichen mats. JBL7 is located just south of the discontinuous permafrost zone and the average summer boundary between the moist Pacific front and the dry Arctic front. JBL7 exists in a watershed with very low relief and surface water moving through meandering streams and rivers; there is a relatively small stream channel downslope 1 km to the south and a larger river downslope 9 km to the north.

I created an age-depth model using multiple radiocarbon (^{14}C) dates and 'Bacon' age-depth modeling software (Fig. 21; Tab 5; Blaauww and Christen, 2011). Methods and results are detailed in Chapter 2. I analyzed macrofossil assemblages based on semi-quantitative lab identification of relative abundances of recognized macrofossil groups, and identified down to the genus or species level when possible (Ch. 2; Fig. 10).

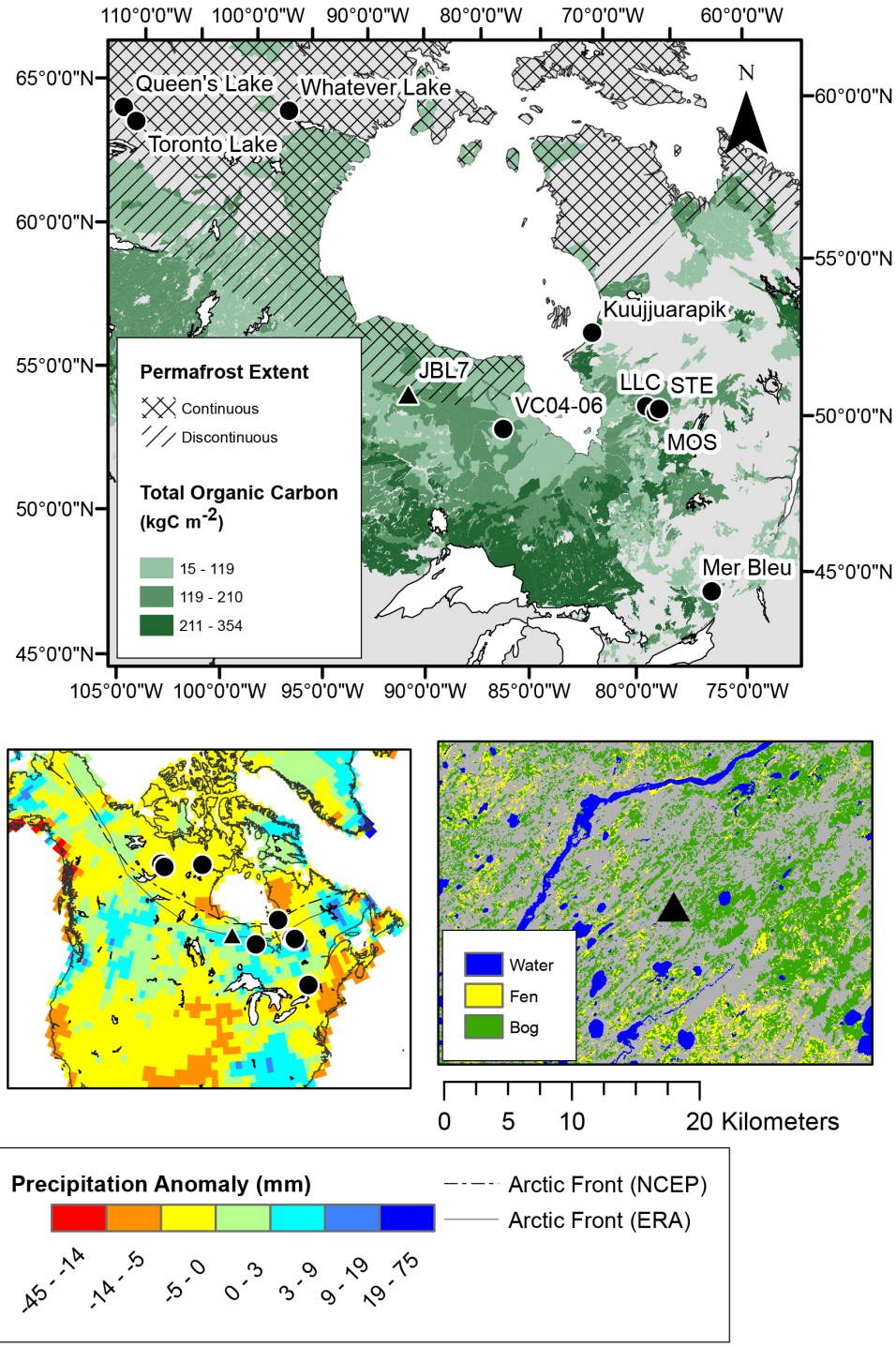

Figure 20: JBL7 is located in area that is crucial to understand because of its high levels of soil C, precipitation anomalies, and local hydrology. Top: JBL7 and notable review sites mentioned in the text, as well a peatland C mass, and permafrost distribution (Brown et al., 1998; Tarnocai, 2011). Bottom left:. A map showing compiled precipitation anomalies for the seven most extreme La Niña events since 1949 according to the Multivariate ENSO Index (1949-51, 1954-56,1964-66,1970-1972,1973-75, 1988-90, 2010-2011; NOAA/ESRL, 2013a,b), as well as the modern position of the arctic front (Ladd and Gajewski, 2009). Bottom right: Local surface hydrology, and both fen and bog distribution near JBL7 (Provincial Land Cover Data Base, Second Edition; 2000).

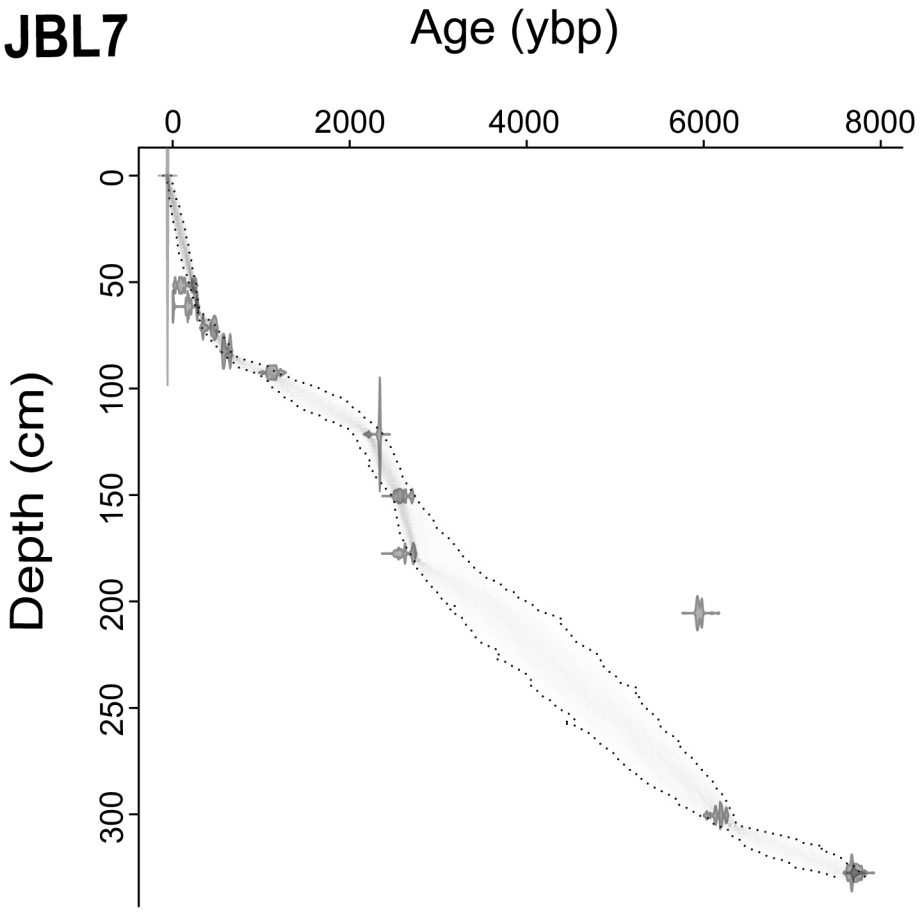

Figure 21: The age-depth Model for JBL7 using multiple ^{14}C ages, and 'Bacon' statistical software (Blaauww et al., 2011).

4.3.2. TA processing

I used a combination of high-resolution sampling, based on age-depth models (Fig. 21), and coarse resolution sampling, to reconstruct hydrological variability in JBL7. The sampling resolution post-2 ka varied depending on the age-depth model, but was generally lower than 60 years sample^{-1}, in order to register relatively short climate evens such as the MCA and LIA. I used a lower resolution standard sampling interval 4 cm on

pre-2 ka sections of the cores to capture broader trends earlier Holocene WTD variability in relation to the HTM, and long-term ecological changes. Temporal resolution pre-2 ka was also limited by low-test counts in some sections.

Processing and identification of TA followed protocols modified from Charman (2000) and Booth et al. (2010). I removed subsamples of peat using a stainless steal tube with a 1 cm diameter, measured them lengthwise with digital calibers to calculated sample volume (Ch. 2), boiled samples gently for 10 minutes, adding 1 tablet spiked with a known number of exotic *Lycopodium* spores, in order to verify the quality of processing and to calculate concentration of amoebae (Booth et al., 2010). I separated TA from peat using two stages of filtration (Booth et al., 2010). I filtered samples through a 250 µm filter and reverse-filtered them through a 7 µm filter. Common North American TA tests sizes typically fall between 10 - 200 µm in length (Charman, 2000; Booth et al., 2008). I centrifuged samples, added Saffron dye, preserved TA in glycerol, and counted tests under a compound microscope at 400 x magnification. I counted 150 tests sample^{-1} except for samples that had fewer than ~6000 tests cc^{-1}, for which I halted the analysis at 50 tests (Payne and Mitchell, 2009).

I identified TA following Charman et al. (2000) as modified by Booth (2008), including shells of the rotifer species, *Habrotrocha angusticollis* (Booth, 2008). The ubiquitous species identified in much previous work as *Amphitrema flavum,* is presented here as *Archerella flavum* to conform to current taxonomy and nomenclature (Gomaa et al., 2013). Several taxa were combined into single categories in this study, due to their ecological or morphological similarity (Tab. 15).

Table 15: A list of taxa (Booth, 2008) that were combined in this analysis because of ecological and morphological similarity.

Booth, 2008	Combined Categories
Heleopera rosea, *Heleopera sphagni,* and *Heleopera perticola*	*Heleopera* spp.
Amphitrema wrightianum, Amphitrema stenostoma	*Amphitrema wrightianum* type
Trignonopyxis minutae, Trigonopyxis arcula	*Trigonopyxis* spp.
Trinema lineare, Corythion dubium type	*Corythion dubium* type
Nebela bohemica, Nebela collaris	*Nebela bohemica* type

4.3.3. Statistics

I described TA percentages using a constrained cluster analysis (Bennett, 1996; Juggins, 2009; R development core team, 2013), and reconstructed WTD using a weighted-average transfer function approach (Booth, 2008). Figure 22 plots the optima and tolerances of major species identified in JBL7. Although North American transfer functions do not yet integrate surface sample data from the HBL-JBL, studies indicate that a transfer function's calibration dataset can affect the magnitude, but not the direction of WTD changes (Turner et al., 2013). I built stratigraphy plots displaying TA percentage, WTD, and LARCA using C2 software (Juggins, 2003). I also extrapolated WTD at 1 cm increments using linear interpolation, while excluding interpolated values from three areas with low TA concentration.

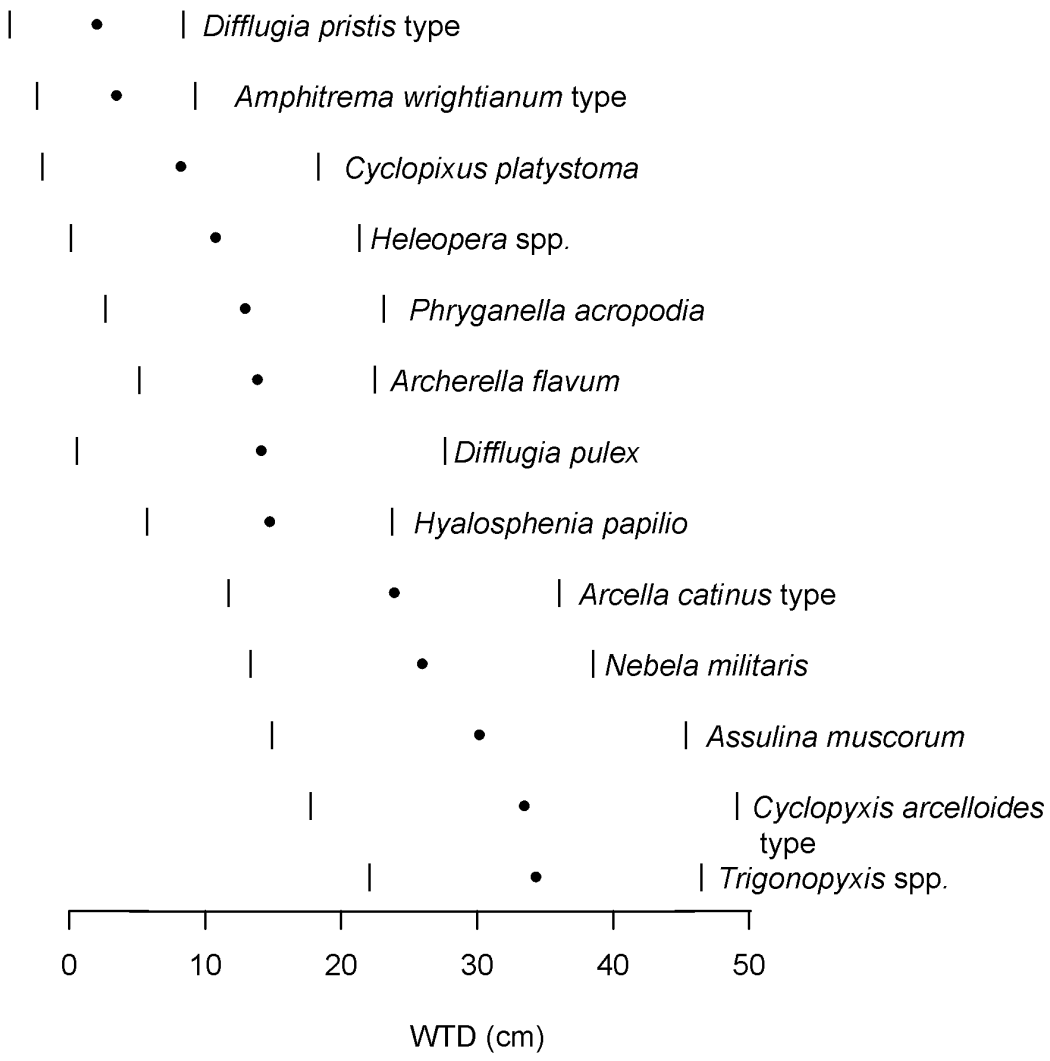

Figure 22: An xy plot with a list of common taxa identified in JBL7, as well as their mean WTD and minimum and maximum tolerances (Booth, 2008).

Table 16: Transfer function performance statistics for JBL7.

Transfer Function	RMSE	r^2
Weighted averaging model (inverse deshrinking) for wtd	8.27	0.70

4.4. RESULTS

4.4.1. TA and WTD

TA clustered into five zones (A–E; Fig. 23; Tab. 17). Zone A spans the mid-Holocene, the longest range of any of the zones, from 7.4 ka to 2.6 ka. The section is dominated by *Amphitrema wrightianum* type, *Archerella flavum*, *Assulina muscorum*, *Cyclopyxis arcelloides* type, *Cyclopyxis platystoma*, *Heleopera* spp., *Hyalosphenia papilio*, *Phyganella acropodia* type, and *Trigonopyxis* spp. WTD was the most variable during this period ranging from 8 - 35 cm and was 17 ± 7 cm on average. This period was marked by three discrete periods of sparse TA abundance ranging from 5976 - 5047 ybp, 4290 - 4083 ybp, and 3145 - 2720 ybp. Zone A ended following a brief dry period indicated by a local increase in *Trigonopyxis* spp. Zone B spans the pre-MCA period of the late-Holocene and had stable, moderate WTD (11 ± 2 cm). Dominant species include *Archerella flavum*, *Difflugia pulex*, and *Heleopera* spp. In Zone C (1258 – 721 ybp), *Archerella flavum* decreased, *Difflugia pulex* increased along with other common species, *Arcella catinus* type, and *Arcella vulgaris*. WTD increased the highest/wettest in the core (10 ± 2 cm). Zone D spans from 674 to 294 ybp and showed decreases in the *Arcella* and *Difflugia* species, as well as the dominance of *Archerella flavum*. WTD dropped to 12 ± 2 cm and ranged from 9 - 17 cm. Zone E ranges from 249 ybp to modern times and coincides with acrotelm peat. *Archerella flavum* was replaced in dominance by *Assulina muscorum*, *Hyalosphenia papilio*, and *Nebela militaris*. WTD was relatively low (20 ± 6 cm).

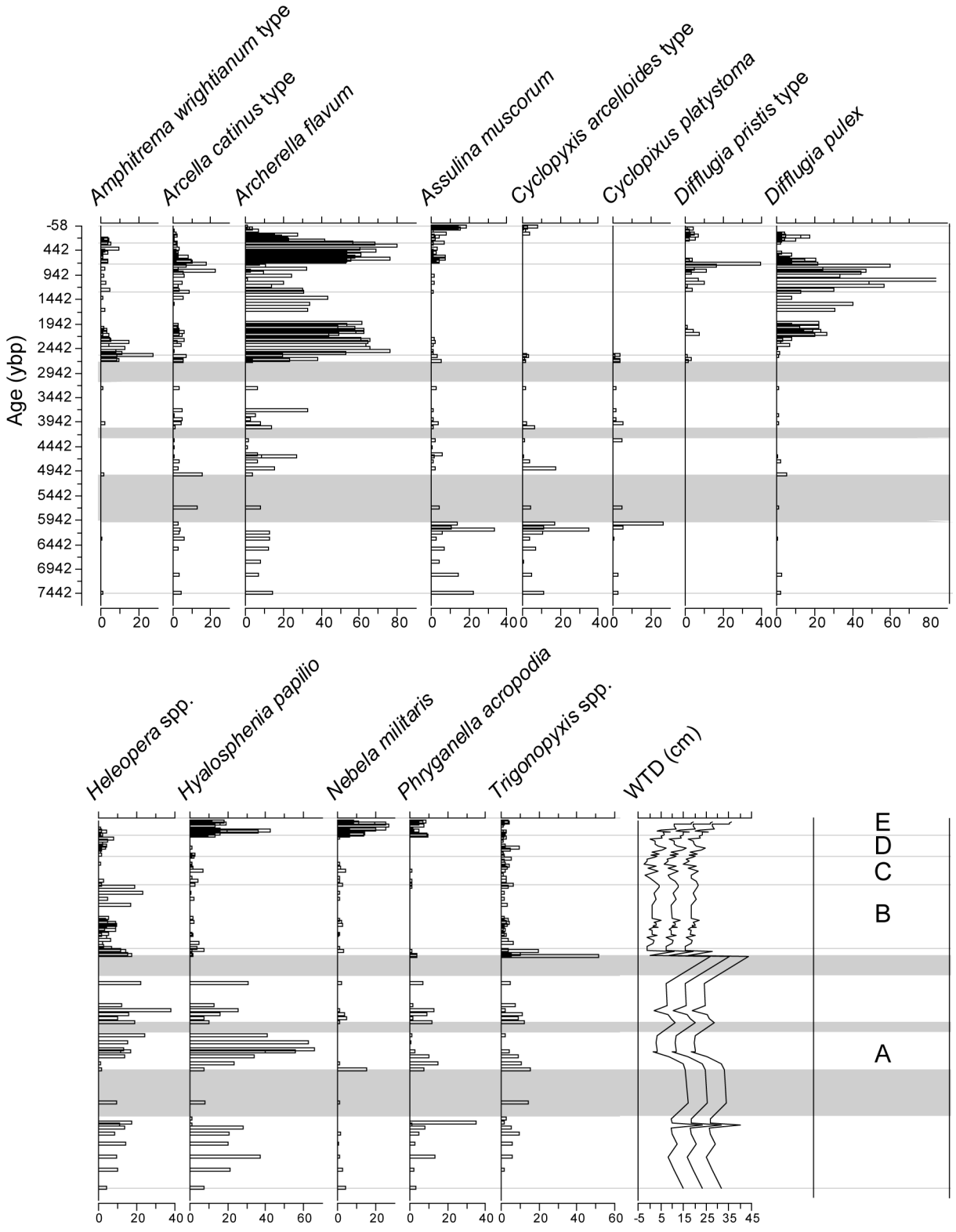

Figure 23: Stratigraphy data for JBL7 including, age, TA species > at least 20% at some point in the core, WTD reconstructions, and TA zones based on a constrained cluster analysis. Grey bars represent periods of low TA data.

Table 17: Zones, dominant taxa, and WTD descriptive statistics for JBL7, listed for each zone.

TA zone	Depth Range (cm)	Age Range (ybp)	Dominant Taxa	WTD Range (cm)	WTD Average (cm)
A	324 - 152	7425 - 2573	*Amphitrema wrightianum* type, *Archerella flavum*, *Assulina muscorum*, *Cyclopixus arcelloides* type, *Cyclopixus platystoma*, *Heleopera* spp., *Hyalsphenia papilo*, *Phryganella acropodia* type, *Trigonopyxis* spp.	8 - 35	17 ± 7
B	148 - 99	2542 - 1285	*Archerella flavum*, *Difflugia pulex*, *Heleopera* spp.,	7 - 14	11 ± 2
C	97 - 86	1258 - 721	*Arcella catinus* type, *Archerella flavum*, *Difflugia pristis* type, *Difflugia pulex*	7 - 13	10 ± 2
D	85 - 58	674 - 294	*Archerella flavum*, *Difflugia pulex*	9 - 16	12 ± 2
E	57 - 8	249 - -37	*Archerella flavum*, *Hyalsphenia papilo*, *Nebela militaris*	12 - 28	19 ± 6

The late-Holocene average WTD (13 cm) was higher than the average mid-Holocene WTD (18 cm). Zone C, corresponds with the timing of the MCA, and was relatively wet. Zone B corresponds with the timing of the LIA, and was relatively dry. Zone A corresponds with the last three centuries and was marked by gradual decline in WTD.

4.4.2. WTD changes associated with Macrofossil and LARCA Record

There were two major changes in the macrofossil assemblage that were associated with extreme hydrological events. The peatland initiated as a *Sphagnum*-dominated system,

transitioned into woody *Sphagnum* peat, and shifted to a herbaceous dominated fen system abruptly (4.5 ka; Fig. 24). This transition was associated with wet conditions compared to previous millennia. *Sphagnum* vegetation became dominant again at 2.4 ka following an extreme dry event.

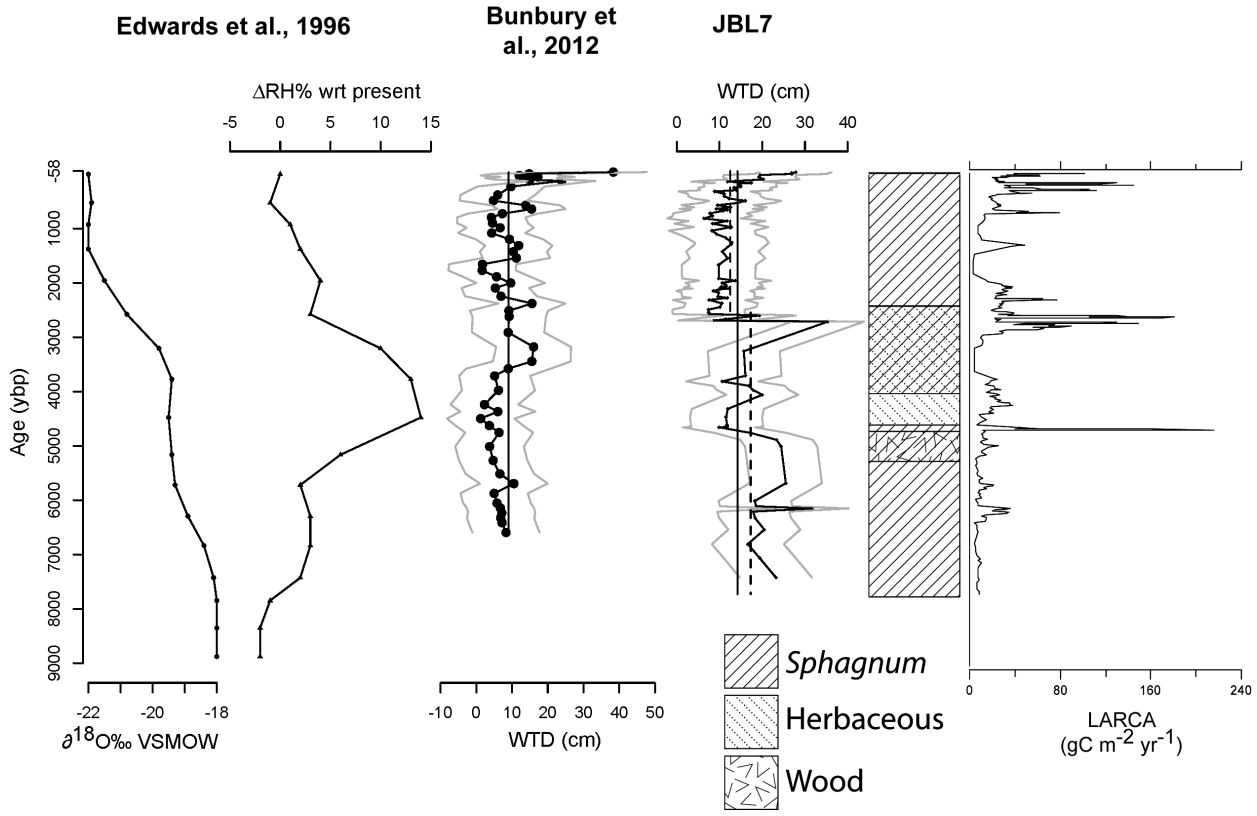

Figure 24: JBL7 shows mid-Holocene synchronicities with a central Canadian compiled record of change in relative humidity with respect to present (ΔRH% wrt present; Edwards et al., 1996), and late-Holocene synchronicities with a WTD reconstruction from another JBL record (Bunbury et al., 2012). JBL7 WTD reconstructions are also compared with macrofossil and LARCA data from the same core (Ch. 2). The solid line indicates the mean WTD value for the entire record. The dashed line represents the mid-Holocene, and late-Holocene averages.

Generally, LARCA changes were associated with extreme hydrological events (Fig. 24). There was a brief increase in LARCA at 6.1 ka associated with a brief drought during *Sphagnum* dominated conditions. At approximately 4.7 ka, LARCA increased to its' highest point in the core associated with the loss of woody peat and wet conditions.

From 2.6 to 2.4 ka dry conditions occurred at the same time as high LARCA. During the last 400 years LARCA increased due to acrotelm process, but was also associated with lower WTD. There is a weak but significant correlation between WTD and LARCA (r^2=0.03; p<0.001; Fig. 25). However both extreme low and extreme high WTD have high residuals compared to the predictions of a linear model. At the wet extreme there was more variability in residuals; at the dry extreme residuals were higher than predicted by the linear model.

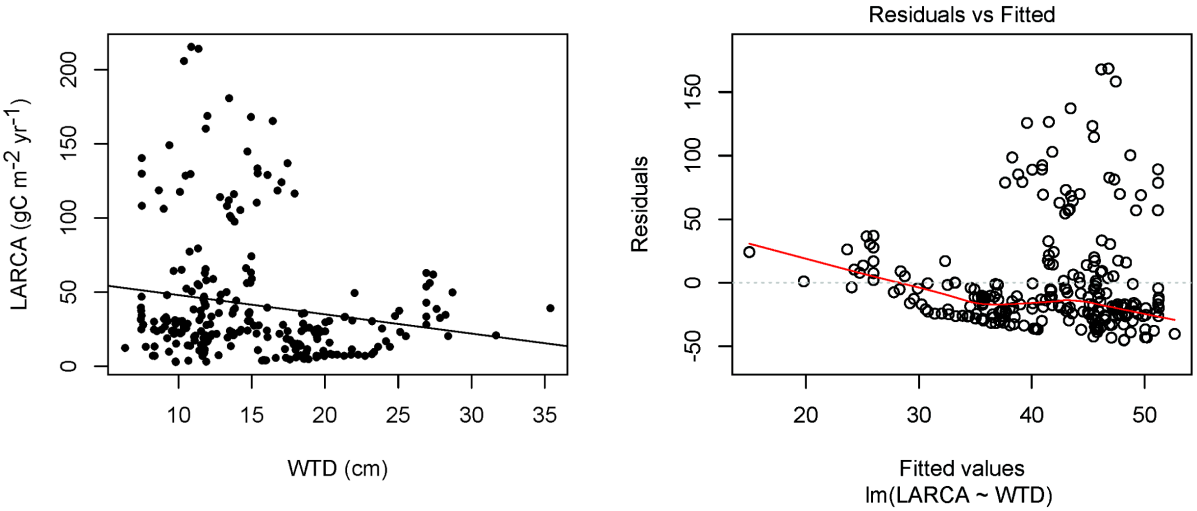

Figure 25: Scatter plot showing correlation between WTD and LARCA, as well as a plot of standard residuals relative to a linear model with WTD as the causal variable and LARCA as the dependent variable.

4.5. DISCUSSION

4.5.1. Mid-Holocene WTD Changes

Although peatland WTD is heavily dependent on local drainage and surface microtopotraphy, and this study is based on single core and a single site, dramatic shifts in WTD Holocene changes in WTD show synchronicities in timing and magnitude for relative humidity reconstructions from Northern Canada (Fig. 24). From 7.4 to 4.6 ka, WTD was generally lower than the full record, and mid-Holocene averages indicating dry conditions. This could have been due to the relatively southerly position of the Arctic front and drier conditions during the cool pre-HTM period. From 4.6 to 3.1 ka WTD was generally higher than the mid-Holocene mean, indicating wet conditions, which may indicate the relatively Northern position of the Arctic front and greater precipitation during the HTM. The transition to moist conditions during the HTM in eastern Canada is also apparent in other paleo-climate records. In Elk Lake, Michigan, a record of ostracodes and diatoms indicate relatively warm, near-modern, air temperatures between 6.7 - 4.0 ka, with peak wet conditions approaching 90% of their modern values between 4.3 - 4.0 ka (Forester et al., 1987). In southern Ontario Pinus forests were replaced by oak savannah in Southern Ontario 6.0 - 4.0 ka. Transition could have been caused by a transition to moist conditions (Szeicz and MacDonald, 1995). The beginning of this wet period was also observed by Bunbury et al. (2012) around 4.5 ka in the Victor fen area, and was associated with a transition from fen to bog conditions. Wet events north of the Great Lakes in this general time period may also be associated with the 4.2 ka drought that is indicated by multiple paleoenvironmental records in the Great Lakes region (Booth et al., 2005).

There were two dry periods recorded for 6.1 and 2.5 ka (Fig. 24). These may have been cause by site-specific changes in drainage or surface microtopography.

However, previous studies indicate that 6 ka was the beginning of a period of drastic climate and ecological shifts in the Canadian arctic (Prentice et al., 1991; Gajewski et al., 2000). Pollen reconstructions in North America indicate longer growing seasons ~6.0 ka (Bartlein et al., 2011). Longer growing seasons could increase the amount of time over which evapotranspiration can occur annually (Bracht-Flyr and Fritz, 2012). This was also a period of rapid isostatic uplift, and shifting watersheds could have caused hydrological changes. Unfortunately there is a paucity of data between 6.0 – 5.0 ka (Fig. 23), possibly due to the increase in aerobic respiration in the rhizosphere associated with wood and *Sphagnum* dominated sections, and the poor preservation of tests. The 2.5 ka drought may be associated with neo-glacial cooling and the return of the dominance of the Arctic front.

4.5.2. Late-Holocene WTD changes

The late-Holocene was generally wetter than the mid-Holocene starting about 2.4 ka. The Pacific front likely dominated central Ontario despite neoglacial cool conditions, similar to modern conditions. The shorter-term variations such as the MCA and LIA indicate wet/dry conditions compared to the late-Holocene mean (Fig. 24). The relatively wet MCA is consistent with other reports in Central Ontario (Bunbury et al., 2012). This also supports modern observations and climate models that indicate positive precipitation anomalies in the JBL region during warm temperature induced La Niña conditions (MacDonald and Case, 2005; Feng et al., 2008; Seager et al., 2008; Fig. 20) and a strong westerly storm-track. The LIA corresponded to the lowest WTD of

the core, and was dry relative to the MCA and moderate relative to the Holocene average. This differs from the other published record from the JBL, which reported a wet LIA. However Bunbury et al. (2012) reported a dry period lagging the MCA. This dry spike many be analogous to my report of the LIA, but differs in timing because of different resolutions of the two age-depth models (Fig. 21). Dry conditions during the LIA may have been due to the southern expansion of the arctic front, or the formation of permafrost, which can increase surface drainage in some cases (van Bellen et al., 2011).

Acrotelm peat spans the last two centuries, and contains species such as *Nebela militaris*, that are not generally present in catotelm sections (Fig. 23; Tab. 17). This could be a recent change due to drying associated with the shapr Arctic temperature amplification of global warming (Overpeck et al. 1997; Kaufman et al., 2009), or it could be an artifact of TA preservation. Other records in Ontario have the same drying trend over than last two centuries (Bunbury et al., 2012), however this is largely absent from similar peatland in the Quebec JBL (Loisel and Garneau, 2010; van Bellen et al., 2011). Future studies could statistically compare modern drying across multiple cores, identify potential problematic taxa, and reapply transfer functions to determine if drying is an artifact, or a robust global trend. If the drying trend in the JBL is representative of modern moisture balance, then reports of MCA precipitation and C cycling need to be interpreted with a caveat. The MCA and modern global warming have different drivers and may not be prudent in all cases to connect C cycle feedback changes during the MCA to future climate change.

The general pattern over the Holocene in JBL7 indicates relatively dry and variable conditions during the mid-Holocene and relatively stable and wet conditions during the late-Holocene. A pollen-based reconstruction focusing on *Tsuga* in Michigan indicates a general increase in precipitation since 7 ka, and relatively little change in precipitation since 2 ka (Calcote, 2003). Three pollen records from central Alberta indicate cooler, stable, moist conditions since 3 ka (Vance et al., 1983).

4.5.3. Vegetation Changes in the Mid-Holocene

Hydroecology in peatlands is complex, and it is possible that autogenic changes or feedbacks between ecology and hydrology could be responsible for changes (Swindels et al., 2012). However, two vegetation changes at approximately 4.5 ka and 2.4 ka, may have been caused by external forcing, either watershed or climate changes. The 4.5 ka shift reversed common succession patterns in peatlands, whereas the 2.4 ka shift followed them (Fig. 24). TA based WTD indicated that the 4.5 ka ecological transition occurred following an extreme wet period, and that the 2.4 ka shift was preceded by a dry period. Ecologically extreme events in the mid-Holocene may have been the result of allogenic transitions that affected both the vegetative composition of the peat and the surface moisture, or allogenic changes due to the complex internal feedbacks of peat forming species.

In JBL7 the 4.5 ka bog-fen transition was coincident with a locally low water table (Fig. 24). This type of change has been observed in North American peatland complexes due to the flooding of bog margins and the upslope expansion of fen

communities (Bauer et al., 2003). In the Netherlands many present-day fens have formed over bogs that were flooded by anthropogenic activity. Lamers et al. (2002) cite the infiltration of riparian water as one mechanism of bog to fen transition. The reestablishment of herbaceous vegetation was also documented in Beckley Bog, Connecticut, over a five-year period due to flooding due to beaver dams (Mitchell and Niering et al., 1993). Watersheds were highly variable during the Holocene in the JBL because of the land's low relief, and the high rates of isotatic uplift (Webber et al., 1970; Dyke et al., 2003; Riley, 2011). A meandering stream could have intersected the peatland at some point, or the area could have been periodically flooded in the spring due to ice jams in nearby streams and rivers (Fig. 20).

A second ecological transition occurred, when vegetation switched back to *Sphagnum* dominated bog ~2.4 ka; this was preceded by relatively dry conditions (Fig. 24). This may indicate autogenic events such as hummock and hollow development (Pouliot et al., 2011), or an allogenic change such as gradual watershed or climate shifts (Edwards and Wolfe, 1996; Glaser et al., 2004a). *Sphagnum fuscum* is a relatively robust competitor in rich fens under persistently dry conditions (Granath et al., 2010). Manipulation studies show that extended periods of low water tables can cause a shift in vascular plant dominance away from graminoid species. Overall, droughts can cause *Sphagnum* and vascular assemblages to switch from a hollow-type community to a lawn or hummock-type community (Breeuwer et al., 2009).

4.5.4.Correlation between WTD and LARCA

WTD had a low, but significant correlation with LARCA in JBL7 (r^2 = 0.03; p = 0.01; Fig. 25). High LARCA values were associated with extreme wet conditions, indicating that wet conditions positively influence net C sequestration through positively influencing plant productivity, negatively influencing peat decay, or both (Blodau et al., 2004). Reconstructed WTD may be intercorrelated winter snow pack, which positively correlates with dry mass production of *Sphagnum fuscum* (Dorrepaal et al., 2004). However, the ecological change occurring during wet shift ~4.5 ka that state changes could decouple any equilibrium or negative feedback between WTD and LARCA, causing a much more complex relationship than a simple linear model can explain.

Less extreme LARCA increases also occurred during dry events. 6.1 ka was a time period that has been identified to have relatively high LARCA across four different sites in the JBL (Fig. 24). In JBL7 this was associated with punctuated dry conditions. Although *Sphagnum* generally produces recalcitrant litter, there is phenotypic plasticity in species response to drought. Hummock species can increase the relative abundance of structural carbohydrates, which can lower the decay potential of litter, whereas hollow species can increase the relative abundance of metabolic carbohydrates, which can increase growth rate (Turetskey et al., 2008). There also may be higher amounts of physical peat compaction during droughts causing higher LARCA (Winston, 1994). The effect of drought on peat compaction, and peat biochemistry should be a topic of further studies to investigate possible complex effects of drought on peat formation and preservation. Future studies should also investigate WTD at 6.1 ka across multiple sites to determine in the same drought conditions exist associated with temporarily high LARCA.

4.6. CONCLUSIONS

A Holocene reconstruction of WTD indicates that patterns in vegetation and hydrology were complex throughout the mid-Holocene likely due to the dominance of Pacific and Arctic air masses, and the strength of the westerly storm track. The pre-HTM period was generally dry indicating the possible dominance of the Arctic summer front, whereas the HTM was wetter possible due to the influence of the Pacific summer front. Punctuated dry conditions occurred around 6.1 ka and 2.5 ka. The late-Holocene had moderate and stable WTD compared to the mid-Holocene, following a general trend of trend of increasing North American moisture and climate stability since ~2.5 ka. The MCA registered as a relatively wet event, whereas the LIA was relatively dry, supporting the conclusions of previous studies, and modern precipitation anomaly data for the region. Two dramatic changes in the macrofossil record were associated with extreme hydrological events with the transition from bog to fen 4.5 ka occurring due to wet events, possibly caused by flooding by mineral rich water, and a 2.4 ka resurgence of bog vegetation, possibly caused by drought or drainage changes returning competitive advantage to *Sphagnum*. LARCA was generally high during wetter periods, but also rose during brief periods of drought, indicating that there are possible contradictory effects of WTD on peat productivity and decay. I view this as a step towards increasing the number of multi-proxy paleoecology and paleo-climate studies in the sensitive boreal zone of Canada, testing the predictions of climate models, and improving peatland C storage models.

5. Impact of the Medieval Climate Anomaly, Little Ice Age, and Recent Warming on Hydrology and Carbon Accumulation in the James Bay Lowlands

5.1. ABSTRACT

The reconstruction and analysis of late-Holocene hydroclimatic variations can be useful to understanding the sensitivity of peatland soil carbon (C) to climate change, and the magnitudes and directions of possible future C cycle feedbacks. Four testate amoeba based reconstructions of peatland hydrology along a north to south transect of the James Bay Lowlands of Ontario record changes in hydrology and C accumulation coincidental with the Medieval Climate Anomaly (MCA; 1000 – 700 calendar years before present [ybp]), the Little Ice Age (LIA; 500 – 200 ybp), and recent warming. The three southern sites indicate that water table depths (WTD) fluctuated relative to the mean, with a wetter MCA and drier LIA. However, the most northern sites indicate that a wet LIA and dry MCA. This could reflect regional variability of late-Holocene precipitation patterns consistent with observed climatic patterns, or the establishment and deterioration of permafrost. All four cores indicated recent drying. Increased moisture detected in the three southern sites is consistent with a geographic pattern of drought in the southwest and central plains region coupled with increased moisture in the Pacific Northwest and north of the Great Lakes that is related to changes in the planetary wave and westerly storm track. These proxy records constrain the geographic extent of MCA drought in the Great Lakes region and support previous model simulations. Despite the hydroclimatic sensitivity of the region no distinct

relationship was observed between variations in WTD over the MCA, LIA, and recent warming and long-term apparent rates C accumulation from the same cores, indicating that at these particular sites at least, C accumulation has not been sensitive to the range of climatic variability associated with the MCA, LIA and recent warming.

5.2. INTRODUCTION

Although there is general agreement between climate models about likely patterns of warming over the 21st century there is less agreement in terms of precipitation and moisture balance. Examination of surface moisture variability over the Holocene can serve as a natural experiment for modern and projected effects of climate change on precipitation, surface moisture and potentially, carbon (C) accumulation in northern peatlands (Loisel and Garneau, 2010; van Bellen et al., 2011; Bunbury et al., 2012; Lamarre et al., 2012). The late-Holocene is of particular interest to reconstructing hydroclimate and peatland C accumulation because past variations may be, in some cases, analogous to future climate change (Berger and Loutre, 1991; Beilman et al., 2009). The Medieval Climate Anomaly (MCA; 1000 – 700 calendar years before present [ybp]; Lamb, 1965) and the Little Ice Age (LIA; 500 – 200 ybp; Viau et al., 2002) have been framed as natural experiments that can elucidate the effects of both depressed and elevated temperatures on surface moisture conditions and the combined effect of both on long-term apparent rate of C accumulation (LARCA; Clymo et al., 1998; Loisel and Garneau, 2010; Bunbury et al., 2012).

The southern extent of the central North American boreal zone is a crucial area for studying climate change and documenting the extent of late-Holocene droughts. Coupled climate models and empirical data indicate that the MCA hydroclimatology was likely analogous to La Niña events, cool-tropical Pacific, coupled with a anomalously warm portions of the North Pacific, and a warm North Atlantic, which caused droughts extending through much of North America, but may have produced greater precipitation in regions north of the Great Lakes (MacDonald and Case, 2005; Feng et al., 2008; Seager et al., 2008).

The hydroclimatic response of the James Bay Lowlands (JBL) is particularly important because they contain the second largest continuous peatland complex, as well as some of the most concentrated peatlands in the world (Riley, 2011; Tarnocai et al., 2011). They also lie in an area where warm medieval climate may have produced moister conditions relative to regions further south (Ch. 4). This geographic pattern is evident in the spatial patterning of La Niña-year (2012) precipitation anomalies (NOAA/ESRL, 2013; Ch. 4). However, records of Holocene surface moisture and precipitation remain sparse in the subarctic and boreal zone, and are unavailable for large areas of the JBL (Bunbury et al., 2012; Ch. 4).

Droughts can have contradictory effects on C accumulation, and their net effect is likely dependent on hydrology interacting with plant productivity, plant-soil interactions, and peat decay (Dise, 2009; McGuire et al., 2009; Yu et al., 2009). Droughts can decrease C accumulation by either decreasing the productivity of plants, which has been observed in controlled growth experiments of *Sphagnum* and *Carex*, or by increasing decay. Droughts can increase acrotelm space, which increases available

oxygen, and can lower apparent C accumulation by increasing the rate of decay (Martikainen et al., 1995; Laiho, 2006). Contradictory, droughts can also increase apparent C accumulation by changing the density, and recalcitrance of peat. C accumulation can increase during droughts because of a state changes to woody peat, changes in *Sphagnum* carbohydrate metabolism, or increases in physical peat compaction (Lahio, 2006; Turetskey et al., 2009; Loisel and Garneau, 2010). Some peatland manipulation studies conclude however that there is very little effect of droughts on *Sphagnum* bogs because bogs can structurally collapse during water table drawdown to maintain equilibrium with the height of the ground water (Bridgeham et al., 2006).

In this chapter I present three new late-Holocene (post-2,000 ybp) testate amoebae (TA) based records of water table depth (WTD). The TA based paleohydrology from JBL7 was previously discussed in Chapter 4, but will be reviewed again here in relation to the other records (JBL2, JBL4, JBL8), when relevant. I also compare WTD to previously discussed LARCA measurements from the same cores. I address three different research questions involving WTD reconstructions in this chapter: 1. Were there consistent wet/dry shifts during the MCA, LIA, and modern times? 2. Are records of medieval moisture status in the JBL, and the rest of North America consistent with, paleoclimate model projections and modern precipitation anomalies under La Niña-like conditions (NOAA/ESRL, 2013)? 3. Did wet/dry shifts correspond with changes in LARCA, and were these changes consistent in all cases?

5.3. MATERIALS AND METHODS

The collection and initial processing of the cores is detailed in Chapter 2. The four peat cores utilized in this study were collected in 2008. The four cores analyzed were collected from ombrotrophic non-permafrost peat bogs (Tab. 1) as part of an eight core transects spanning non-permafrost to discontinuous permafrost regions (Fig. 26). I established well-constrained chronologies of the cores by using multiple AMS radiocarbon (^{14}C) dates and 'Bacon' age-depth modeling software (Blaauww and Christen, 2011; Fig. 4 - 11; Tab. 3 - 5). I subsampled cores at 1 cm intervals and estimated the mass of C using bulk density (BD), loss-on ignition (LOI_{550}), and an assumption of 0.5 gC g Organic Matter $(OM)^{-1}$. I calculated long term apparent C accumulation rates (LARCA) from the mass C estimates and rates of peat accumulation inferred from the 'Bacon' age-depth models (Clymo, 1998). TA processing is detailed in Chapter 4, and no changes were made to the major protocols in this chapter. Figure 27 plots the WTD optimum, and minimum and maximum tolerances for key dominant species are represented in JBL2, JBL4 and JBL8. Table 18 lists the descriptive statistics for the transfer function used in WTD reconstruction.

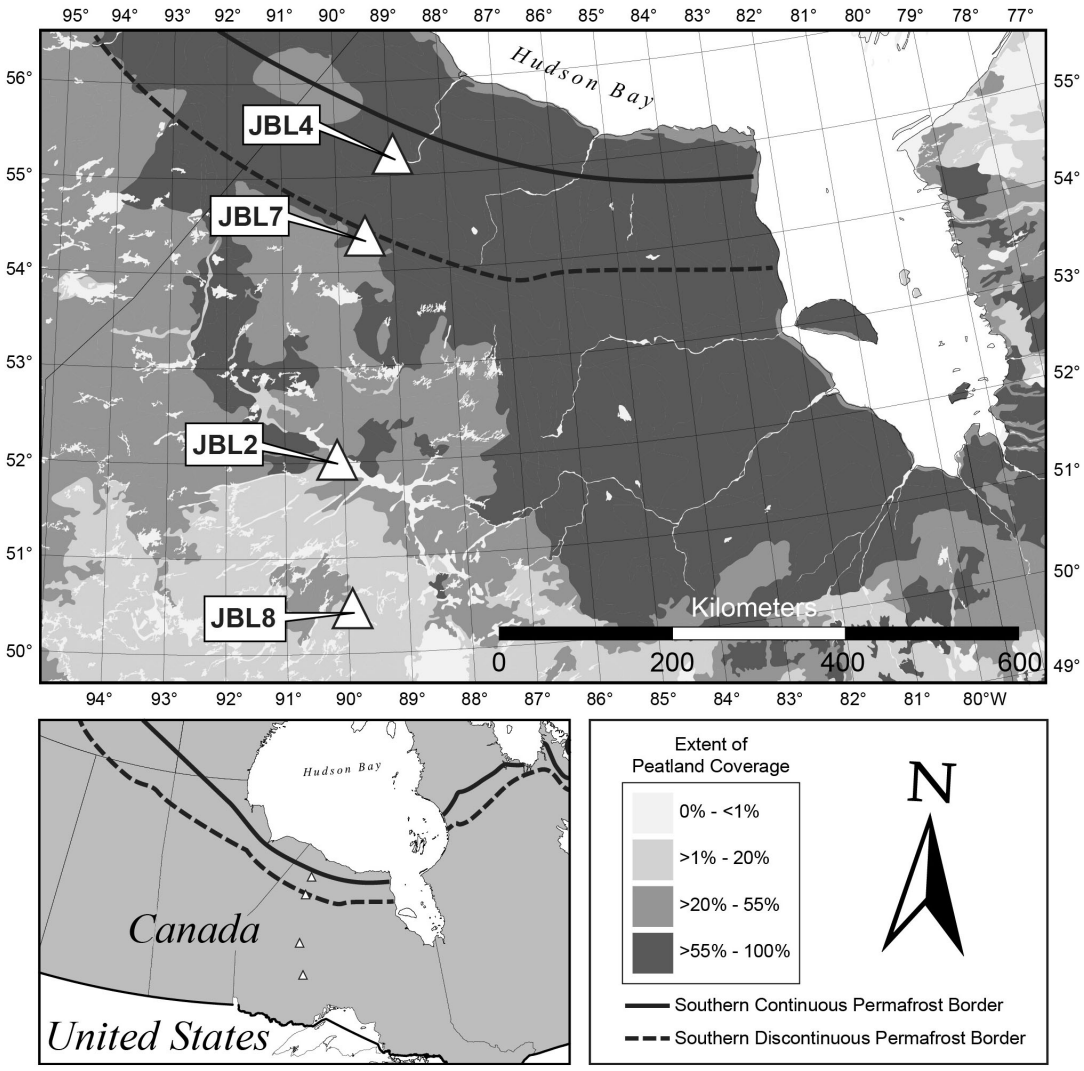

Figure 26: A map of the JBL, showing the sites of testate amoeba based reconstructions, notable review sites mentioned in the text, peatland concentration (Tarnocai, 2011), and the southern boarders of continuous and discontinuous permafrost in the region (Brown et al., 1998).

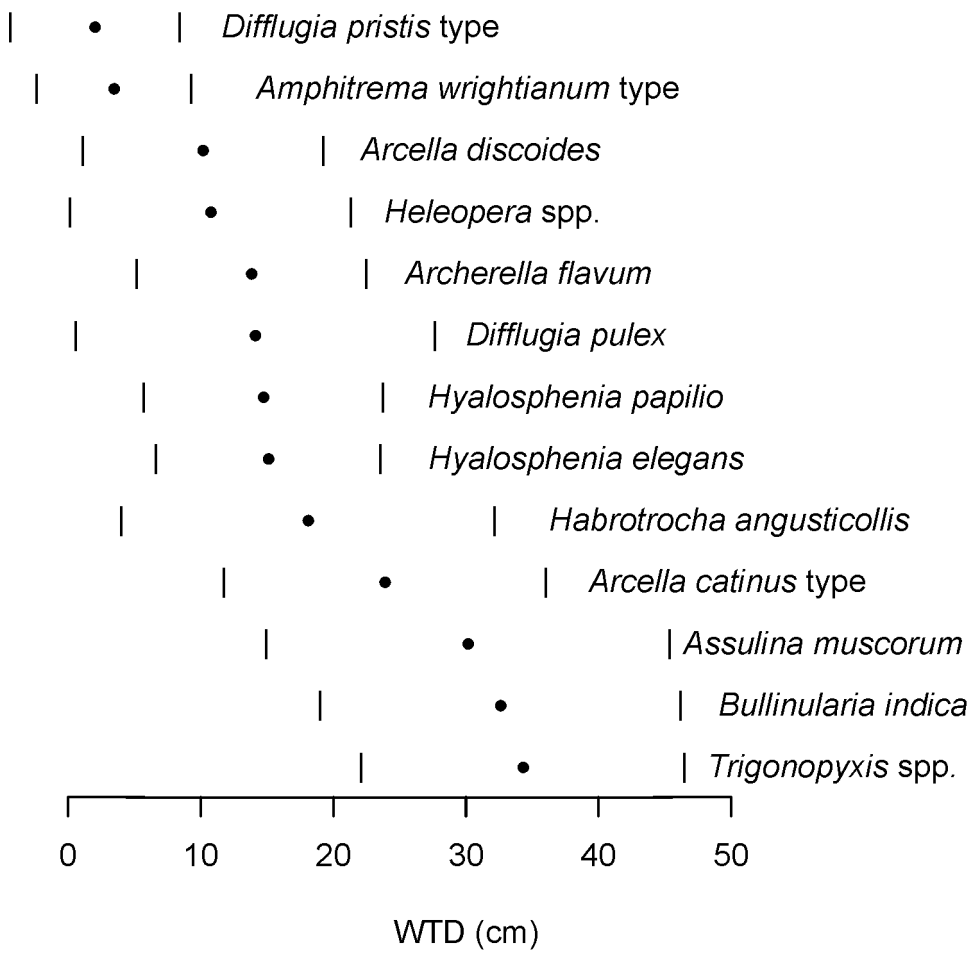

Figure 27: A xy plot with a list of common taxa identified in JBL8, JBL2, JBL4, as well as their mean WTD and minimum and maximum tolerances (Booth, 2008).

Table 18: Transfer function performance statistics for JBL8, JBL2, and JBL4.

Core	Model	RMSE	r^2
JBL8, JBL2, JBL4	Weighted averaging - Inverse Deshrinking	8.27	0.70

5.4. RESULTS

5.4.1. Testate Amoebae Assemblages

Figure 28 displays twelve common and morphologically representative species from JBL2, JBL4 and JBL8. The four records range in age from 2119 ybp to 1044 ybp (Fig. 29 - 31; Tab. 19). Canonical cluster analysis determined that three to five stratigraphic zones were apparent in the TA assemblages. All species that have an occurrence of 20% or greater within any zone of the core are displayed in figures and tables.

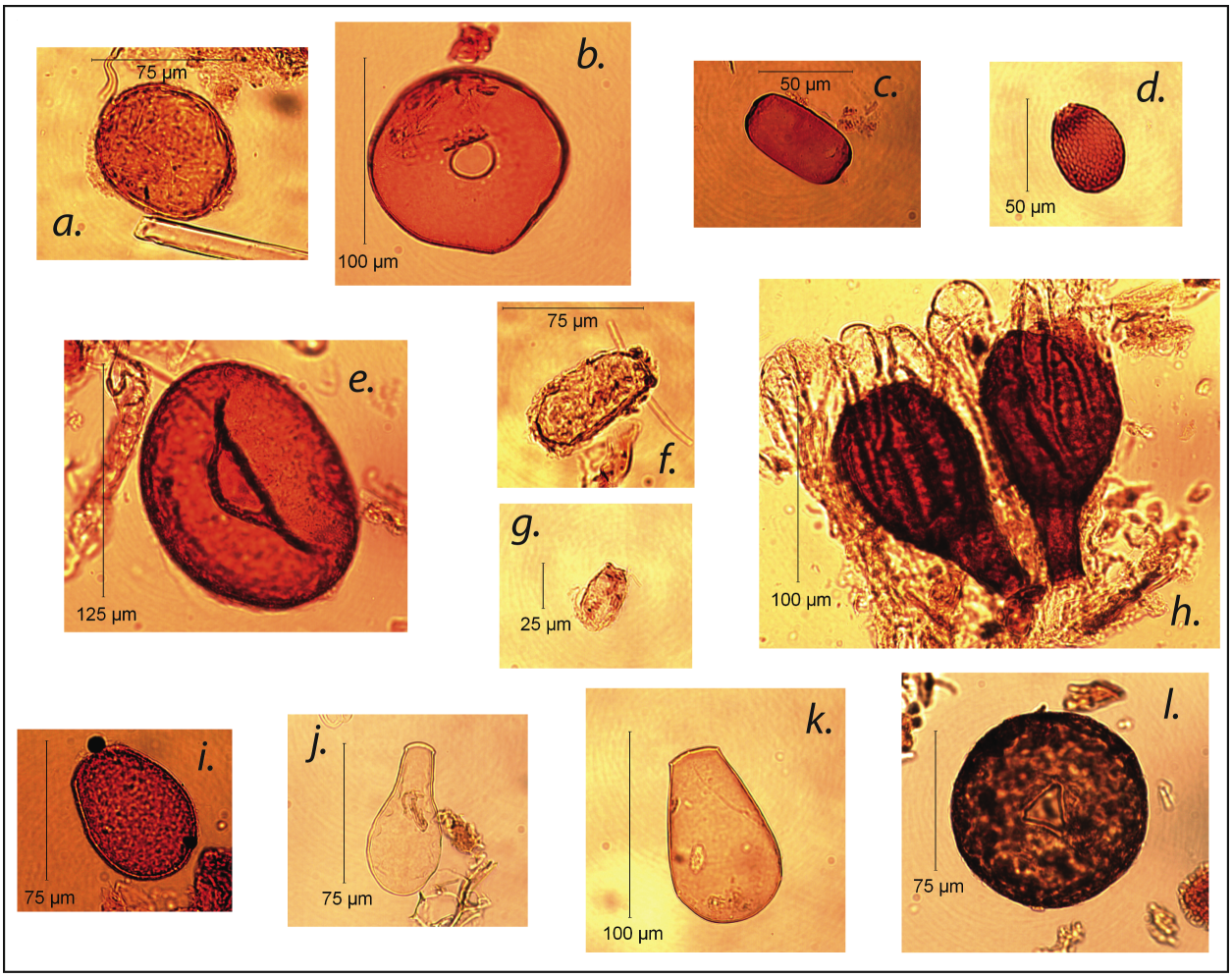

Figure 28: Representations of common and notable tests found in JBL material: a. *Amphitrema wrightianum* type, b. *Arcella catinus* type, c. *Archerella flavum,* d. *Assulina muscorum,* e. *Bullinularia indicum,* f. *Difflugia pristis* type, g. *Difflugia pulex,* h. *Habrotrocha angusticollis*, i. *Heleopera* spp., j. *Hyalosphenia elegans,* k. *Hyalosphenia papilio,* l. *Trigonopyxis* spp.

Table 19: Zones, dominant taxa, and WTD descriptive statistics for four cores in the JBL, listed for the entire core, and for each zone.

Core	Zone	Depth (cm)	Age Range (ybp)	Dominant Taxa	WTD range (cm)	WTD mean (cm)
JBL8	A	128 - 104	1307 - 661	*Arcella discoides, Archerella flavum, Difflugia pulex, Habrotrocha angusticolis, Heleopera* spp., *Trigonipixus* spp.	11 - 25	16 ± 4
	B	102 - 72	632 - 215	*Arcella discoides, Archerella flavum, Assulina muscorum, Difflugia pulex, Habrotrocha angusticolis, Heleopera* spp., *Trigonipixus* spp.	17 - 30	25 ± 4
	C	68 - 9	188 - -39	*Assulina muscorum, Difflugia pulex, Hyalsphinia paplio, Trigonipixus* spp.	21 - 37	28 ± 5
JBL2	A	110 - 101	1044 - 926	*Amphitrema wrightianum* type, *Archerella flavum, Heleopera* spp., *Hyalsphenia papilio*	-5 - -1	-3 ± 1
	B	100 - 82	915 - 594	*Amphitrema wrightianum* type, *Archerella flavum, Heleopera* spp., *Hyalsphenia papilio*	-1 - 14	5 ± 4
	C	78 - 42	555 - 154	*Archerella flavum, Difflugia pristis* type, *Difflugia pulex, Heleopera* spp., *Hyalsphenia papilio*	9 - 18	12 ± 2
	D	24 - 6	64 - -41	*Archerella flavum, Heleopera* spp., *Hyalsphinia elegans, Hyalsphenia*	6 - 15	12 ± 4
JBL7	A	324 - 152	7425 - 2573	*Amphitrema wrightianum* type, *Archerella flavum, Assulina muscorum, Cyclopixus arcelloides* type, *Cyclopixus platystoma, Heleopera* spp., *Hyalsphenia papilo, Phryganella acropodia, Trigonopyxis* spp.	8 - 35	17 ± 7
	B	148 - 99	2542 - 1285	*Archerella flavum, Difflugia pulex, Heleopera* spp.,	7 - 14	11 ± 2
	C	97 - 86	1258 - 721	*Arcella catinus* type, *Archerella flavum, Difflugia pristis* type, *Difflugia pulex*	6 - 13	10 ± 2
	D	85 - 58	674 - 294	*Archerella flavum, Difflugia pulex*	9 - 16	12 ± 2
	E	57 - 8	249 - -37	*Archerella flavum, Hyalsphenia papilo, Nebela militaris*	12 - 28	19 ± 6
JBL4	A	94 - 83	1385 - 1170	*Archerella flavum, Difflugia pulex, Hyalsphenia elegans, Hyalsphenia papilio*	9 - 12	10 ± 1
	B	80 - 62	1150 - 675	*Bullinularia indica, Difflugia pristis* type, *Difflugia pulex*	9 - 20	12 ± 3
	C	61 - 50	618 - 296	*Archerella flavum, Difflugia pulex*	1 - 13	7 ± 4
	D	48 - 5	274 - -54	*Archerella flavum, Difflugia pulex*	10 - 23	15 ± 3

JBL8 had a record extending from modern times to 1307 ybp and can be divided into three zones (Fig. 29; Tab. 19). JBL8-A extends from 1307 to 661 ybp, and is dominated by *Archerella flavum, Arcella discoides, Difflugia pulex, Habrotrocha angusticolis, Heleopera* spp., and *Trigonopyxis* spp. JBL8-B extends from 632 to 215 ybp and is dominated by the same taxa as JBL8-A with the addition of *Assulina muscorum*. From 188 to -39 (JBL8-C) ybp there is a decline in *Archerella flavum*, and dominance by *Assulina muscorum, Difflugia pulex, Hyalosphenia papilio,* and *Trigonopyxis* spp.

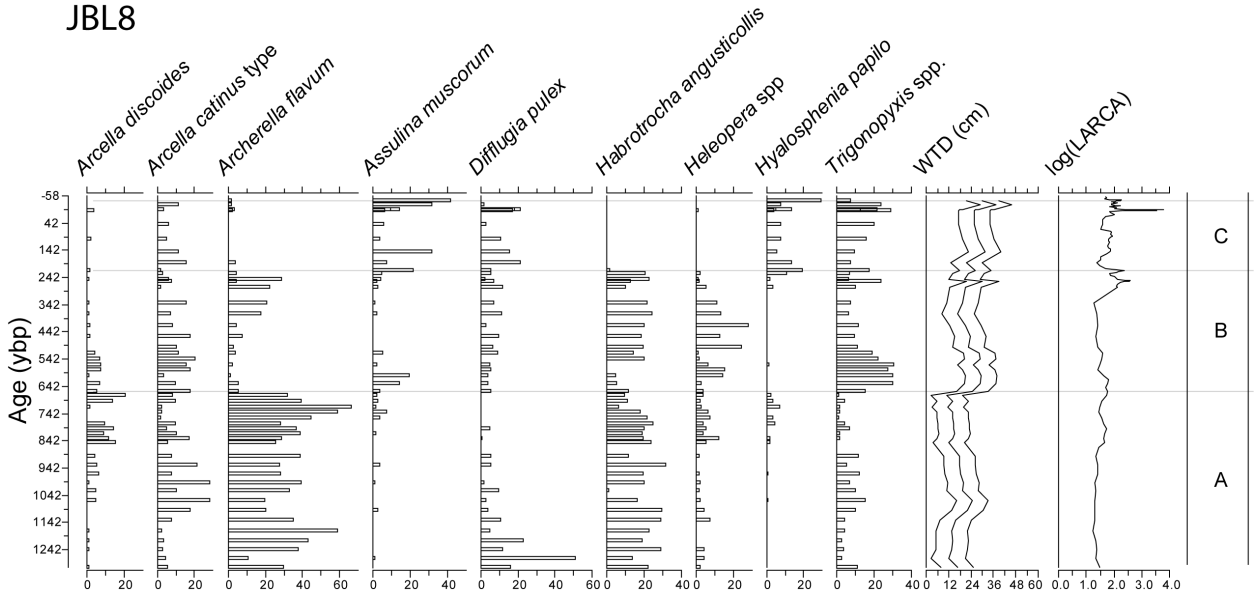

Figure 29: Stratigraphy data for JBL8 including, age, notable TA species, WTD reconstructions, LARCA, and TA zones based on a cluster analysis.

In JBL2 the TA record extends from 1044 ybp to modern times, and can be divided into four zones (Fig. 30; Tab. 19). All four zones contain, or are dominated by *Archerella flavum*. JBL2-A spans from 1044 to 926 ybp and is dominated by

Amphitrema wrightianum type*, Heleopera* spp., and *Hyalosphenia papilio.* JBL2-B extends from 915 to 594 ybp and is similar to the previous zone, but has a shift in dominance from *A. wrightianum* type to *A. flavum*. From 555 to 154 ybp (JBL2-C) *A. wrightianum* declined drastically, and *Difflugia pristis* type and *Difflugia pulex* occurred with *A. flavum* still dominant. *Heleopera* spp., and *Hyalosphenia papilio* still occured at lower concentrations. In the youngest zone (JBL2-D; 64 to -41 ybp), *A. flavum*, *D. pristis* type, and *D. pulex* declined, while *Hyalosphenia elegans* and *Hyalosphenia papilio* increased in relative abundance.

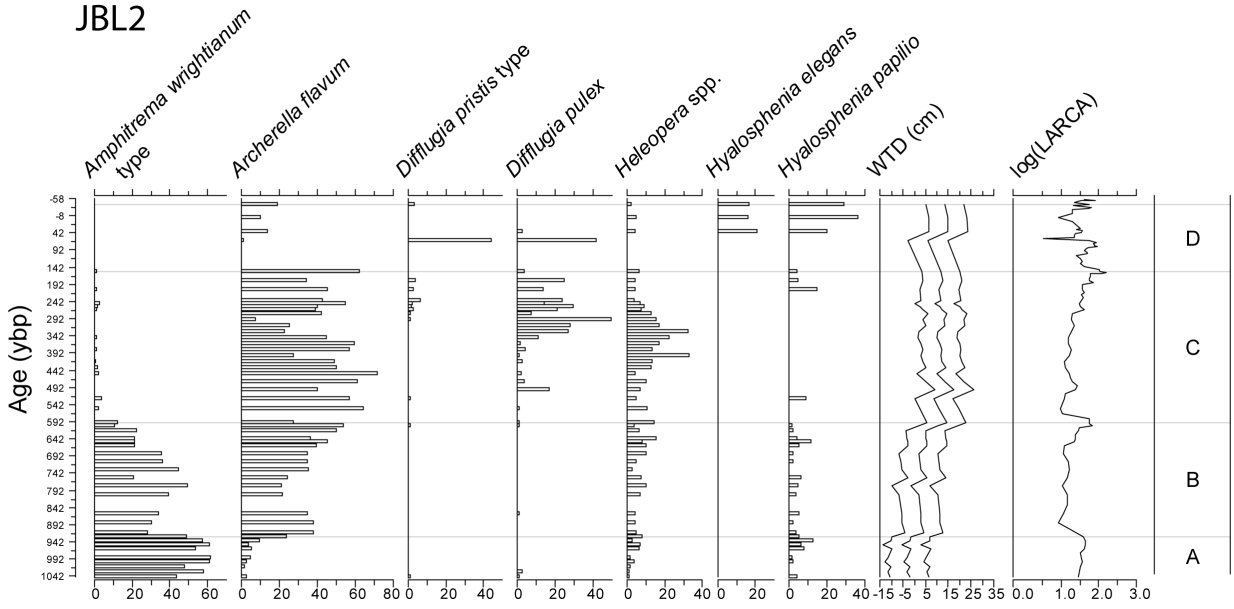

Figure 30: Stratigraphy data for JBL2 including, age, notable TA species, WTD reconstructions, LARCA, and TA zones based on a cluster analysis.

The TA record of JBL7 extends from 2119 ybp to modern times, and is divided into four zones (Fig. 23; Tab. 19). All four zones contain, or are dominated by *Archerella flavum* and *Difflugia pulex*. From 2119 to 1285 ybp, JBL7-A also contains abundant *Heleopera* spp. From 1258 to 721 ybp (JBL7-B). *A. flavum* decreases in

concentration and *D. pulex* increases between 674 to 294 ybp. There were also spikes in *Arcella catinus* type, and *Arcella vulgaris*. The youngest zone (JBL7-D) ranges from 249 to -37 ybp, and shows a decline in *A. flavum*, a slight increase in *D. pristis* type and *D. pulex*, as well as sharp increases in the concentrations of *Hyalosphenia papilio* and *Nebela militaris*.

The TA record of JBL4 extends from 1385 ybp to modern times and is divided into four zones (Fig. 31; Tab. 19). A major feature in the record is the alternation of dominance between *Archerella flavum* and *Difflugia pulex*, which are both present throughout the core. The first two zones, JBL4-A and JBL4-B, span 1385 to 1170 ybp, and 1150 to 675 ybp respectively. *D. pulex* is dominant , whereas *A. flavum* is dominant in JBL-B. From 618 to 296 ybp (JBL4-C) *A. flavum* decreased drastically, and *D. pulex* became dominant. *Bullinularia indica* and *Difflugia pristis* type were also present during this time period. The most recent zone (JBL4-D) spans from 274 to -54 ybp, and contained a slight increase in *A. flavum*, a slight decrease in *D. pulex*, and the presence of *Hyalosphenia elegans* and *Hyalosphenia papilio*.

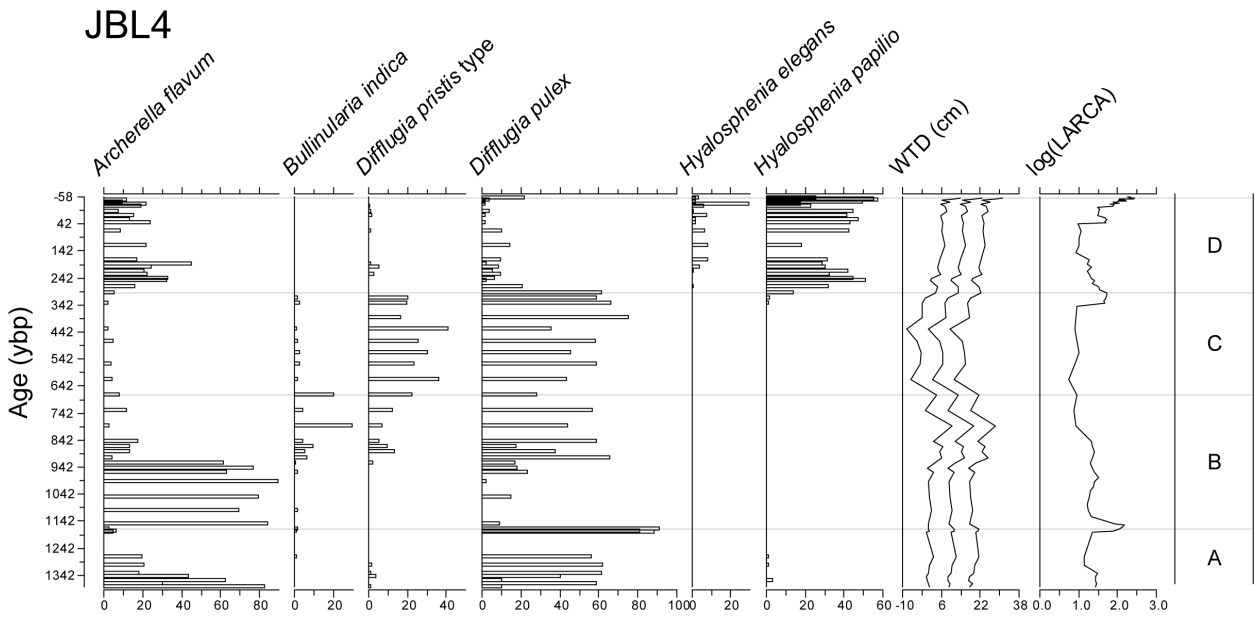

Figure 31: Stratigraphy data for JBL4 including, age, notable TA species, WTD reconstructions, LARCA, and TA zones based on a cluster analysis.

5.4.2. Water Table Depth

WTD at JBL8 ranged from 11.2 to 37.3 cm between 1385 ybp and modern times, and had a mean of 21 ± s. dev. (±) 7 cm. JBL2 has persistently shallow water tables ranging from -5 to 18 cm between 1044 ybp and modern times. In JBL7, WTD ranged from 6 to 28 cm and averaged 13 ± 5 cm from 7.4 ka until modern times. WTD at JBL4 ranged from 1 to 23 cm and averaged 12 ± 4 cm between 1385 ybp and modern times (Tab. 19).

The timing of the MCA was represented by TA inferred WTD depth changes in all four cores (Fig. 23; Fig. 29; Fig. 30; Fig. 31; Tab. 19). JBL8-A had the highest average WTD out of any zone in JBL8 (16 ± 4 cm) and timed between 1307 – 661 ybp. JBL2-A closely followed the succession from fen to bog conditions, and indicated constant pooling beteen 1044 and 926 ybp. JBL7-C contained the wettest conditions of JBL7

averaging 10 ± 2 cm between 1258 – 721 ybp. In contrast to the other sites, JBL4-B indicated dry conditions in JBL4 with WTD averaging 12 ± 3 cm between 1150 and 675 ybp.

The timing of the LIA was also represented in the TA inferred WTD of all four cores (Fig. 23; Fig. 29; Fig. 30; Fig. 31; Tab. 19). JBL8-B had relatively low water tables ranging from 17 to 30 cm and averaging 25 ± 4 cm from 632 – 215 ybp. JBL2-C contains the driest conditions averaging 12 ± 2 cm from 555 – 154 ybp. JBL7-D contained drier conditions similar to JBL7-A ranging averaging 12 ± 2 cm from 674 – 294 ybp. JBL4-C indicated the wettest conditions in JBL4, and averaged 7 ± 4 cm from 618 - 296.

Dry conditions appear to be represented in the modern portions of all four cores (Fig. 23; Fig. 29; Fig. 30; Fig. 31). JBL8-C displays the driest conditions with WTD ranging from 21 to 37 cm, and averaging 28 ± 5 cm from 188 - -39 ybp (Tab. 19). JBL2-D represents the last century and indicates variable, but generally dry conditions ranging from 6 to 15 cm 64 - -41 ybp. JBL7-E spans 249 - -37 ybp and indicated the driest conditions of JBL7 ranging from 12 to 28 cm. JBL4-D indicated the driest conditions of JBL4, from 274 - -54 ybp, ranging from 10 to 23 cm.

5.4.3. TA assemblages, WTD, and LARCA

I compared late-Holocene reconstructions of WTD to previously discussed records of LARCA. LARCA varied over four orders of magnitude over the last 2 ka (ka = 1,000 ybp) in these four sites, so I present log transformed LARCA values in Figures 29 - 31.

In JBL8, LARCA increases occurred at the same time as quick fluctuations to dry conditions occurred near the transition between JBL8-B and JBL8-C. LARCA changes in JBL8 are dominated by a spike in peat accumulation rate in the acrotelm (JBL8-C), discussed in Chapter 2. This major change cannot be explained by any observed change in TA based WTD reconstruction. In JBL2-A, there were locally wet conditions, and generally high LARCA values during the MCA (36.2 ± 5.5 gC m^{-2} yr^{-1}). Productivity may have been high due to residual minerotrophy or mesotrophy from the recent fen to bog transition. It is also possible that LARCA was high because of increased temperature and seasonality increasing productivity and high water tables increasing peat preservation during the MCA. In JBL2-B and JBL2-C LARCA was generally moderate except for a spike that was coincident with the transition between the two zones. LARCA in JBL7-A and JBL7-B greatly fluctuated in the absence of WTD fluctuations, with LARCA values between 2.8 and 38.3 gC m^{-2} yr^{-1} in JBL7-A, 7.0 to 48.2 to gC m^{-2} yr^{-1}, and a spike of 144.7 gC m^{-2} yr^{-1} during the transition from JBL7-A to JBL7-B (Fig. 23). LARCA was also stable throughout JBL7-C with a spike following the transitions from JBL7-B to JBL7-C. LARCA in JBL4-A, JBL4-B, and JBL4-C were fairly constant with a spike of 87.9 gC m^{-2} yr^{-1} during the transition from JBL4-A to JBL4-B (Fig. 30).

Out of the four records of LARCA and WTD, there is no consistent pattern in linear models with LARCA as the predictor WTD in JBL7 there is a negative, low but significant, relationship between WTD and LARCA (Fig. 25). Of the three cores published in this chapter, only JBL4 has a significant, but positive correlation between WTD and LARCA (Tab. 20).

Table 20: The results of linear models with WTD as the independent variable and LARCA as the dependent variable for all four cores

	r^2	p-value	Intercept	Slope
JBL2	0.01	0.26	32.54	0.57
JBL4	0.35	1.44×10^{-9}	-57.49	8.85
JBL8	0.01	0.28	-52.39	18.17
JBL7	0.03	0.01	60.89	-1.30

5.5. DISCUSSION

5.5.1. Hydroclimatology and WTD During the MCA, LIA, and Recent Periods

Peatland records of past moisture variability are likely affected by both autogenic dynamics (Swindles et al. 2012) as well as allogenic changes; however, synchronous changes among sites likely indicate that climate conditions either directly, or indirectly affected WTD in bogs in the JBL. All four records show synchronous multi-centennial changes in WTD centering on MCA (1000 - 700 ybp) and LIA (500 – 200 ybp; Fig. 32). The three southern sites indicate a wet MCA and a dry LIA, while JBL4 in the north indicates a dry MCA and a wet LIA. WTD was approximately 4 to 10 cm higher than the average in JBL8, JBL2 and JBL7 between and 1000 - 700 ybp. In the three southern cores, WTD ranged from 1 cm above to 5 cm below the average WTD. The one other central Ontario TA based record (VC04-06) also indicated a wet MCA with WTD ranging from 4.2 to 6.7 cm followed by a 150 year 10 cm drop in WTD (Bunbury et al., 2012). This brief dry period may be analogous to our reconstruction of the LIA. In JBL4, the most dramatic change occurred during the LIA when the WTD rose 5 cm above the

average. Two TA based studies in Quebec cite the formation of permafrost as a possible driver of surface hydrology, although whether permafrost creates relatively dry conditions, or relatively moist conditions due to summer pooling, is uncertain (van Bellen et al., 2011; Lammare et al., 2012). LIA surface moisture changes may have been more spatially variable in the JBL, due to interactions between, precipitation, evaporation, seasonality, and permafrost, (Camil, 2010; Bracht-Flyr and Fritz, 2012).

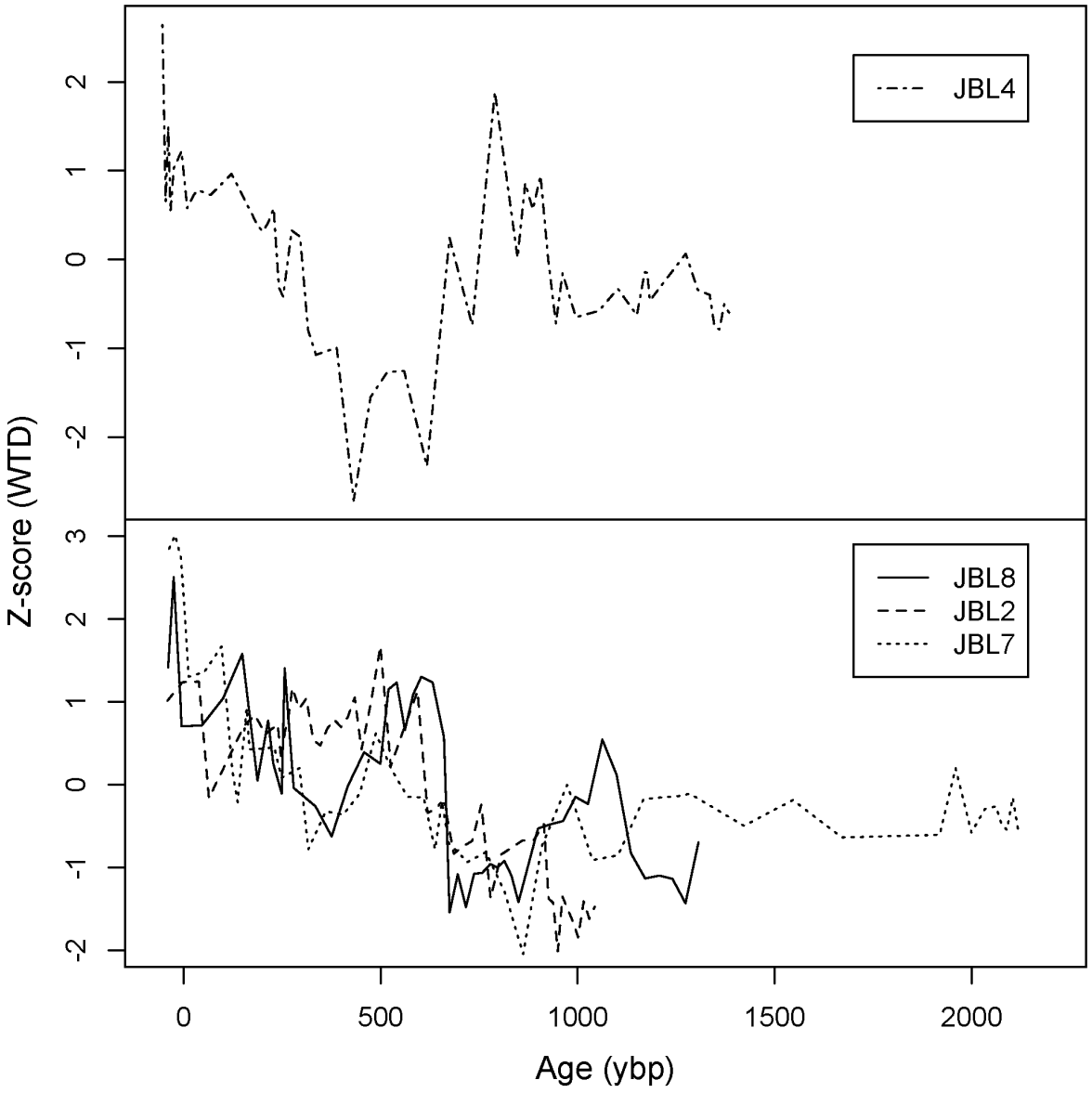

Figure 32: Z-scores of WTD for JBL8, JBL2, JBL7, and JBL4 over the late-Holocene.

Each site showed synchronous shifts towards lower WTD during the last two centuries (Fig. 32). There are two possible explanations for this. The recent reconstructed dry conditions could be an artifact of TA preservation, with some tests being common in lower zone because of their high level of preservation rather than their initial abundance. In most cores, the shift in communities during the past 200 years is

characterized by decreasing *Archerella flavum* and increasing *Hyalosphenia papilio*. *H. papilio* is found abundantly in many fossil peats (Bunbury et al., 2012), but a preservation bias is possible, particularly given that a few cores have increased amounts of *Nebela* and *Assulina*, which may be more prone to decay and therefore underrepresented in catotelm peat (Loisel and Garneau, 2010; Fig. 23; Fig. 29; Fig. 30; Fig. 31; Tab 17; Tab. 20). However, it is striking that all records show the same recent response. If decreases in WTD during the last two centuries represents drying due to anthropogenic climate change, then the MCA may not be a good analog for our modern climate. It may not be appropriate to frame paleorecords during the MCA as natural experiments because modern warming may have already exceeded MCA warming, and the drivers of modern warming are different from the MCA.

Although three of the JBL records display well constrained, consistent and synchronous changes during the MCA, LIA, and last two centuries, interpretation of the patterns in the northernmost record require further examination, and a better understanding of the potential effect that permafrost establishment or thaw can have on surface moisture. More information on the ecology of TA in the region is also needed, as morphologically variable taxa such as *Difflugia pristis* type are common, but not well constrained ecologically or taxonomically (Booth, Personal Communication).

5.5.2. MCA Hydroclimatology in North America

To examine the spatial pattern of drought during the MCA and see if it is similar to episodes during La Niña conditions in North America, I supplemented my JBL TA

records with a review of lake level, surface moisture, or precipitation reconstructions during the MCA (Fig. 33; Tab. 21, 22). These studies utilize diatoms, stable isotopes, pollen, or lake varves, and charcoal, and other geochemical and physical properties. This is not a comprehensive overview of every proxy and every site tied to precipitation in North America, but instead serves to add perspective to new TA data from central Ontario and assess if the inferred hydrology during the MCA is consistent with known climate dynamics.

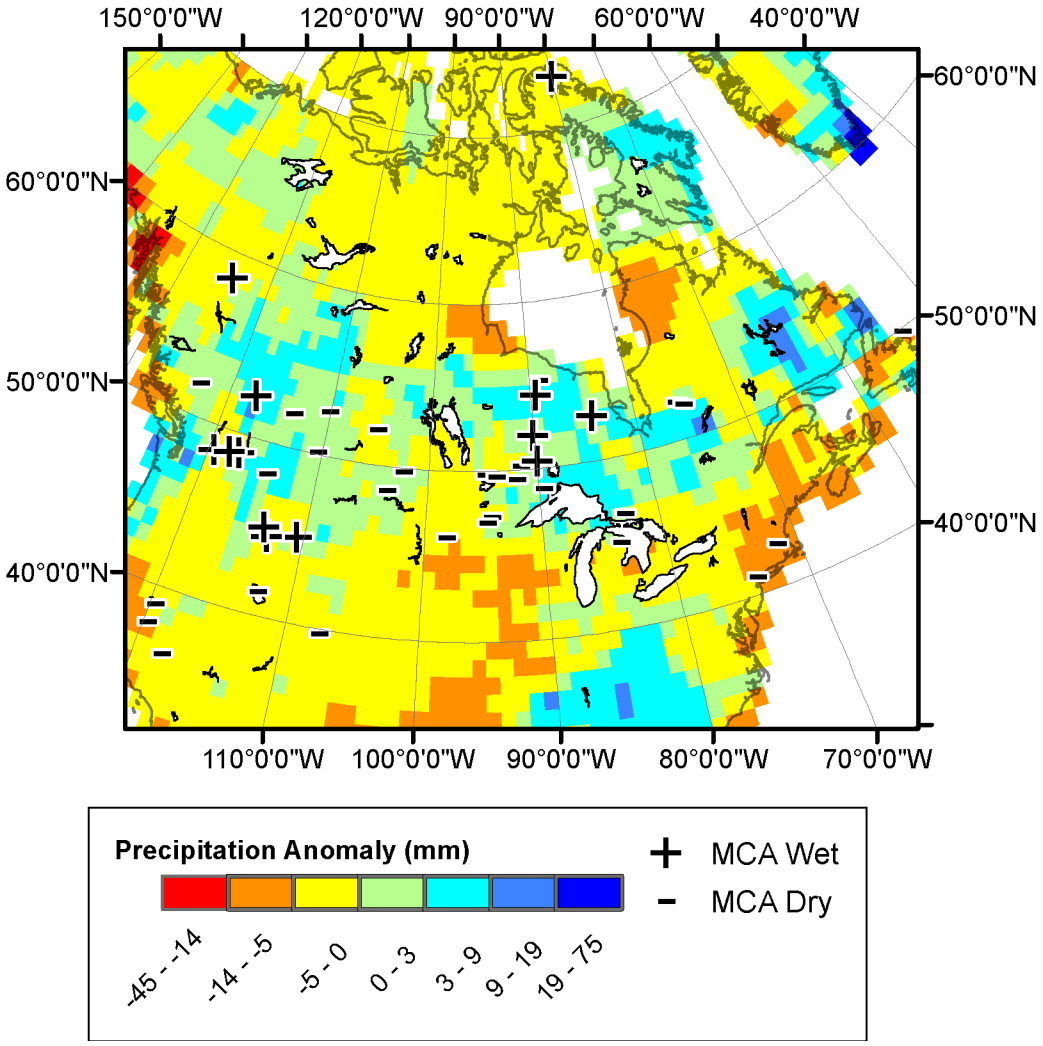

Figure 33: A map showing reported medieval surface moisture conditions from Ch. 4, Ch. 5, and a review of literature (Tab. 21, 22), as well as compiled precipitation anomalies for the seven most extreme La Niña events since 1949 according to the Multivariate ENSO Index (1949-51, 1954-56,1964-66,1970-1972,1973-75, 1988-90, 2010-2011; NOAA/ESRL, 2013a,b)

Table 21: The results of a literature review of reported moisture conditions across various proxies in North America.

Core Name	Source	Lat., Long. (DMS)	Proxy	MCA (+/-)
Bison Lake	Anderson, 2011	39.764°N, 107.346°W	^{18}O	-
Burnt Knob Lake	Brunelle et al., 2000; Cooke et al., 2004	45°42'16" N, 114°59'12" W	Charcoal	-
Chappice Lake	Vance et al., 1992	50°10' N, 110°22 W	Laminates	-
Chauvin Lake	Vance and Wolfe, 1996; Bonsal et al., 2011	52.69°N, 110.10°W	Diatoms	-
Crater Lake	Brunelle et al., 2003; Cooke et al., 2004	41°24' N, 122°35' W	Charcoal	-
Dog Lake	Hallet et al., 2003	48°48'11" N, 89°32'51" W	Diatoms	-
Felker Lake	Galloway et al. 2011	51°57.00' N, 121°59.90' W	Diatoms	-
Foy Lake	Stevens et al., 2006; Bracht-Flyr and Fritz, 2012	48°10' N, 114°21 W	Diatoms and ^{18}O	-
Gall Lake	Haig, 2011	50°14’ N, 91°27’ W	Diatoms	-
Hole Bog	Booth et al., 2005	47°18'00" N, 94°14'57" W	Testate Amoebae	-
Humbolt Lake	Vance and Wolfe, 1996; Bonsal et al., 2011	52°08'37" N, 105°07'04" W	Diatoms	-
Irwin Smith Peatland	Booth et al., 2012	45°1'51.02" N, 83°37'1.43" W	Beech Pollen, Testate Amoebae	-
JBL4	-	55°16'09" N, 88°55'50" W	Testate Amoebae	-
Kenosee Lake	Vance et al., 1997	49°49' N, 102°18' W	Sediments, Macrofossils, Ostracodes, Isotopes	-
Kettle Lake	Hobbs et al., 2011	48°36'25" N, 103°37'27" W	Diatoms	-
Little Pond	Oswald and Foster, 2011	42° 25' 20.2794" N, 71° 35' 15.7194" W	Pollen	-
Little Raliegh Lake	Ma, 2011; Ma et al., 2012	49°27’13" N, 91°53’46’’ W	Diatoms	-
LLC	Van Bellen et al., 2011	52°17' N, 75°50' W	Testate Amoebae	-
Meekin Lake	Laird et al., 2011	49°49'01 N, 94°46'12" W	Diatoms	-
Minden Bog	Booth et al., 2005, 2012	46°36'38" N, 82°50'05" W	Testate Amoebae	-
Moon Lake	Laird et al., 1998; Fritz et al., 2009	46°5'27" N, 98°09'30" W	Diatoms	-
Nordan's Pond Bog	Hughes et al., 2006	49°19'5" N, 53°36'0" W	Plant Macros, Testate Amoebae, Humification	-

Table 22: The results of a literature review of reported moisture conditions across various proxies in North America.

Core Name	Source	Lat., Long. (DMS)	Proxy	MCA (+/-)
Owens Lake	Benson et al., 2002	36°26'10" N, 117°57'36" W	^{18}O and Tree Stump Death	-
Piermont Marsh	Pederson et al., 2005	41°00' N, 73°55' W	Pollen and Charcoal	-
Pine Lake	Cambell et al., 2000	52°04’ N, 113°27’ W	charcoal, granulometry, geochemistry, mineralogy, and pollen	-
Pyramid Lake	Benson et al., 2002; Cooke et al., 2004	38°57'33" N, 119°35'35" W	^{18}O and Tree Stump Death	-
Rawson Lake	Laird and Cummings, 2009	49°40' N, 93°44' W	Diatoms	-
Siesta Lake	Brunelle and Anderson, 2003	37°51' N, 119°40' W	Charcoal	-
STE	Van Bellen et al., 2011	52°02'37" N, 75°10'23" W	Testate Amoebae	-
Steel Lake	Tian et al., 2006	46°58’N, 94°41’W	^{18}O	-
Athabsca	Edwards et al., 2008	52°24' N, 117°30' W	Dendrochronology and Stable Isotopes	+
BC2	Karst-Riddoch et al., 2005	58°28’ N, 124°28’ W	Diatoms	+
Castor Lake	Steinman et al., 2012	48.54° N, 119.56° W	^{18}O	+
Crevice Lake	Bracht-Flyr and Fritz, 2012; Steinman et al., 2012	45°0' N, 110°36' W	^{18}O	+
JBL2	-	52°01'07" N, 90°07'53" W	Testate Amoebae	+
JBL7	-	54°23'43" N, 89°31'20" W	Testate Amoebae	+
JBL8	-	50°27'33" N, 89°55'42" W	Testate Amoebae	+
Lime Lake	Steinman et al., 2012	48.87° N, 117.34° W	^{18}O	+
Morisson	Bracht-Flyr and Fritz, 2012	44°36' N, 113°2' W	Diatoms	+
Qunguliqtut Valley	Ellis and Rochefort, 2006	73.08° N; 80.00° W	Macrofossils and ^{18}O	+
Renner Lake	Steinman et al., 2012	48.78 °N, 118.19 °W	^{18}O	+
Resevoir	Bracht-Flyr and Fritz, 2012	45°7' N, 113°27' W	Diatoms	+
VC04-06	Bunbury et al., 2012	52°42'36" N, 84°10'48" W	Testate Amoebae	+

Out of the 41 sites I investigated, 13 reported anomalously moist, humid, or high lake stand periods, and 28 reported anomalously dry, or low lake stand periods (Fig. 33;

Tab. 21, 22). The wet MCA reconstructed in JBL8, JBL2 and JBL7 differ from surrounding areas, most notably, the Quebec JBL, and the more southerly Great Lakes region. The extent of medieval precipitation anomalies roughly corresponds to the extent of precipitation anomalies under La Niña conditions since 1949 AD. Modern positive precipitation anomalies also correspond with reconstructed medieval precipitation in the Pacific Northwest (Bracht-Flyr and Fritz, 2012; Steinman et al., 2012), and the Rocky Mountain range (Karst-Riddoch, 2005; Edwards et al., 2008; Bracht-Flyr and Fritz, 2012). During the late-Holocene, some glacial expansion in Alaska and Pacific Northwest may be due to increasing medieval wetness (Reyes et al., 2006; Edwards et al., 2008). In many areas, such as the American southwest (Benson et al., 2002; Brunelle et al., 2003; Anderson, 2011), the Great Plains (Vance et al., 1992; Fritz et al., 2000; Stevens et al., 2006; Bonsal et al., 2011; Galloway et al. 2011; Bracht-Flyr and Fritz, 2012), the more southerly Great Lakes regions (Booth et al., 2005; Tian et al, 2006; Vance et al., 2007; Laird and Cummings, 2009; Haig, 2011; Hobbs et al., 2011; Laird et al., 2011; Booth et al. 2012; Laird et al., 2012), American northeast (Pederson et al., 2005; Hughes, 2006; Oswald and Foster; 2011), and Quebec JBL (van Bellen et al., 2011), the MCA appears to have been dominated by drought conditions. Studeis in the Great Lakes Region indicate several quick droughts interspersed with moderate or wet periods (Booth et al., 2012). Medieval wetness in central and northern Ontario can be explained by likely negative Pacific Southern Oscillation phase, coupled with an anomalously warm Northern Atlantic, which could have pushed the westerly storm track north (Graham et al., 2011; Bracht-Flyr and Fritz 2012).

There are many data gaps and outstanding issues that could lend themselves to future studies. Biological proxies can have a complex relationship to precipitation, and often require interpretation. There is general agreement that medieval droughts did not extend far into the boreal regions of northern and central Ontario, and Quebec (Fig. 33). Few studies have directly compared TA based WTD reconstructions to nearby diatom inferred lake-depth records. There are many possible drivers, such as the seasonality of precipitation (Shabbar et al., 2007), the length of the season, (Karst-Riddoch, 2005; Camill, 2012), and watershed properties (Klein et al., 2013) that could potentially make records derived from different proxies difficult to compare. There is also a paucity of surface moisture reconstruction data for the American and Canadian coastal Atlantic region. Therefore, future studies should focus on creating high-resolution, multi-proxy records from permafrost zones, and southern boreal zones of Canada, as well as the North Atlantic coast and the Pacific Northwest.

The four TA based WTD reconstructions presented in this dissertation, as well as my review of medieval climate proxy reconstructions, reinforce the importance of Pacific sea surface temperatures and their stochastic interactions with the atmosphere on North American precipitation/drought patterns. In the future, some increased precipitation in the HBL-JBL can be expected due to the general poleward shift of westerly storms. Although future warming will likely weaken tropical easterly winds, warm tropical surface waters, shoal the equatorial thermocline, and increase the temperature gradient of the equitorial thermocline, there is no current consensus on whether the future will be more El Niño or La Niña-like (Collins et al., 2010). One possibility for the future is an increase in frequency of El Niño and La Niña conditions

with anomalous central Pacific convection patterns, known as El Niño and La Niña-Modoki (Ashok and Yamagata, 2009). In North America, one possible pattern includes a northeastern shift in the North American teleconnections (Stevenson et al., 2012). Some models indicate that positive precipitation in the Pacific Northwest will be robust in the future (Zhang et al., 2012), but the same regional application of general circulation models to ENSO teleconnections has not yet been applied to the HBL-JBL.

5.5.3. Inconsistent relationships between WTD and LARCA

Variation in LARCA did not have a constant relationship with WTD, but did accompany general changes in TA assemblage. I have three possible hypotheses to explain this pattern. 1. Changes in TA assemblage and LARCA could be intercorrelated with shifts in surface ecology that were not detected in the coarse macrofossil analysis, such as hummock-hollow alternation (Booth, 2008). Different species of *Sphagnum* could have different species of TA associated with them, as well as differential rates of preservation. 2. LARCA could have increased due to fluctuating water tables. Some studies indicate that *Sphagnum* has a competitive advantage during unstable hydrological conditions (Granath et al., 2010). 3. The lack of an apparent response of LARCA to changes in WTD could be due to a return to growth-decay-WTD equilibrium following a disturbance (Bridgeham et al., 2006). Although LARCA was variable over the late-Holocene, those variations do not show the positive relationship between WTD and LARCA that I reported for the mid and late-Holocene for JBL7 in Chapter 4.

5.6. CONCLUSION

In the JBL, TA records in *Sphagnum* peat cores over the late-Holocene showed statistical zonation and variability in reconstructed WTD. I observed a consistent trend in the three most southern sites of a generally wet MCA, and a generally dry LIA. JBL4 showed synchronous changes, with a wet LIA, and a dry MCA. This difference may be due to past permafrost dynamics, autogenic processes, or spatial precipitation variability during the MCA and LIA. All four sites show conditions drying over the last 100 to 250 ybp. Fluctuations in WTD did not apparently coincide with variation in LARCA; *Sphagnum* bogs may have been resilient to allogenic changes in WTD because of structural negative feedbacks. North American mega-droughts were widespread during in the MCA in the Great Plains, the Great Lakes regions, and western Ontario, but severe droughts do not appear to have extended into the JBL and adjacent portions boreal regions of Ontario and Quebec. This pattern is roughly consistent in some areas of North America with modern precipitation anomalies in Canada involving Pacific Southern Oscillation and the movement of the Northern storm front. If positive precipitation anomalies persist in the JBL promotes low decomposition, and temperature driven increase productivity, then the JBL may continue to serve as sink for C. However if recent drying is indicative of anthropogenic climate change rather than an artifact of TA preservation, then soil C in the JBL may be vulnerable to future shifts in precipitation patterns.

6. Conclusion

The overall focus of this dissertation was the relationship between Holocene soil carbon (C) and climate in the remote James Bay Lowlands (JBL) region of Canada. I filled data gaps, tested hypothesis, and reconstructed hydrology for the understudied JBL regions of central and northern Ontario. I also provided synthesis when possible for the Hudson Bay Lowlands (HBL)–JBL as a whole. Average peatland initiation occurred around 6.2 ka (ka = 1,000 calendar years before present [ybp]) following deglaciation and glacial lake drainage. Average fen to bog transitions had occurred before the late-Holocene meaning that the JBL likely contributed to the decline in atmospheric CH_4 during this time (Ch. 2). 40% of the C stored had been stored since 2 ka (Ch. 3). Growing degree-days > 0°C (GDD_0) and photosynthetically active radiation integrated over days > 0°C (PAR_0) were the major drivers of vertical peat accumulation over the last 2 ka, for the HBL-JBL, although precipitation sets the climatic envelope and may be an important local driver (Ch. 3). Apparent C accumulation was highly variable, but was limited in the north by the establishment of modern permafrost conditions (Ch. 2; Ch. 3). In the early Holocene, the Arctic Front likely dominated central Ontario from 7.4 – 4.5 ka, whereas the Pacific Front dominated from 4.5 ka to modern time (Ch. 4). The Medieval Climate Anomaly (MCA) was a regionally wet event, while the Little Ice Age (LIA) was regionally dry, except for the most northern site in the discontinuous permafrost zone (Ch. 4; Ch. 5). Modern warming is unprecedented and may be responsible for the modern drying trend observed (Ch. 5). Although I have provided original data, synthesis, and insight

into the possible allogenic drivers of peatland C cycle feedbacks, current knowledge of JBL history is still evolving, and there are many possible areas for future study.

This dissertation adds eight new sites to the JBL, and synthesizes currently available data, but there are many regions within the HBL-JBL, and elsewhere, that are still under-represented. The far northeastern regions of Ontario are under researched although they are remote and contain dense C-stores (Glaser et al., 2004a; MacDonald et al., 2006; Tarnocai et al., 2011; Bunbury et al., 2012). The southern discontinuous peatland regions of Ontario are also under represented although they represent the high end of the temperature gradient amenable to peat formation (Ch. 3; Elliott et al., 2012). Coring efforts, combined with seasonality and precipitation data from the southernmost documented extent of peatlands in the JBL could lead to more accurate estimates of the effect of climate on productivity and decay. This dissertation also dealt exclusively with modern-day bogs, and ombrotrophic permafrost formations, leaving fen peatlands still under-represented in the JBL (Ch. 2; O'Reilly, 2012). There have been no regional syntheses of fen C accumulation even though they are also likely sensitive to changes in GDD_0 and PAR_0 (Charman et al., 2013). For fens and bogs, there is a lack of C accumulation, and paleohydrology data from the Mackenzie River Basin (Beilman et al., 2008), Alaska (Klein et al., 2013; Loisel and Yu, 2013a), some regions of Siberia (Beilman et al., 2009), and Patagonia (Loisel and Yu, 2013b), as well as tropical, and high altitude peatlands (Page et al., 2011).

The data in this dissertation, including: average core depths, C-content estimates, the positive correlations between GDD_0/PAR_0 and 2 ka depth, and negative correlations between permafrost occurrence and 2 ka depth (Ch. 2), could be used to

parameterize a spatial model of C accumulation in the JBL. However there are still very few %C estimates for the JBL (Bunbury et al., 2012; O'Reilly, 2012). There are many outstanding issues with peatland mapping including, limited resolution and reliability of peatland maps. Current maps of C stocks in Ontario are based on shapefiles with varied and limited resolution (Tarnocai et al., 2011), and high-resolution remotely sensed data has not yet been used to estimate peatland types for more than the provincial level (Provincial Land Cover Data Base, 2000). As new C accumulation data is published, and spatial data is revised and combined with climate data (Beilman et al., 2009; Charman et al., 2013), and hydrological models (Glaser et al., 2004b), soil C estimates of the JBL will become more detailed and accurate.

One of the limitations of this study was the single core approach. Multi-core studies of a single site show that initiation can vary within a peatland. Multi-core studies in the JBL could better constrain the average initiation time following deglaciation (Bauer et al., 2003). Lateral expansion could have been important to peatland C sinks (MacDonald et al., 2006). In the case of JBL7, a multi-core macrofossil analysis, could determine if the bog to fen succession event was an ecosystem-wide phenomenon, or a function of microtopography, such as hummock – hollow alternation, or the flooding of a bog or poor fen margin (Bauer et al., 2003). A multi-core analysis could also be helpful with the testate amoebae (TA) reconstruction of precipitation because water table depth (WTD) in bogs can be influenced by autogenic and allogenic events (Loisel and Garneau, 2010; Klein et al., 2013).

The peat initiation dates and fen to bog succession timings showed spatial variation with southern sites having longer lags in both initiation and succession, relative

to northern sites (Ch. 3). Future studies could investigate this trend relative to sediment types. Different initiation and succession timing patterns could be the result of different pH or different permeability of boreal shield and lacustrine/marine sediments, or could reflect the results of different bog forming processes, paludification and terrestrialization (Josenhans and Zevenhuizen, 1990; Korhola, 1995).

Another limitation of this dissertation is that past peat decay was not investigated in detail. Some studies have used a modeling approach to estimate C losses over time (Beilmen et al., 2009; Loisel and Yu, 2013b). One case observed that modern productivity was high relative to model projections, indicating that modern warming has been having a positive effect on peat growth and formation (Loisel and Yu, 2013b). Other studies have combined WTD reconstruction with C to nitrogen (N) ratios to investigate the linked relationship between past ecohydrology (Andersson and Schoning, 2010), and decay/production balance (Malmer and Wallén, 2004; Broder et al., 2012). Although I did not observe significant increase in LARCA during the MCA and LIA due to WTD fluctuations, a C:N analysis could determine whether this could have been due to a change in the balance between productivity and decay.

Future studies should focus on improving TA reconstructions in the JBL by adding new surface samples to the calibration dataset. The taxonomy and ecology of TA could also be improved. Taxa such as *Difflugia pristis* type are ubiquitous and morphologically variable, and taxonomically not well constrained (Booth, 2008). Currently TA based WTD reconstructions use transfer function calibration datasets that were developed for the Great Lakes, and Rocky Mountain regions (Booth, 2008; Loisel and Garneau, 2010; Bunbury et al., 2012; O'Reilly, 2012). Although TA are ubiquitous

and studies comparing different regional transfer functions indicate little effect of a transfer function's regional origin, future studies should still integrate surface samples from the JBL into transfer function calibration datasets (Turner et al., 2013).

Future studies could focus on increasing the number of Holocene-length TA based WTD reconstructions, as well as increase the number of multi-proxy studies, and develop new proxies for important climate variables. The mid-Holocene reconstruction of WTD revealed that there was a 6.1 ka dry event, along with a spike in LARCA (Ch. 3; Ch. 4). TA analysis, on other Holocene length cores that contain 6.1 ka LARCA spikes could provide evidence for a larger scale climate or watershed event. A multiproxy surface wetness reconstruction using ^{13}C records and TA analysis could substantiate reports of extreme values (Lamentowicz et al., 2008). There are increased margins of error towards dry extremes in TA due to the relatively shallow WTD optimum for the most extreme dry taxa (~40 cm; Booth, 2008). Although GDD_0 and PAR_0 were the dominant drivers of late-Holocene vertical peat accumulation, there is currently no way to reconstruct growing season length in the JBL. One possible future proxy that could be adapted are dwarf birch leaf cuticle characteristics (Wagner-Cremer et al., 2010). The undulation index of epidermal cells correlate with growing degree days in a Scandinavian dwarf birch, *Betula nana*, however studies have not yet investigated the closely related Canadian *Betula glandulosa* or attempted growing season length reconstruction using sub-fossil birch leaf cuticles.

Future studies should document the extent of medieval wetness and better constrain precipitation anomalies during the LIA for the JBL. In Chapter 5 I presented a brief review of surface moisture proxies in North America in relation to TA based

reconstructions in the JBL, and modern precipitation anomaly data. There is a rough relationship between modern North American precipitation anomalies under large-scale drought conditions and reported MCA precipitation anomalies. However there are a few issues when comparing records from multiple sources. Bog WTD can be influenced by autogenic factors that do not occur in lakes such as hummock-hollow alternation, succession, mound collapse, and recharge. It would also be beneficial to reconstruct WTD in other areas that contain significant stores of soil C, and exhibit positive or negative precipitation anomalies under modern La Niña-like conditions such as portions of the Mackenzie River Basin, and the northern coast of Labrador and Quebec, Canada (Ch. 5).

In this dissertation I provided data and insight into the post-glacial history, soil C storage patterns, and mid to late-Holocene hydrology in one of the most immense, and possibly vulnerable, terrestrial C sinks. There is a lot potential to introduce climate controls into peatland development models, to scale up estimates of soil C using spatial models, to develop and improve climate proxies, and to further document the past effect of warming on precipitation anomalies, in order to better predict the role of peatland C cycle feedbacks to anthropogenic global warming.

7. Works Cited

Adkinson, A. C., Syed, K. H., & Flanagan, L. B. (2011). Contrasting responses of growing season ecosystem CO_2 exchange to variation in temperature and water table depth in two peatlands in northern Alberta, Canada. *Journal of Geophysical Research*, *116*(G1), G01004.

Anderson, L. (2011). Holocene record of precipitation seasonality from lake calcite $\delta^{18}O$ in the central Rocky Mountains, United States. *Geology*, *39*(3), 211-214.

Andersson, S., & Schoning, K. (2010). Surface wetness and mire development during the late-Holocene in central Sweden. *Boreas*, *39*(4), 749-760.

Arlen-Pouliot, Y., & Bhiry, N. (2005). Palaeoecology of a palsa and a filled thermokarst pond in a permafrost peatland, subarctic Québec, Canada. *The Holocene*, *15*(3), 408-419.

Asada, T., Warner, B. G., & Banner, A. (2003). Growth of mosses in relation to climate factors in a hypermaritime coastal peatland in British Columbia, Canada. *The Bryologist*, *106*(4), 516-527.

Ashok, K., Behera, S. K., Rao, S. A., Weng, H., & Yamagata, T. (2007). El Niño Modoki and its possible teleconnection. *Journal of Geophysical Research: Oceans (1978–2012)*, *112*(C11).

Barber, K. E. (1981). *Peat stratigraphy and climatic change: a palaeoecological test of the theory of cyclic peat bog regeneration*. Rotterdam: Balkema.

Barber, D. C., Dyke, A., Hillaire-Marcel, C., Jennings, A. E., Andrews, J. T., Kerwin, M. W., Bilodeau, G., McNeely, R., Southon, J., Morehead, M. D., & Gagnon, J. M. (1999). Forcing of the cold event of 8,200 years ago by catastrophic drainage of Laurentide lakes. *Nature*, *400*(6742), 344-348.

Bartlein, P. J., Harrison, S. P., Brewer, S., Connor, S., Davis, B. A. S., Gajewski, K., Guiot, J., Harrison-Prentice, T. I., Henderson, A., Peyron, O., Prentice, I. C., Scholze, M., Seppä, H., Shuman, B., Sugita, S., Thompson, R. S., Viau, A. E., & Wu, H. (2011). Pollen-based continental climate reconstructions at 6 and 21 ka: a global synthesis. *Climate Dynamics*, *37*(3-4), 775-802.

Bauer, I. E., Gignac, L. D., & Vitt, D. H. (2003). Development of a peatland complex in boreal western Canada: lateral site expansion and local variability in vegetation succession and long-term peat accumulation. *Canadian Journal of Botany*, *81*(8), 833-847.

Beaulieu-Audy, V., Garneau, M., Richard, P. J., & Asnong, H. (2009). Holocene palaeoecological reconstruction of three boreal peatlands in the La Grande Riviere region, Quebec, Canada. *The Holocene*, *19*(3), 459-476.

Beilman, D. W., MacDonald, G. M., Smith, L. C., & Reimer, P. J. (2009). Carbon accumulation in peatlands of West Siberia over the last 2000 years. *Global Biogeochemical Cycles*, *23*(1): GB1012.

Beilman, D. W., Vitt, D. H., Bhatti, J. S., & Forest, S. (2008). Peat carbon stocks in the southern Mackenzie River Basin: Uncertainties revealed in a high-resolution case study. *Global Change Biology*, *14*(6), 1221-1232.Belyea, L. R., & Baird, A. J. (2006). Beyond "the limits to peat bog growth": cross-scale feedback in peatland development. *Ecological Monographs*, *76*(3), 299-322.

Bennett, K., (1996). Determination of the number of zones in a biostratigraphic sequence. *New Phytologist*, 132, 155-170.

Benson, L., Kashgarian, M., Rye, R., Lund, S., Paillet, F., Smoot, J., Kester, C., Mensing, S., Meko, D., & Lindström, S. (2002). Holocene multidecadal and multicentennial droughts affecting Northern California and Nevada. *Quaternary Science Reviews*, *21*(4), 659-682.

Beringer, J., Tapper, N. J., McHugh, I., Chapin, F. S., Lynch, A. H., Serreze, M. C., & Slater, A. (2001). Impact of Arctic treeline on synoptic climate. *Geophysical Research Letters*, *28*(22), 4247-4250.

Blaauw, M., & Christen, J. A. (2011). Flexible paleoclimate age-depth models using an autoregressive gamma process. *Bayesian Analysis*, *6*(3), 457-474.

Blaauw, M., & Heegaard, E. (2012). Estimation of age-depth relationships. In *Tracking environmental change using lake sediments* (pp. 379-413). Springer Netherlands.

Blodau, C. (2002). Carbon cycling in peatlands: A review of processes and controls. *Environmental Reviews*, *10*(2), 111-134.

Blodau, C., Basiliko, N., & Moore, T. R. (2004). Carbon turnover in peatland mesocosms exposed to different water table levels. *Biogeochemistry*, *67*(3), 331-351.

Bonsal, B. R., Wheaton, E. E., Chipanshi, A. C., Lin, C., Sauchyn, D. J., & Wen, L. (2011). Drought research in Canada: A review. *Atmosphere-Ocean*, *49*(4), 303-319.

Booth, R. K. (2008). Testate amoebae as proxies for mean annual water-table depth in *Sphagnum*-dominated peatlands of North America. *Journal of Quaternary Science*, *23*(1), 43-57.

Booth, R. K., Jackson, S. T., Forman, S. L., Kutzbach, J. E., Bettis III, E. A., Kreigs, J., & Wright, D. K. (2005). A severe centennial-scale drought in midcontinental North America 4200 years ago and apparent global linkages. *The Holocene*, *15*(3), 321-328.

Booth, R. K., Jackson, S. T., Sousa, V. A., Sullivan, M. E., Minckley, T. A., & Clifford, M. J. (2012). Multi-decadal drought and amplified moisture variability drove rapid forest community change in a humid region. *Ecology*, 93(2), 219-226.

Booth, R. K., Lamentowicz, M., & Charman, D. J. (2010). Preparation and analysis of testate amoebae in peatland paleoenvironmental studies. *Mires and Peat*, *7*(7).

Booth, R. K., Notaro, M., Jackson, S. T., & Kutzbach, J. E. (2006). Widespread drought episodes in the western Great Lakes region during the past 2000 years: geographic extent and potential mechanisms. *Earth and Planetary Science Letters*, *242*(3), 415-427.

Bracht-Flyr, B., & Fritz, S. C. (2012). Synchronous climatic change inferred from diatom records in four western Montana lakes in the US Rocky Mountains. *Quaternary Research, 77*, 456-467.

Breeuwer, A., Heijmans, M. M., Robroek, B. J., & Berendse, F. (2008). The effect of temperature on growth and competition between *Sphagnum* species. *Oecologia*, *156*(1), 155-167.

Breeuwer, A., Robroek, B. J., Limpens, J., Heijmans, M. M., Schouten, M. G., & Bridgham, S. D., Megonigal, J. P., Keller, J. K., Bliss, N. B., & Trettin, C. (2006). The carbon balance of North American wetlands. *Wetlands*, *26*(4), 889-916.

Bridgham, S. D., Megonigal, J. P., Keller, J. K., Bliss, N. B., & Trettin, C. (2006). The carbon balance of North American wetlands. *Wetlands*, *26*(4), 889-916.

Broder, T., Blodau, C., Biester, H., & Knorr, K. H. (2012). Peat decomposition records in three pristine ombrotrophic bogs in southern Patagonia. *Biogeosciences*, *9*(4), 1479-1491.

Broecker, W. S. (2001). Paleoclimate: Was the medieval warm period global?. *Science*, *291*(5508), 1497.

Brook, E. J., Harder, S., Severinghaus, J., Steig, E. J., & Sucher, C. M. (2000). On the origin and timing of rapid changes in atmospheric methane during the last glacial period. *Global Biogeochemical Cycles*, *14*(2), 559-572.

Brown, J., Ferrians Jr., O. J., Heginbottom, J. A., & Melnikov, E. S., (1998). revised February 2001. Circum-Arctic map of permafrost and ground-ice conditions. Boulder, CO: National Snow and Ice Data Center/World Data Center for Glaciology. Digital Media: accessed 13 August, 2012

Brunelle, A., & Whitlock, C. (2003). Postglacial fire, vegetation, and climate history in the Clearwater Range, Northern Idaho, USA. *Quaternary Research*, *60*(3), 307-318.

Bunbury, J., Finkelstein, S. A., & Bollmann, J. (2012). Holocene hydro-climatic change and effects on carbon accumulation inferred from a peat bog in the Attawapiskat River watershed, Hudson Bay Lowlands, Canada. *Quaternary Research*: 275-284.

Calcote, R. (2003). Mid-Holocene climate and the hemlock decline: the range limit of *Tsuga canadensis* in the western Great Lakes region, USA. *The Holocene, 13*(2), 215-224.

Camill, P., Umbanhowar, C. E., Geiss, C., Hobbs, W. O., Edlund, M. B., Shinneman, A. C., & Lynch, J. (2012). Holocene climate change and landscape development from a low-Arctic tundra lake in the western Hudson Bay region of Manitoba, Canada. *Journal of Paleolimnology*, 1-18.

Campbell, I. D., Last, W. M., Campbell, C., Clare, S., & McAndrews, J. H. (2000). The late-Holocene paleohydrology of Pine Lake, Alberta: a multiproxy investigation. *Journal of Paleolimnology*, *24*(4), 427-441.

Carlson, M., Chen, J., Elgie, S., Henschel, C., Montenegro, Á., Roulet, N., Scott, N., Tarnocai, C., & Wells, J. (2010). Maintaining the role of Canada's forests and peatlands in climate regulation. *The Forestry Chronicle*, *86*(4), 434-443.

Chambers, F. M., Booth, R. K., De Vleeschouwer, F., Lamentowicz, M., Le Roux, G., Mauquoy, D., Nichols, J. E., & van Geel, B. (2011). Development and refinement of proxy-climate indicators from peats. *Quaternary International 268*, 21-33.

Charman, D. J. (2000). Biostratigraphic and palaeoenvironmental applications of testate amoebae. *Quaternary Science Reviews*, *20*(16), 1753-1764.

Charman, D. J., Beilman, D. W., Blaauw, M., Booth, R. K., Brewer. S., Chambers, F. M., Christen, J. A., Gallego-Sala, A., Harrison, S. P., Hughes, P. D. M., Jackson, S. T., Korhola. A., Mauquoy, D., Mitchell, F. J. G., Prentice, I. C., van der Linden, M., De Vleeschouwer, F., Yu, Z. C., Alm, J., Bauer, I. E., Corish, Y. M. C., Garneau, M., Hohl, V., Huang, Y., Karofeld, E., Le Roux, G., Loisel, J., Moschen, R., Nichols, J. E., Nieminen, T. M., MacDonald, G. M., Phadtare, N. R., Rausch, N., Sillasoo, Ü., Swindles, G.T., Tuittila, E.-S., Ukonmaanaho, L., Vä Iiranta, M., van Bellen, S., van Geel, B., Vitt, D. H., & Zhao, Y, (2013). Climate-related changes in peatland carbon accumulation during the last millennium. *Biogeociences, 10*: 929-944.

Charman, D. J., & Hendon, D. (2000). Long-Term Changes in Soil Water Tables over the past 4500 Years: Relationships with Climate and North Atlantic Atmospheric Circulation and Sea Surface Temperature. *Climatic Change*, *47*(1-2), 45-59.

Christen, J. A., & Pérez, S. (2011). A new robust statistical model for radiocarbon data. *Radiocarbon*, *51*(3), 1047-1059.

Christiansen, B., & Ljungqvist, F. C. (2011). Reconstruction of the extratropical NH mean temperature over the last millennium with a method that preserves low-frequency variability. *Journal of Climate*, *24*(23), 6013-6034.

Clymo, R. S. (1984). The limits to peat bog growth. *Philosophical Transactions of the Royal Society of London. B, Biological Sciences*, *303*(1117), 605-654.

Clymo, R. S., Turunen, J., & Tolonen, K. (1998). Carbon accumulation in peatland. *Oikos*, 368-388.

Collins, M., An, S. I., Cai, W., Ganachaud, A., Guilyardi, E., Jin, F. F., ... & Wittenberg, A. (2010). The impact of global warming on the tropical Pacific Ocean and El Niño. *Nature Geoscience*, *3*(6), 391-397.

Cook, E. R., Woodhouse, C. A., Eakin, C. M., Meko, D. M., & Stahle, D. W. (2004). Long-term aridity changes in the western United States. *Science*, *306*(5698), 1015-1018.

Davidson, E. A., & Janssens, I. A. (2006). Temperature sensitivity of soil carbon decomposition and feedbacks to climate change. *Nature*, *440*(7081), 165-173.

Dise, N. B. (2009). Peatland response to global change. *Science*, *326*(5954), 810.

Dorrepaal, E., Aerts, R., Cornelissen, J. H., Callaghan, T. V., & Van Logtestijn, R. S. (2004). Summer warming and increased winter snow cover affect *Sphagnum fuscum* growth, structure and production in a sub‐arctic bog. *Global Change Biology*, *10*(1), 93-104.

Dredge, L. A. (2001). Late Pleistocene and Holocene glaciation and deglaciation of Melville Peninsula, northern Laurentide Ice Sheet. *Géographie physique et Quaternaire*, *55*(2), 159-170.

Dredge, L. A. (1990). The Melville Moraine: sea-level change and response of the western margin of the Foxe Ice Dome, Melville Peninsula, Northwest Territories. *Canadian Journal of Earth Sciences*, *27*(9), 1215-1224.

Dredge, L. A., & Mott, R. J. (2003). Holocene pollen records and peatland development, northeastern Manitoba. *Géographie physique et Quaternaire*, *57*(1), 7-19.

Dunn, C., & Freeman, C. (2011). Peatlands: our greatest source of carbon credits?. *Carbon Management*, *2*(3), 289-301.

Dyke, A. S., Moore, A., Robertson, L., 2003: Geological survey of Canada <geoscan.ess.nrcan.gc.ca>, accessed 5 February 2010.

Edwards, T. W., Birks, S. J., Luckman, B. H., & MacDonald, G. M. (2008). Climatic and hydrologic variability during the past millennium in the eastern Rocky Mountains and northern Great Plains of western Canada. *Quaternary Research*, *70*(2), 188-197.

Edwards, T. W., Wolfe, B. B., & Macdonald, G. M. (1996). Influence of changing atmospheric circulation on precipitation δ18O-temperature relations in Canada during the Holocene. *Quaternary Research*, *46*(3), 211-218.

Ellis, C. J., & Rochefort, L. (2006). Long-term sensitivity of a High Arctic wetland to Holocene climate change. *Journal of Ecology*, *94*(2), 441-454.

Elliott, S. M., Roe, H. M., & Patterson, R. T. (2012). Testate amoebae as indicators of hydroseral change: An 8500 year record from Mer Bleue Bog, eastern Ontario, Canada. *Quaternary International*, *268*, 128-144.

Environment Canada: National Climate Data and Information Archive. <www.climate.weatheroffice.gc.ca>, accessed 7 January 2013.

Eppinga, M. B., de Ruiter, P. C., Wassen, M. J., & Rietkerk, M. (2009). Nutrients and hydrology indicate the driving mechanisms of peatland surface patterning. *The American Naturalist*, *173*(6), 803-818.

Feng, S., Oglesby, R. J., Rowe, C. M., Loope, D. B., & Hu, Q. (2008). Atlantic and Pacific SST influences on Medieval drought in North America simulated by the Community Atmospheric Model. *Journal of Geophysical Research: Atmospheres (1984–2012)*, *113*(D11).

Fenner, N., & Freeman, C. (2011). Drought-induced carbon loss in peatlands. *Nature geoscience*, *4*(12), 895-900.

Forester, R. M., Delorme, L. D., & Bradbury, J. P. (1987). Mid-Holocene climate in northern Minnesota. *Quaternary Research, 28*(2), 263-273.

Freeman, C., Fenner, N., & Shirsat, A. H. (2012). Peatland geoengineering: an alternative approach to terrestrial carbon sequestration. *Philosophical Transactions of the Royal Society A: Mathematical, Physical and Engineering Sciences*, *370*(1974), 4404-4421.

Fritz, S. C., Ito, E., Yu, Z., Laird, K. R., & Engstrom, D. R. (2000). Hydrologic variation in the northern Great Plains during the last two millennia. *Quaternary Research*, *53*(2), 175-184.

Frolking, S., & Roulet, N. T. (2007). Holocene radiative forcing impact of northern peatland carbon accumulation and methane emissions. *Global Change Biology*, *13*(5), 1079-1088.

Frolking, S., Roulet, N. T., Moore, T. R., Richard, P. J., Lavoie, M., & Muller, S. D. (2001). Modeling northern peatland decomposition and peat accumulation. *Ecosystems, 4*(5), 479-498.

Frolking, S., Roulet, N. T., Tuittila, E., Bubier, J. L., Quillet, A., Talbot, J., & Richard, P. J. H. (2010). A new model of Holocene peatland net primary production, decomposition, water balance, and peat accumulation. *Earth System Dynamics*, *1*(1), 1.

Gajewski, K., Vance, R., Sawada, M., Fung, I., Gignac, L. D., Halsey, L., John, J., Maisongrande, P., Mandell, P., Mudie, P.J., Richard, P.J.H., Sherin, A.G., Soroko J., & Vitt, D. H. (2000). The climate of North America and adjacent ocean waters ca. 6 ka. *Canadian Journal of Earth Sciences*, *37*(5), 661-681.

Galloway, J. M., Lenny, A. M., & Cumming, B. F. (2011). Hydrological change in the central interior of British Columbia, Canada: diatom and pollen evidence of millennial-to-centennial scale change over the Holocene. *Journal of Paleolimnology*, *45*(2), 183-197.

Glaser, P. H., Hansen, B., Siegel, D. I., Reeve, A. S., & Morin, P. J. (2004). Rates, pathways and drivers for peatland development in the Hudson Bay Lowlands, northern Ontario, Canada. *Journal of Ecology*, *92*(6), 1036-1053.

Glaser, P. H., Siegel, D. I., Reeve, A. S., Janssens, J. A., & Janecky, D. R. (2004). Tectonic drivers for vegetation patterning and landscape evolution in the Albany River region of the Hudson Bay Lowlands. *Journal of Ecology*, *92*(6), 1054-1070.

Gomaa, F., Mitchell, E. A., & Lara, E. (2013). Amphitremida (Poche, 1913) Is a New Major, Ubiquitous Labyrinthulomycete Clade. *PloS one*, 8(1), e53046.

Gorham, E. (1991). Northern peatlands: role in the carbon cycle and probable responses to climatic warming. *Ecological applications*, *1*(2), 182-195.

Gorham, E., Janssens, J. A., & Glaser, P. H. (2003). Rates of peat accumulation during the postglacial period in 32 sites from Alaska to Newfoundland, with special emphasis on northern Minnesota. *Canadian Journal of Botany*, *81*(5), 429-438.

Gorham, E., Lehman, C., Dyke, A., Janssens, J., & Dyke, L. (2007). Temporal and spatial aspects of peatland initiation following deglaciation in North America. *Quaternary Science Reviews*, *26*(3), 300-311.

Graham, N. E., Ammann, C. M., Fleitmann, D., Cobb, K. M., & Luterbacher, J. (2011). Support for global climate reorganization during the “Medieval Climate Anomaly”. Climate dynamics, 37(5), 1217-1245.

Granath, G., Strengbom, J., & Rydin, H. (2010). Rapid ecosystem shifts in peatlands: linking plant physiology and succession. *Ecology*, *91*(10), 3047-3056.

Gunnarsson, U. (2005). Global patterns of *Sphagnum* productivity. *Journal of Bryology*, *27*(3), 269-279.

Haig, H. A. (2011). Diatom-inferred changes in effective moisture from gall lake, northwestern, Ontario, over the base two millenia. Thesis (Master, Biology) -- Queen's University, 2011-05-27 17:41:02.022 <http://hdl.handle.net/1974/6542>

Hallett, D. J., Mathewes, R. W., & Walker, R. C. (2003). A 1000-year record of forest fire, drought and lake-level change in southeastern British Columbia, Canada. *The Holocene*, *13*(5), 751-761.

Harley, P. C., Tenhunen, J. D., Murray, K. J., & Beyers, J. (1989). Irradiance and temperature effects on photosynthesis of tussock tundra *Sphagnum* mosses from the foothills of the Philip Smith Mountains, Alaska. *Oecologia*, *79*(2), 251-259.

Halsey, L. A., Vitt, D. H., & Gignac, L. D. (2000). *Sphagnum*-dominated peatlands in North America since the last glacial maximum: their occurrence and extent. *The Bryologist*, *103*(2), 334-352.

Hillaire-Marcel, C., & Fairbridge, R. W. (1978). Isostasy and eustasy of Hudson Bay. *Geology, 6*(2), 117-122.

Hobbs, W. O., Fritz, S. C., Stone, J. R., Donovan, J. J., Grimm, E. C., & Almendinger, J. E. (2011). Environmental history of a closed-basin lake in the US Great Plains: Diatom response to variations in groundwater flow regimes over the last 8500 cal. yr BP. *The Holocene*, 21(8), 1203-1216.

Hua, Q., & Barbetti, M. (2007). Review of tropospheric bomb ^{14}C data for carbon cycle modeling and age calibration purposes. *Radiocarbon*, *46*(3), 1273-1298.

Hughes, P. D. M., Blundell, A., Charman, D. J., Bartlett, S., Daniell, J. R. G., Wojatschke, A., & Chambers, F. M. (2006). An 8500cal. year multi-proxy climate record from a bog in eastern Newfoundland: contributions of meltwater discharge and solar forcing. *Quaternary Science Reviews*, *25*(11), 1208-1227.

IPCC. (2007). Climate Change 2007: Synthesis Report. Contribution of Working Groups I, II and III to the Fourth Assessment Report of the Intergovernmental Panel on Climate Change Pachauri RK & Reisinger A. (eds.). IPCC, Geneva, Switzerland.

Jansson, K. N., & Kleman, J. (2004). Early Holocene glacial lake meltwater injections into the Labrador Sea and Ungava Bay. *Paleoceanography*, *19*(1).

Jeong, S., Ho, C., Gim, H., & Brown, M. E. (2011). Phenology shifts at start vs. end of growing season in temperate vegetation over the Northern Hemisphere for the period 1982–2008. *Global Change Biology*, *17*(7), 2385-2399.

Jia, G. J., Epstein, H. E., & Walker, D. A. (2009). Vegetation greening in the Canadian Arctic related to decadal warming. *Journal of Environmental Monitoring*, *11*(12), 2231-2238.

Jorgenson, M. T., & Osterkamp, T. E. (2005). Response of boreal ecosystems to varying modes of permafrost degradation. *Canadian Journal of Forest Research*, *35*(9), 2100-2111.

Josenhans, H. W., & Zevenhuizen, J. (1990). Dynamics of the laurentide ice sheet in Hudson Bay, Canada. *Marine Geology, 92*(1), 1-26.

Juggins, S. (2003). C2: software for ecological and palaeocological data analysis and visualization, version 1.3. *Department of Geography, University of Newcastle*.

Juggins, S., Juggins, M. S., WA, W., & IKFA, M. (2009). Package 'rioja'.

Kaislahti Tillman, P., Holzkämper, S., Kuhry, P., Sannel, A. B. K., Loader, N. J., & Robertson, I. (2010). Long-term climate variability in continental subarctic Canada: A 6200-year record derived from stable isotopes in peat. *Palaeogeography, Palaeoclimatology, Palaeoecology*, *298*(3), 235-246.

Karst-Riddoch, T. L., Pisaric, M. F., Youngblut, D. K., & Smol, J. P. (2005). Postglacial record of diatom assemblage changes related to climate in an alpine lake in the northern Rocky Mountains, Canada. *Canadian journal of botany*, *83*(8), 968-982.

Kaplan, J. O., Bigelow, N. H., Bartlein, P. J., Christensen, T. R., Cramer, W., Harrison, S. P., Matveyeva, N. V., McGuire, A. D., Murray, D. F., Prentice, I. C., Razzhivin, V. Y., Smith, B., Walker, D. A., Anderson, P. M., Andreev, A. A., Brubaker, L. B., Edwards, M. E., Lozhkin, A. V., & Ritchie, J. (2003). Climate change and Arctic ecosystems II: Modeling, palaeodata-model comparisons, and future projections. *Journal of Geophysical Research: Atmospheres 108*, 8171.

Kaufman, D. S., Ager, T. A., Anderson, N. J., Anderson, P. M., Andrews, J. T., Bartlein, P. J., & Wolfe, B. B. (2004). Holocene thermal maximum in the western Arctic (0–180 W). *Quaternary Science Reviews*, *23*(5), 529-560.

Kaufman, D. S., Schneider, D. P., McKay, N. P., Ammann, C. M., Bradley, R. S., Briffa, K. R., Miller, G. H., Otto-Bliesner, B. L., Overpeck, J. T., Vinther, B. M., Arctic Lakes 2k Project Members - Abbott, M., Axford, Y., Bird, B., Birks, H. J. B., Bjune, A. E., Briner, J., Cook, T., Chipman, M., Francus, P., Gajewski, K., Geirsdóttir, Á., Hu F. S., Kutchko, B., Lamoureux, S., Loso, M., MacDonald, G., Peros, M., Porinchu, D., Schiff, C., Seppä, H., & Thomas, E. (2009). Recent warming reverses long-term Arctic cooling. *Science*, *325*(5945), 1236-1239.

Keddy, P. (2000). The World's Largest Wetlands. *Wetland Ecology: Principles and Conservation, Cambridge University Press,< http://www. selu. edu/Academics/Faculty/pkeddy/world2. htm>(1 3.03. 2003)*.

Klein, E. S., Booth, R. K., Yu, Z., Mark, B. G., & Stansell, N. D. (2013). Hydrology-mediated differential response of carbon accumulation to late-Holocene climate change at two peatlands in Southcentral Alaska. *Quaternary Science Reviews*, *64*, 61-75.

Klinger, L. F., & Short, S. K. (1996). Succession in the Hudson Bay Lowland, Northern Ontario, Canada. *Arctic and Alpine Research*, 172-183.

Korhola, A. (1995). Holocene climatic variations in southern Finland reconstructed from peat-initiation data. *The Holocene*, *5*(1), 43-57.

Koven, C. D., Ringeval, B., Friedlingstein, P., Ciais, P., Cadule, P., Khvorostyanov, D., Krinner, G., & Tarnocai, C. (2011). Permafrost carbon-climate feedbacks accelerate global warming. *Proceedings of the National Academy of Sciences*, *108*(36), 14769-14774.

Kuhry, P. (2008). Palsa and peat plateau development in the Hudson Bay Lowlands, Canada: Timing, pathways and causes. *Boreas*, *37*(2), 316-327.

Kuhry, P., & Turunen, J. (2006). The Postglacial Development of Boreal and Subarctic Peatlands. *Boreal and Peatland Ecosystems*, *188*: 21-46.

Ladd, M. J., & Gajewski, K. (2010). The North American summer Arctic front during 1948–2007. *International Journal of Climatology*, *30*(6), 874-883.

Lamentowicz, M., Cedro, A., Gałka, M., Goslar, T., Miotk-Szpiganowicz, G., Mitchell, E. A. D., & Pawlyta, J. (2008). Last millennium palaeoenvironmental changes from a Baltic

bog (Poland) inferred from stable isotopes, pollen, plant macrofossils and testate amoebae. *Palaeogeography, Palaeoclimatology, Palaeoecology*, *265*(1), 93-106.

Lamentowicz, M., Lamentowicz, Ł., van der Knaap, W. O., Gąbka, M., & Mitchell, E. A. (2010). Contrasting Species—Environment Relationships in Communities of Testate Amoebae, Bryophytes and Vascular Plants Along the Fen–Bog Gradient. *Microbial ecology, 59*(3), 499-510.

Laiho, R. (2006). Decomposition in peatlands: reconciling seemingly contrasting results on the impacts of lowered water levels. *Soil Biology and Biochemistry*, *38*(8), 2011-2024.

Laird, K. R., & Cumming, B. F. (2009). Diatom-inferred lake level from near-shore cores in a drainage lake from the Experimental Lakes Area, northwestern Ontario, Canada. *Journal of Paleolimnology*, *42*(1), 65-80.

Laird, K. R., Fritz, S. C., & Cumming, B. F. (1998). A diatom-based reconstruction of drought intensity, duration, and frequency from Moon Lake, North Dakota: a sub-decadal record of the last 2300 years. *Journal of Paleolimnology*, *19*(2), 161-179.

Laird, K. R., Haig, H. A., Ma, S., Kingsbury, M. V., Brown, T. A., Lewis, C. F., & Cumming, B. F. (2012). Expanded spatial extent of the Medieval Climate Anomaly revealed in lake-sediment records across the boreal region in northwest Ontario. *Global Change Biology 18*(9), 2869-2881.

Laird, K. R., Kingsbury, M. V., Lewis, C. F., & Cumming, B. F. (2011). Diatom-inferred depth models in 8 Canadian boreal lakes: inferred changes in the benthic: planktonic depth boundary and implications for assessment of past droughts. *Quaternary Science Reviews*, *30*(9), 1201-1217.

Lajeunesse, P., & St-Onge, G. (2008). The subglacial origin of the Lake Agassiz–Ojibway final outburst flood. *Nature Geoscience*, *1*(3), 184-188.

Lamarre, A., Garneau, M., & Asnong, H. (2012). Holocene paleohydrological reconstruction and carbon accumulation of a permafrost peatland using testate amoeba and macrofossil analyses, Kuujjuarapik, subarctic Québec, Canada. *Review of Palaeobotany and Palynology*, *186*, 131-141.

Lamb, H. H. (1965). The early medieval warm epoch and its sequel. *Palaeogeography, Palaeoclimatology, Palaeoecology*, 1, 13-37.

Lamers, L. P., Smolders, A. J., & Roelofs, J. G. (2002). The restoration of fens in the Netherlands. *Hydrobiologia*, *478*(1-3), 107-130.

Lévesque, P. E. M., Dinel, H., & Larouche, A. (1988). *Guide to the identification of plant macrofossils in Canadian peatlands*. Land Resource Research Centre, Research Branch, Agriculture Canada.

Li, Y. X., Yu, Z., & Kodama, K. P. (2007). Sensitive moisture response to Holocene millennial-scale climate variations in the Mid-Atlantic region, USA. *The Holocene*, *17*(1), 3-8.

Ljungqvist, F. C. (2010). A regional approach to the medieval warm period and the little ice age. *Climate Change and Variability*, 1-26.

Loisel, J., Gallego-Sala, A. V., & Yu, Z. (2012). Global-scale pattern of peatland *Sphagnum* growth driven by photosynthetically active radiation and growing season length. *Biogeosciences*, *9*(84), 2169-2196.

Loisel, J., & Garneau, M. (2010). Late-Holocene paleoecohydrology and carbon accumulation estimates from two boreal peat bogs in eastern Canada: Potential and limits of multi-proxy archives. *Palaeogeography, Palaeoclimatology, Palaeoecology*, *291*(3), 493-533.

Loisel, J., & Yu, Z. (2013). Holocene peatland carbon dynamics in Patagonia. *Quaternary Science Reviews*, *69*, 125-141.

Loisel, J., & Yu, Z. (2013). Recent acceleration of carbon accumulation in a boreal peatland, south central Alaska. *Journal of Geophysical Research: Biogeosciences 118*(1), 41-53.

Ma, S. (2011). Climate change and water availability over the last two millennia in Little Raleigh Lake, northwestern Ontario. Thesis (Master, Biology) -- Queen's University, Kingston Ontario. http://qspace.library.queensu.ca/jspui/bitstream/1974/6627/1/Ma_Susan_201107_MSc.pdf

Ma, S., Laird, K. R., Kingsbury, M. V., Lewis, C. M., & Cumming, B. F. (2012). Diatom-inferred changes in effective moisture during the Late-Holocene from nearshore cores in the southeastern region of the Winnipeg River Drainage Basin (Canada). *The Holocene*.

MacDonald, G. M., Beilman, D. W., Kremenetski, K. V., Sheng, Y., Smith, L. C., & Velichko, A. A. (2006). Rapid early development of circumarctic peatlands and atmospheric CH_4 and CO_2 variations. *Science*, *314*(5797), 285-288.

MacDonald, G. M., & Case, R. A. (2005). Variations in the Pacific Decadal Oscillation over the past millennium. *Geophysical Research Letters*, *32*(8), L08703.

MacDonald, G. M., Stahle, D. W., Diaz, J. V., Beer, N., Busby, S. J., Cerano-Paredes, J., & Woodhouse, C. A. (2008). Climate warming and 21st-century drought in southwestern North America. *Eos, Transactions American Geophysical Union*, *89*(9), 82.

MacDonald, G. M., Szeicz, J. M., Claricoates, J., & Dale, K. A. (1998). Response of the central Canadian treeline to recent climatic changes. *Annals of the Association of American Geographers*, *88*(2), 183-208.

Makila, M. (1994). Calculation of the energy content of mires on the basis of peat properties. *Geological Survey of Finland, Report of Investigation, 121*:1-73.

Malmer, N., & Wallén, B. (2004). Input rates, decay losses and accumulation rates of carbon in bogs during the last millennium: internal processes and environmental changes. *The Holocene*, *14*(1), 111-117.

Mamet, S. D., & Kershaw, G. P. (2011). Radial-Growth Response of Forest-Tundra Trees to Climate in the Western Hudson Bay Lowlands. *Arctic*, 446-458.

Mann, M. E., Zhang, Z., Rutherford, S., Bradley, R. S., Hughes, M. K., Shindell, D., & Ni, F. (2009). Global signatures and dynamical origins of the Little Ice Age and Medieval Climate Anomaly. *Science*, *326*(5957), 1256-1260.

Martikainen, P. J., Nykänen, H., Alm, J., & Silvola, J. (1995). Change in fluxes of carbon dioxide, methane and nitrous oxide due to forest drainage of mire sites of different trophy. *Plant and Soil*, *168*(1), 571-577.

Matsuura, K., & Willmott, C. J. (2009). Terrestrial Air Temperature and Precipitation: Monthly Climatologies, version 4.01 (1975-2005), available at <http://climate.geog.udel.edu/`climate/html_page/archive.html>, accessed 4 September 2012.

Mauquoy, D., Hughes, P. D. M., & van Geel, B. (2010). A protocol for plant macrofossil analysis of peat deposits. *Mires and Peat*, *7*(06), 1-5.

Mauquoy, D., van Geel, B., Blaauw, M., & van der Plicht, J. (2002). Evidence from northwest European bogs shows 'Little Ice Age' climatic changes driven by variations in solar activity. *The Holocene*, *12*(1), 1-6.

Mauquoy, D., Yeloff, D., Van Geel, B., Charman, D. J., & Blundell, A. (2008). Two decadally resolved records from north-west European peat bogs show rapid climate changes associated with solar variability during the mid–late-Holocene. *Journal of Quaternary Science, 23*(8), 745-763.

Mcglone, M. S., & Wilmshurst, J. M. (1999). A Holocene record of climate, vegetation change and peat bog development, east Otago, South Island, New Zealand. *Journal of Quaternary Science, 14*(3), 239-254.

McGuire, A. D., Anderson, L. G., Christensen, T. R., Dallimore, S., Guo, L., Hayes, D. J., & Roulet, N. (2009). Sensitivity of the carbon cycle in the Arctic to climate change. *Ecological Monographs*, *79*(4), 523-555.

McMullen, J. A., Barber, K. E., & Johnson, B. (2004). A paleoecological perspective of vegetation succession on raised bog microforms. *Ecological monographs*, *74*(1), 45-77.

Meinders, M., & Van Breemen, N. (2005). Formation of soil-vegetation patterns. In *Ecosystem Function in Heterogeneous Landscapes* (pp. 207-227). Springer New York.

Mitchell, C. C., & Niering, W. A. (1993). Vegetation change in a topogenic bog following beaver flooding. *Bulletin of the Torrey Botanical Club*, 136-147.

Mitchell, E. A., Charman, D. J., & Warner, B. G. (2008). Testate amoebae analysis in ecological and paleoecological studies of wetlands: past, present and future. *Biodiversity and Conservation*, *17*(9), 2115-2137.

Moberg, A., Sonechkin, D. M., Holmgren, K., Datsenko, N. M., & Karlén, W. (2005). Highly variable Northern Hemisphere temperatures reconstructed from low-and high-resolution proxy data. *Nature, 433*(7026), 613-617.

Moore, T. R., & Knowles, R. (1989). The influence of water table levels on methane and carbon dioxide emissions from peatland soils. *Canadian Journal of Soil Science*, *69*(1), 33-38.

Murray, K. J., Tenhunen, J. D., & Nowak, R. S. (1993). Photoinhibition as a control on photosynthesis and production of *Sphagnum* mosses. *Oecologia*, *96*(2), 200-207.

Nichols, J. E., Walcott, M., Bradley, R., Pilcher, J., & Huang, Y. (2009). Quantitative assessment of precipitation seasonality and summer surface wetness using ombrotrophic sediments from an *Arctic Norwegian peatland. Quaternary Research, 72*(3), 443-451.

NOAA/ESRL (2013). GPCC Precipitation V6 Combined Precipitation (mm) Composite Anomaly, 1981-2010 climate. <http://www.esrl.noaa.gov/psd/cgi-bin/data/composites/comp.pl>. Accessed 17 April 2013.

NOAA/ESRL (2013). Multivariate El Niño Index (MEI). <http://www.esrl.noaa.gov/psd/enso/mei/>. Accessed 12 June 2013.

Olefeldt, D., Roulet, N. T., Bergeron, O., Crill, P., Bäckstrand, K., & Christensen, T. R. (2012). Net carbon accumulation of a high-latitude permafrost palsa mire similar to permafrost-free peatlands. *Geophysical Research Letters*, *39*(3).

Olsson, I. U. (1986). A study of errors in ^{14}C dates of peat and sediment. *Radiocarbon*, *28*(2A), 429-435.

O'Reilly, B., (2012). Paleoecological and Carbon Accumulation Dynamics of a Fen Peatland in the Hudson Bay Lowlands, Northern Ontario, from the Mid-Holocene to Present. Masters Thesis, Department of Geography, University of Toronto.

Oswald, W. W., & Foster, D. R. (2011). A record of late-Holocene environmental change from southern New England, USA. *Quaternary Research*, *76*(3), 314-318.

Overpeck, J., Hughen, K., Hardy, D., Bradley, R., Case, R., Douglas, M., ... & Zielinski, G. (1997). Arctic environmental change of the last four centuries. *Science*, *278*(5341), 1251-1256.

Page, S. E., Rieley, J. O., & Banks, C. J. (2011). Global and regional importance of the tropical peatland carbon pool. *Global Change Biology*, *17*(2), 798-818.

Pastor, J., Peckham, B., Bridgham, S., Weltzin, J., & Chen, J. (2002). Plant community dynamics, nutrient cycling, and alternative stable equilibria in peatlands. *The American Naturalist*, *160*(5), 553-568.

Payette, S., Delwaide, A., Caccianiga, M., & Beauchemin, M. (2004). Accelerated thawing of subarctic peatland permafrost over the last 50 years. *Geophysical Research Letters*, *31*(18).

Payne, R. J., & Mitchell, E. A. (2009). How many is enough? Determining optimal count totals for ecological and palaeoecological studies of testate amoebae. *Journal of Paleolimnology, 42*(4), 483-495.

Pederson, D. C., Peteet, D. M., Kurdyla, D., & Guilderson, T. (2005). Medieval Warming, Little Ice Age, and European impact on the environment during the last millennium in the lower Hudson Valley, New York, USA. *Quaternary Research, 63(3)*, 238-249.

Pouliot, R., Rochefort, L., Karofeld, E., & Mercier, C. (2011). Initiation of *Sphagnum* moss hummocks in bogs and the presence of vascular plants: Is there a link?. *Acta Oecologica*, *37*(4), 346-354.

Prentice, I. C., Bartlein, P. J., & Webb III, T. (1991). Vegetation and climate change in eastern North America since the last glacial maximum. *Ecology 12*(6), 2038-2056.

Prentice, I. C., Sykes, M. T., & Cramer, W. (1993). A simulation model for the transient effects of climate change on forest landscapes. *Ecological modeling*, *65*(1), 51-70.

Provincial Land Cover Data Base, Second Edition [computer file]. (2000). Peterborough, ON: Ministry of Natural Resources. Available: Brock University Map Library Controlled Access S:\MapLibrary\DATA\MNR\Provincial_Land_Cover (22 January 2013).

Quillet, A., Frolking, S., Garneau, M., Talbot, J., & Peng, C. (2013). Assessing the role of parameter interactions in the sensitivity analysis of a model of peatland dynamics. *Ecological Modelling*, *248*, 30-40.

R Development Core Team (2012). R: A language and environment for statistical computing. R Foundation for Statistical Computing, Vienna, Austria. ISBN 3-900051-07-0, <http://www.R-project.org/>.

Raghoebarsing, A. A., Smolders, A. J., Schmid, M. C., Rijpstra, W. I. C., Wolters-Arts, M., Derksen, J., Jetten, M. S. M., Schouten S., Sinninghe Damsté, J. S., Lamers, L. P. M., Roelofs, J. G. M., Op den Camp, H. J. M., & Strous, M. (2005). Methanotrophic symbionts provide carbon for photosynthesis in peat bogs. *Nature, 436*(7054), 1153-1156.

Reimer, P. J., Baillie, M. G. L., Bard, E., Bayliss, A., Warren, B. J., Blackwell, P. G., Ramsey, C. B., Buck, C. E., Burr, G. S., Edwards, R. L., Friedrich, M., Grootes, P. M., Guilderson, T. P., Hajdas, I., Heaton, T. J., Hogg, A. G., Hughen, K. A., Kaiser, K. F., Kromer, B., Manning, S. W., McCormac, F. G, Reimer, R. W., Richards, D. A., Southon,

J. R., Talamo, S., Turney, C. S. M., van der Plicht, J., Weyhenmeyer, C. E. (2009). IntCal09 and Marine09 radiocarbon age calibration curves, 0–50,000 years cal BP. *Radiocarbon, 51*: 1111-1150.

Reyes, A. V., Wiles, G. C., Smith, D. J., Barclay, D. J., Allen, S., Jackson, S., Larocque, S., Laxton, S., Lewis, D., Calkin, P.E., & Clague, J. J. (2006). Expansion of alpine glaciers in Pacific North America in the first millennium AD. *Geology*, *34*(1), 57-60.

Riley, J. L., (2005). Flora of the Hudson Bay Lowlands and its postglacial origins. *National Research Council of Canada*. ISBN 0-660-18941-0.

Riley, J. L. (2011). Wetlands of the Ontario Hudson Bay Lowland: an regional overview. *Nature Conservancy of Canada, Toronto, Ontario, Canada*.

Riordan, B., Verbyla, D., & McGuire, A. D. (2006). Shrinking ponds in subarctic Alaska based on 1950–2002 remotely sensed images. *Journal of Geophysical Research: Biogeosciences (2005–2012)*, *111*(G4).

Robroek, B. J., Schouten, M. G., Limpens, J., Berendse, F., & Poorter, H. (2009). Interactive effects of water table and precipitation on net CO_2 assimilation of three co-occurring *Sphagnum* mosses differing in distribution above the water table. *Global Change Biology*, *15*(3), 680-691.

Roulet, N. T., Jano, A., Kelly, A., Klinger, L. F., Moore, T. R., Protz, R., Ritter, J. A., & Roulet, N. T. (2000). Peatlands, carbon storage, greenhouse gases, and the Kyoto protocol: prospects and significance for Canada. *Wetlands*, *20*(4), 605-615.

Roulet, N. T., Jano, A., Kelly, C. A., Klinger, L. F., Moore, T. R., Protz, R., Ritter, J. A., & Rouse, W. R. (1994). Role of the Hudson Bay lowland as a source of atmospheric methane. *Journal of Geophysical Research*, *99*(D1), 1439-1454.

Sannel, A. B. K, & Kuhry, P. (2009). Holocene peat growth and decay dynamics in sub-arctic peat plateaus, west-central Canada. *Boreas*, *38*(1), 13-24.

Szeicz, J. M., & Macdonald, G. M. (1995). Recent white spruce dynamics at the subarctic alpine treeline of north-western Canada. *Journal of Ecology*, 873-885.

Seager, R., Burgman, R., Kushnir, Y., Clement, A., Cook, E., Naik, N., & Miller, J. (2008). Tropical Pacific Forcing of North American Medieval Megadroughts: Testing the Concept with an Atmosphere Model Forced by Coral-Reconstructed SSTs. *Journal of Climate, 21*(23), 6175-6190.

Shabbar, A., Bonsal, B., & Khandekar, M. (1997). Canadian precipitation patterns associated with the Southern Oscillation. *Journal of Climate*, *10*(12), 3016-3027.

Sheng, Y., Smith, L. C., MacDonald, G. M., Kremenetski, K. V., Frey, K. E., Velichko, A. A., Lee, M., Beilman, D. W., & Dubinin, P. (2004). A high-resolution GIS-based inventory of the west Siberian peat carbon pool. *Global Biogeochemical Cycles*, *18*(3).

Steinman, B. A., Abbott, M. B., Mann, M. E., Stansell, N. D., & Finney, B. P. (2012). 1,500 year quantitative reconstruction of winter precipitation in the Pacific Northwest. *Proceedings of the National Academy of Sciences*, *109*(29), 11619-11623.

Stevens, L. R., Stone, J. R., Campbell, J., & Fritz, S. C. (2006). A 2200-yr record of hydrologic variability from Foy Lake, Montana, USA, inferred from diatom and geochemical data. *Quaternary Research*, *65*(2), 264-274.

Stevenson, S., Fox-Kemper, B., Jochum, M., Neale, R., Deser, C., & Meehl, G. (2012). Will there be a significant change to El Niño in the twenty-first century?. *Journal of Climate*, *25*(6), 2129-2145.

Strack, M., Waddington, J. M., Lucchese, M. C., & Cagampan, J. P. (2009). Moisture controls on CO_2 exchange in a *Sphagnum*-dominated peatland: results from an extreme drought field experiment. *Ecohydrology*, *2*(4), 454-461.

Swindles, G. T., Morris, P. J., Baird, A. J., Blaauw, M., & Plunkett, G. (2012). Ecohydrological feedbacks confound peat-based climate reconstructions. *Geophysical Research Letters, 39*(11).

Tarnocai, C. (2006). The effect of climate change on carbon in Canadian peatlands. *Global and planetary Change*, *53*(4), 222-232.

Tarnocai, C., Kettles, I. M., Lacelle, B. (2011). Geological Survey of Canada, Open File 6561. Natural Resources Canada, accessed 13 August 2012.

Tian, J., Nelson, D. M., & Hu, F. S. (2006). Possible linkages of late-Holocene drought in the North American midcontinent to Pacific Decadal Oscillation and solar activity. *Geophysical research letters*, *33*(23), L23702.

Tuittila, E. S., Juutinen, S., Frolking, S., Väliranta, M., Laine, A. M., Miettinen, A., Seväkivi, M., Quillet, A., & Merilä, P. (2013). Wetland chronosequence as a model of peatland development: Vegetation succession, peat and carbon accumulation. *The Holocene*, *23*(1), 25-35.

Turetsky, M. R., Crow, S. E., Evans, R. J., Vitt, D. H., & Wieder, R. K. (2008). Trade-offs in resource allocation among moss species control decomposition in boreal peatlands. *Journal of Ecology*, *96*(6), 1297-1305.

Turetsky, M., Wieder, K., Halsey, L., & Vitt, D. (2002). Current disturbance and the diminishing peatland carbon sink. *Geophysical Research Letters*, *29*(11), 21-1.

Turetsky, M. R., Wieder, R. K., Vitt, D. H., Evans, R. J., & Scott, K. D. (2007). The disappearance of relict permafrost in boreal north America: Effects on peatland carbon storage and fluxes. *Global Change Biology*, *13*(9), 1922-1934.

Turner, T. E., Swindles, G. T., Charman, D. J., and Blundell, A. (2013). Comparing regional and supra-regional transfer functions for palaeohydrological

Turunen, J., Tomppo, E., Tolonen, K., & Reinikainen, A. (2002). Estimating carbon accumulation rates of undrained mires in Finland–application to boreal and subarctic regions. *The Holocene*, *12*(1), 69-80.

Van Bellen, S., Garneau, M., & Booth, R. K. (2011). Holocene carbon accumulation rates from three ombrotrophic peatlands in boreal Quebec, Canada: Impact of climate-driven ecohydrological change. *The Holocene, 21*(8): 1217-1231.

van Breemen, N. (1995). How *Sphagnum* bogs down other plants. *Trends in Ecology & Evolution*, *10*(7), 270-275.

Vance, R. E., Emerson, D., & Habgood, T. (1983). A mid-Holocene record of vegetative change in central Alberta. *Canadian Journal of Earth Sciences*, *20*(3), 364-376.

Vance, R. E., Last, W. M., & Smith, A. J. (1997). Hydrologic and climatic implications of a multidisciplinary study of late-Holocene sediment from Kenosee Lake, southeastern Saskatchewan, Canada. *Journal of Paleolimnology*, *18*(4), 365-393.

Vance, R. E., Mathewes, R. W., & Clague, J. J. (1992). 7000 year record of lake-level change on the northern Great Plains: A high-resolution proxy of past climate. *Geology*, *20*(10), 879-882.

Vance, R. E., & Wolfe, S. A. (1996). Geological indicators of water resources in semi-arid environments: Southwestern interior of Canada. *Geoindicators: Assessing Rapid Environmental Changes in Earth Systems, AA Balkema, Lisse*, 251-263.

Viau, A. E., & Gajewski, K. (2009). Reconstructing millennial-scale, regional paleoclimates of boreal Canada during the Holocene. *Journal of Climate*, *22*(2), 316-330.

Viau, A. E., Gajewski, K., Fines, P., Atkinson, D. E., & Sawada, M. C. (2002). Widespread evidence of 1500 yr climate variability in North America during the past 14 000 yr. *Geology*, *30*(5), 455-458.

Vitt, D. H., Halsey, L. A., Bauer, I. E., & Campbell, C. (2000). Spatial and temporal trends in carbon storage of peatlands of continental western Canada through the Holocene. *Canadian Journal of Earth Sciences*, *37*(5), 683-693.

Vitt, D. H., Halsey, L. A., & Zoltai, S. C. (2000). The changing landscape of Canada's western boreal forest: the current dynamics of permafrost. *Canadian Journal of Forest Research*, *30*(2), 283-287.

Waddington, J. M., Plach, J., Cagampan, J. P., Lucchese, M., & Strack, M. (2009). Reducing the carbon footprint of Canadian peat extraction and restoration. *AMBIO: A Journal of the Human Environment*, *38*(4), 194-200.

Wagner-Cremer, F., Finsinger, W., & Moberg, A. (2010). Tracing growing degree-day changes in the cuticle morphology of Betula nana leaves: a new micro-phenological palaeo-proxy. *Journal of Quaternary Science*, *25*(6), 1008-1017.

Wania, R., Ross, I., & Prentice, I. C. (2009). Integrating peatlands and permafrost into a dynamic global vegetation model: 1. Evaluation and sensitivity of physical land surface processes. *Global Biogeochemical Cycles*, *23*(3): GB3014.

Warner, B. G., & Chmielewski, J. G. (1992). Testate amoebae (Protozoa) as indicators of drainage in a forested mire, northern Ontario, Canada. *Archiv für Protistenkunde*, *141*(3), 179-183.

Webber, P. J., Richardson, J. W., & Andrews, J. T. (1970). Post-glacial uplift and substrate age at Cape Henrietta Maria, southeastern Hudson Bay, Canada. *Canadian Journal of Earth Sciences*, *7*(2), 317-325.

Whalen, S. C. (2005). Biogeochemistry of methane exchange between natural wetlands and the atmosphere. *Environmental Engineering Science*, *22*(1), 73-94.

Winston, R. B. (1994). Models of the geomorphology, hydrology, and development of domed peat bodies. *Geological Society of America Bulletin*, *106*(12), 1594-1604.

Yu, Z. (2011). Holocene carbon flux histories of the world's peatlands Global carbon-cycle implications. *The Holocene*, *21*(5), 761-774.

Yu, Z., Beilman, D. W., & Jones, M. C. (2009). Sensitivity of northern peatland carbon dynamics to Holocene climate change. *Carbon Cycling in Northern Peatlands, Geophysical Monograph Series*, *184*, 55-69.

Zhang, Y., Qian, Y., Dulière, V., Salathé Jr, E. P., & Leung, L. R. (2012). ENSO anomalies over the Western United States: present and future patterns in regional climate simulations. *Climatic change*, *110*(1-2), 315-346.

Zoltai, S. C., & Tarnocai, C. (1975). Perennially frozen peatlands in the western Arctic and Subarctic of Canada. *Canadian Journal of Earth Sciences*, *12*(1), 28-43.